How a Dry Year Affects Spatial Variability of Ground Thaw and Changes the Hydrology of a Small Arctic Watershed

by

Brampton Dakin

A thesis

presented to the University of Waterloo

in fulfillment of the

thesis requirements for the degree of

Master of Science

in

Earth Sciences (Water)

Waterloo, Ontario, Canada 2023

Author's Declaration

I hereby declare that I am the sole author of this thesis. This is a true copy of the thesis, including any required final revision, as accepted by my examiners.

I understand that my thesis may be made electronically available to the public.

Abstract

The summer of 2021 in the Inuvik area, NWT was warm and dry. As recorded in Siksik Creek, a sub-catchment of Trail Valley Creek located 50 km north-east of Inuvik, this was the 7th warmest summer and driest July recorded to date. This presented a unique opportunity to study the drying phenomena of Arctic ecosystems. This is pertinent to the study of permafrost degradation, as the drying phenomena is still vastly understudied and there are few datasets available that record abnormally dry conditions in Arctic catchments. These data sets are needed to properly show the influence that this has on active layer thicknesses. It is unknown whether these conditions may pose a risk to permafrost, if this is spatially variable, and what other processes might amplify or hinder this. The main objective of this thesis is to explore how a dry year affects active layer thaw and the hydrology of Siksik Creek so that we may better understand how catchments such as Siksik will respond to ongoing climate change. To do this a mix of field results and modelling was used to show and quantify how these may affect active layer thaw as well as water balance components. The three main research chapters of this thesis divide this by analyzing active layer thaw as physically measured in the catchment to previous years, by using the model GEOtop to assess how this affects water balance components, and then by simulating wetter conditions to show the affect soil moisture has.

Field data were collected from May 25th to August 29th in Siksik Creek during the summer of 2021, where the data collected included active layer thicknesses, depth to the water table, as well as stratigraphy and soil thicknesses across a variety of terrain type throughout the entirety of the catchment. This study specifically focused on measuring these data across hummocks and inter-hummocks throughout the catchment, as these features are ubiquitous in the Mackenzie uplands. In addition to analyzing the 2021 field data, the GEOtop physically based hydrology model was used to explore the processes controlling active layer thicknesses, water table depths, and various water balance components over the course of the summer of 2021. GEOtop is designed to handle microtopographies, such as hummocks and other terrain features. Further, we compare the physical and simulated results from the summer of 2021 to a more normal and wetter year (2016) to assess the differences that soil moisture has on the hydrology and active layer thaw of Siksik Creek. We explored how the movement of water impacted thaw depths in these landscapes, how spatial variability of thaw is influenced by soil moisture, and by the terrain features that control this.

We found that peat thicknesses in this area are controlled by the presence of hummocks, where peat is thickest between hummock mounds in an area called the inter-hummock zone. This variability of peat thicknesses directly controls the spatial variability of soil moisture, and this had implications on thaw. In Chapter Two it was found that thaw for the summer of 2021 was shallower than expected in the inter-hummock zones by as much as 20cm compared to similar studies in Siksik and in similar landscapes in Alaska. This chapter also showed that the overlying vegetation, specifically lichens and mosses, were statistically linked to peat thicknesses representative of hummocks and inter-hummocks - where lichens tended to be overtop of hummocks, and mosses overtop of inter-hummocks. This correlation was then used with UAV imagery, taken in mid-June, to map mosses and lichens across the catchment and by proxy the locations of hummocks and inter-hummocks. This map was built into the model GEOtop to simulate Siksik Creek for the summer of 2021.

Starting in Chapter Three, the modelled portion of this thesis covered a wide aspect of simulations, where the influence of hummocks was assessed, as well as shrubs and snow when they were added to the model, and finally assessing the role soil moisture plays within all of these various processes. It was found that hummocks, when they were specifically discretized and compared to a simple soil column, reached freshet and max discharge sooner by as much as two days, a lag that existed in the evapotranspiration outputs as well. However, these results were relatively consistent and the only major difference between these two simulations was seen in the 2d active layer depth maps. It was found that microtopography by the end of the summer seemed to influence local patterns of thaw more than larger topographical features such as natural depressions in the landscape did. When shrubs and snow were added to the model domain and simulated it was found that the presence of snow or lack thereof was the main component of difference in the discharge and evapotranspiration data. The active layer depth maps changed between simulations, with the shrub only simulations having the lowest degree of thaw, with a degree of variability seen between simulations. In comparison, the water table depths hardly changed between simulations, and it was hypothesized that the dryness of the summer and the lack of soil moisture was the main culprit for this.

To test if this was the case, in Chapter Four, precipitation and snow water-equivalent data was taken from a wetter year (2016) and replaced the values for the dry summer of 2021. This

was done so that only moisture available to the system was changed. It was found that soil moisture was in fact the main cause for this lack of variability. The wetter simulations because of this had deeper thaw throughout the catchment, with both the extent, max thaw depths, and min thaw depths increasing. The water table depths on the other hand became shallower and the ground surface was much more inundated with water. The spatial variability in the water table depth maps was found to match where the presence of taller shrubs in the catchment exist, where these areas had the least amount of soil moisture and the shallowest thaw depths. Whereas the areas with the highest amount of soil moisture content had the deepest thaw depths in the catchment.

Overall, this thesis helps to improve our understanding of how peat catchments similar to Siksik Creek might respond to either the wetting or drying of the Arctic. This thesis also advances our understanding on the controls of soil moisture variability and ground thaw, as well as its spatial variability. One can infer from this study that for posterity it is the warm and wet summers rather than the warm and dry summers that pose the largest risk to permafrost and its degradation.

Acknowledgements

It has been an incredible opportunity and experience to conduct and write down all of the research that went into this thesis. I am grateful for the opportunity to have worked in the Arctic and at Trail Valley Creek over the last six years, which has culminated in this thesis. I will cherish the memories I have of the months I have spent in camp and of all the friendships and connections that have been made from this. I am grateful to my family who has always supported me in my endeavors, no matter how roundabout the journey was.

Thank you to my supervisor David Rudolph who gave me the opportunity to do all this exciting research at the university of Waterloo, and without whom none of this would have been possible. Thank you also to my supervisor Philip Marsh, who helped me organize my thoughts and put them into written form, for first letting me into the research group six years ago, and for his continuing support in academic research. Thank you to Robin Thorne for the incredible attention to detail, ideas, and support while editing this thesis. Lastly, to Jackson Seto who spent most of the summer with me isolated in camp due to COVID-19, who helped me carry all of the equipment around Siksik Creek, and without whom my time in the field would not have been nearly as enjoyable.

I am appreciative of the financial support from Northern Water Futures without whom this thesis would likely not have been funded. This research was also supported by the Northern Scientific Training Program, and the Polar Continental Shelf Program.

Finally, a huge amount of gratitude goes to Ellen, who has supported me from the beginning and whom continues to do so.

Table of Contents

List of Figures

List of Tables

List of Terms

Active Layer: The top layer of ground subject to annual thawing and freezing in areas underlain by permafrost (Glossary of Permafrost and Related Ground-Ice Terms).

Permafrost: Ground that has been continuously at or below 0 degrees Celsius for at least two years (Glossary of Permafrost and Related Ground-Ice Terms).

Frost-table: A surface in the ground that represents the thawed depth within seasonally frozen ground (American Meteorological Society).

Acrotelm: one of two layers in peat, it overlies the catotelm and is composed of mostly living organic peats and mosses (Holden and Burt, 2003).

Catotelm: one of two layers of peat, it resides underneath the acrotelm and is composed of dead plant material. It is typically associated with the lowest level of the water table (Holden and Burt, 2003).

Depth of zero amplitude: The distance from the ground surface downward to the level beneath which there is practically no annual fluctuation in ground temperature (Glossary of Permafrost and Related Ground-Ice Terms).

Snow Water Equivalent: abbreviated for snow water equivalent, refers to how much water is stored in the snowpack were the snowpack to be melted (American Meteorological Society).

Freshet: The rising of streams in the spring in colder climates due to snowmelt (American Meteorological Society).

List of Abbreviations

TMM: Trail Valley Main Meteorological station in Siksik Creek.

MSC: Environments Canada's Meteorological Service, it is a secondary meteorological station found in Siksik Creek.

Chapter 1

1.1 The Wetting and Drying of Arctic Catchments.

Northernmost latitudes are undergoing the most rapid rate of terrestrial ecosystem changes due to climate change across the globe. The global average for warming is on the scale of 0.4 to 0.8 °C (IPCC, 2011), and according to Young et al., (2006) and Tetzlaf et al., (2018) Arctic temperatures have increased at twice this rate. Burn & Kokelj (2009) showed that average temperatures in Arctic climates have increased by as much as 3-4 °C over the last century. This drastic rate of increase led the United Nations (UN) declaring in March of 2019 that these regions are stuck in a progressive and destructive rate of temperature increase (Schoolmeester et al., 2019), and it is also believed that accelerated permafrost degradation across the Arctic has begun as well (IPCC, 2014). Much of the hydrological regime in these Arctic climates is going to drastically change. This has direct implications to northern communities, and where permafrost degradation becomes extreme could even cause migrations of communities.

One common debate among northern researchers is whether the Arctic will become more wet or more dry, and while there are general climate patterns over the past 30 years that can loosely be followed, there is still no real way to predict whether a year is going to be more wet or dry (Olthof & Rainville, 2022; Webb et al., 2022) as it appears parts of the Arctic are undergoing drying while other parts are becoming more wet. It is extremely difficult to research as field data to validate predictions against wet or dry years are few and far between. Even in places where temperature and precipitation have both increased, Webb et al., (2022) showed that Arctic lowlands in lake dominated areas are becoming drier, a trend seen in Greenland as well (Higgins et al., 2019). Recent studies have shown that in general more regions of the Arctic are becoming wetter than compared to the regions that are becoming dryer (Olthof & Rainville, 2021).

To predict how the wetting or drying of Arctic catchments is going to affect these landscapes, it is pertinent to understand how the hydrology of these catchments change during wet or dry years. Field data collection is necessary, including establishing years that are wet, dry, or average, and understanding how topographical elements such as mineral earth hummocks, vegetation cover, and active layer depths will affect and be affected. Better knowledge of how these changes occur under varying climate conditions can then be used to predict which areas of

the Arctic might become more likely to dry or be more wet as climate change and global warming progress.

1.2 Past Research and Knowledge Gaps

Canadian Arctic hydrology suffers from a lack of continuous, long-standing research stations, and what few stations do exist are slowly dwindling (Tetzlaff et al., 2017). While it is still possible to analyze historical data for change detection, observing dry and wet summer conditions can be sporadic, making the collection of field data that can capture these changes difficult and important. While larger trends in climate change have been analyzed (Vavrus et al., 2017; Rinke et al., 2019; Webb et al., 2022), there is still no concrete consensus on what catchments in the Arctic might become more wet or dry, as noted previously. Field data collected for individual catchments in the Arctic are uncommon for proper analysis.

Perhaps the largest issue to capturing these changes in individual catchments though is the sheer variety and quantity of both processes that need to be considered, as well as the differences in landcover and topography that can be found even in smaller catchments. In the Mackenzie uplands, catchments typical of this area are ubiquitously covered in mosses and lichens; have a variety of both taller alder, willow, and birch shrubs, as well as smaller dwarf shrubs; a variety of sedges and tussocks that litter the terrain; and the presence of mineral-earth hummocks at or near the ground surface (Wilcox et al., 2019). Mineral earth hummocks are composed of mostly clays and silts and are relatively impervious compared to the surrounding inter-hummock zones (Quinton et al., 2000). They create a tortuous network for groundwater flow, and effectively control the spatial variability of soil moisture (Quinton et al., 2000; Endrizzi et al., 2011). Some recent research has begun to analyze how a variety of shrubs and hummock are beginning to affect both water balances as well as active layer depths. An example of this type of research is presented by Wilcox et al (2019), where frost table depths were measured across the summer for both mineral earth hummocks, as well as shrub-tundra vegetation types. Mackay (1980) explored how these mineral-earth hummocks formed, while Quinton and Marsh (1999) and Quinton et al. (2000) explored how these features affect both the sub-surface flow of water, as well as how the physical properties of the soils around these features change. Endrizzi and Marsh (2010), and Endrizzi et al. (2011) showed how these may, in a simplified model, affect soil moisture and thus active layer thaw.

The spatial variability of mineral earth hummocks influences moisture and thaw across a basin. The size of these features are typically less than 1 m, which makes them extremely difficult to map without the use of UAV technology such as a fixed wing drone. Further, the modelling efforts that Endrizzi et al. (2011) did were simplistic in nature, lacking snow or vegetation in the model, and only used a single layer of soil that averaged the properties of hummocks and inter-hummocks into one layer. The use of a numerical model that properly includes the spatial locations of hummocks and inter-hummocks, as well as incorporating snow, vegetation, and active layer thaw, would be the first of its kind to our knowledge. These studies also lacked a detailed analysis of the water balance such as stream discharge, evapotranspiration, and snowmelt, and how mineral earth hummocks could influence each aspect. Analysis of this water balance in this level of detail, based on wet, dry, or average years has not been conducted in the Arctic tundra. While we can expect climate induced changes to active layer thaw and water balances, being able to answer what may increase or decrease these elements is crucial to continuing research in the north.

1.3 Objectives and Approach

The overall objective of this thesis is to better understand how a dry summer in a small Arctic catchment will influence both its hydrological regime as well as active layer thaw, and if these conditions might accelerate permafrost degradation. This study takes place in the Siksik Creek catchment, a sub-catchment of Trail Valley Creek watershed, in the tundra uplands found between Inuvik and Tuktoyaktuk in the Northwest Territories. This area is within the continuous permafrost zone and the thawing of the active layer, which rests above the permafrost, is directly controlled by both the timing of snowmelt; as well as those landforms at, or near, the surface that control the distribution of soil moisture; and intercept incoming solar radiation, such as hummocks and shrubs (Gray and Granger, 1986; Wilcox et al., 2019). Meteorological data was recorded at Siksik Creek for the entirety of the summer of 2021 at the Trail Valley Creek Main Meteorological station (TMM). Field work was conducted in Siksik Creek from May 14th to August 18th with a focus on the spatial variability of peat thickness throughout the catchment, as well as how different landscape characteristics affect active layer thaw. Alongside the measurement of discharge and pre-melt snow water equivalent, a water balance was calculated

for the summer. Measurements and analysis were then used in conjunction with the numerical model GEOtop to further examine any changes in the basin hydrology and rate of thaw. As this was a singular summer, observations from 2021 were compared with previously collected data from the summer of 2016. The summer of 2016 is considered a "wet" year in this study, even though in the longer record of TVC it is average in many aspects. A comparison of the two summers was conducted, where elements of the water balance calculation were analyzed alongside water table depths and active layer thaw to understand how a wet or dry summer might affect these properties. The objective of these research questions:

1. How do peat thicknesses across the catchment vary? How does this affect active layer thaw during a dry year? What does this mean for future permafrost degradation? (Chapter 1)
2. How does active layer thaw and water balances change when hummocks and inter-hummocks, shrubs and vegetation, and snow are added to GEOtop individually during a dry year? (Chapter 2)
3. How do these results compare to a more wet year? (Chapter 3)

1.4 Thesis Outline

There are five chapters in this thesis. The first chapter is a brief introduction to the wetting and/or drying of the Arctic along with a discussion of climate change. Chapters 2, 3, and 4 will answer the research questions stated in the previous section. The fifth chapter reiterates the findings of this research and future work. The following sections are synopses of Chapters 2 to 4.

1.4.1 Chapter Two

Chapter two explores how peat thicknesses vary with hummocks and inter-hummocks, and underneath of surficial features, such as mosses and lichens. These features were compared with active layer thaw across the entirety of the catchment and rates of thaw throughout the summer were measured on a weekly basis. Hummocks are the cornerstone to understanding how groundwater flows in these areas, as they force runoff to be conveyed through the inter-hummock zones, which are composed of highly porous soils and peat. As they control the pathways that runoff must take, they are also essential for understanding the spatial variability of thaw as the rates of thaw are different for hummock and inter-hummock zones. The rate of active

layer thaw underneath hummocks and inter-hummocks will influence permafrost degradation. Results show that the rate of active layer thaw in the inter-hummock zones was shallower than what was originally anticipated, and that there was very little movement of water within these zones. It is highly unlikely that thaw in these zones posed any risk to permafrost thaw. More work needs to be done to collect data on permafrost depths below these features before this can be fully answered.

1.4.2 Chapter Three

Chapter three focuses on the interplay between hummocks and inter-hummocks, shrubs, and snow, and how these individually affect the hydrology and active layer thaw in Siksik Creek. This chapter specifically analyzes how discharge and evapotranspiration are affected, and their influence on the end of summer active layer thicknesses and water table depths. We use the numerical model GEOtop to further explore the water balance during a dry year. Results show that GEOtop was able to properly incorporate microtopography into its domain and was able to model adequately the hydrological components and active layer thaw in Siksik Creek. The simulations comparing a one-soil domain, that averages hummocks and inter-hummocks together, to a two-soil domain, that specifically includes hummocks and inter-hummocks, show that the specific discretization of hummocks in the two-soil domain respond and reach freshet two days sooner than the one-soil simulations. Active layer thaw was influenced by microtopography more so than larger topographical features. The simulations that included shrubs generated an earlier freshet than the snow-only simulations but had smaller rates of evapotranspiration for most of the summer. Shrub-only simulations had a lower rate of active layer thaw possibly due to the lack of available moisture and/or increased vegetation coverage.

1.4.3 Chapter Four

Chapter four, with the use of GEOtop, compares the data collected in a dry year (2021) to observations from a normal year (2016). What made Chapter Four necessary for us was the surprising lack of variability in the results from Chapter 3. It was hypothesized that these results were because of a lack of available soil moisture, which reduces thermal conductivity of peat soils, and thus directly limits both active layer thaw and water table depths. It was found that soil moisture does play a significant role in determining the maximum and minimum thaw depths. These depths were also highly influenced by the presence of shrubs, causing deeper than normal depths to the water table. The volume of water for both daily peaks, and cumulative over the

summer, were significantly different. The daily peak discharge doubled, and the cumulative volume of water leaving the basin as discharged almost tripled. Evapotranspiration on the other hand barely changed, but this is likely because of how the model calculates evapotranspiration and simulation design.

Chapter 2

Spatial Variability of Active Layer Thaw During a Dry Summer in the Western Canadian Arctic

2.1 Introduction

Arctic regions are under a rapid rate of change due to global warming with rates 2-3x higher than the global average (IPCC 2019; Rantanen et al., 2022) – a process that has been called Arctic Amplification (AMAP, 2021). Concerns arise from northern communities in regard to these landscapes and how they will be affected due to warming in these continuous permafrost landscapes. There is a limited number of long-term research stations to help answer their concerns, which have slowly been declining (Tetzlaff et al., 2017). This poses major logistical challenges and hinders the ability of researchers to understand observed changes and is crucial to continuing research. While we know that these landscapes will begin to thaw, we do not yet fully understand the rate at which this will happen, or the factors that may quicken or slow down this rate of thaw; nor what may happen to the region in regard to becoming more dry or more wet.

Permafrost is defined as frozen ground that remains continuously at a temperature below 0°C for at least two years. The active layer is the ground above the permafrost that thaws and then freezes in the summer and winter seasons. The extent of Arctic warming will inherently increase the depth of the active layer and increase the distance of the permafrost from the ground surface. This does vary spatially and temporally as it depends on the rate at which heat is transferred into the subsurface (Wilcox et al, 2019).

Understanding permafrost degradation includes examining the microtopography, biogeochemistry, and hydrogeological processes, as well as an understanding of the regional climate (Juszak et al., 2016; Bolduc, 2015; O'Connor et al., 2020). Specifically, those variables that affect the energy budget at the surface and near-surface interface, as well as those that affect the movement of heat within the sub-surface (Bolduc, 2015). Above surface processes that can affect heat transfer into the ground include cloud cover, shrub and canopy cover, aspect, snow cover, albedo, and the presence of water. Sub-surface processes include the thickness and type of overburden – i.e., moss / lichen and peat, as well as stratigraphy and physical properties of the soil that affect the lateral movement of water and heat, and thus thaw.

Groundwater is the primary transporter of heat laterally, where the lateral movement of water is directly related to thaw depths in a basin and the development of the active layer (Quinton & Marsh, 1999). The movement of water is affected both by the water stored in the subsurface as a legacy of the previous season before the ground froze, as well as the water that gets stored as snow aboveground throughout the winter (Marsh and Woo, 1981; Atchley et al., 2016). In the Arctic, due to permafrost and the active layer, the depth to the water table can be shallow (on the scale of metres to sub-metre) – where the movement of water is confined to the active layer and the permafrost acts as an impermeable barrier underneath this (Quinton and Marsh, 1999).

The majority of streamflow and subsurface flow (as high as 90%) in these Arctic catchments typically happens within a short period of time, called freshet, which ranges from 2-5 weeks on average during snowmelt in late April to mid-May (Marsh et al., 1981). The timing of this event is one of the primary controls of active layer development throughout the summer months (Gray and Granger., 1986). When considering the impacts this might have on stream discharge, the ability of the subsurface soils to convey and release water is crucial to this process for streamflow to occur past the initial melting of snow. It has been shown that the movement of water in the subsurface typically does not happen until the snowpack has been removed, as the ground will not begin to thaw before this (Gray and Granger, 1986).

Snow depth and density throughout the winter and right before freshet are also important as they affect the ability of the snow to insulate the ground, and thus keep it warmer or colder than air temperature depending on the time of year (Frauenfeld et al., 2004). The distribution of snow across these landscapes varies, as shrub patches (taller alder and willow shrubs) and steep hillslopes have been associated with both deeper snowpacks, as well as those that persist longer into the thaw season than snow stored on the open tundra (Pomeroy et al., 1993; Woo and Marsh, 2005; Grunberg et al., 2020). These persistent snowpacks are associated with a shallow active layer. However, in cases where the shrubs are taller than the snowpack, snowmelt tends to occur earlier due to emitted long-wave radiation from the shrubs (Wilcox et al., 2019). These lingering snow patches, both in shrub patches and on hillslopes, are important to controlling the local timing of snowmelt as well as the spatial distribution of depth of snow and Snow Water Equivalent (SWE) (Gray & Granger, 1986). They can also influence the rate of active layer thawing (Ling and Zhang, 2003; Frauenfeld et al., 2004; Burn & Kokelj, 2009; Yanhui et al.,

2022). Lingering snow patches on hill slopes are primarily attributed to aspects of the slope (Lafaysse et al., 2017) and exist on the north facing slopes in these Arctic catchments, receiving less incoming radiation than the other degrees of aspect.

At the surface-ground interface and below shrub canopies, landscape types and surficial vegetation are important factors that affect the ability of radiation to migrate into the subsurface. Sedges, tussocks, hummocks, moss, and lichen all have different thermal conductivities and pore spaces / soil water retention properties, all of which affect the ability of heat to transfer into the ground. For sedges, tussocks, and hummocks, local relative height above the tundra are the most important factors towards shading the ground (O'Connor et al, 2020). There has been some effort in recent years to better understand the relationship between vegetation and permafrost within Siksik Creek (Wilcox et al, 2019; Grunberg et al, 2020); this study aims to build upon these efforts. Literature suggests that shading from vegetative canopies helps prolong the development of the active layer leading to shallower thaw depths. However, recent research has shown that low birch shrubs may be associated with increased frost table depths, and alder areas do not significantly differ from tundra frost depths (Lantz et al, 2013; Wilcox et al, 2019). How these shallow active layer depths caused by these features affect the ability of water to flow through, or around them, needs to be fully explored.

At the surface-ground interface these Arctic catchments are typically dominated by mosses and lichens. Mosses act as a thick mat that can store water in its pore spaces and are a great insulator compared to lichens which have almost no ability to retain water in their pore spaces (O'Connor et al, 2020). Generally, the albedo and thermal conductivities of the top-most layer of soil plays a larger role than above ground vegetation in determining frost thaw depths at the end of the summer (Juszak et al., 2016). While there has been some work done on correlating these with the underlying geology and ability to allow the transport of water, more work needs to be done to associate these with peat thicknesses alongside spatial patterns throughout Arctic catchments (Juszak et al, 2016; Way & Lewkowicz, 2017).

Mapping geological units in the Arctic can be complex, as the surficial units most associated with active layer development originate from the last glaciation, and after the retreat of the glaciers was subjected to cryogenic and fluvial processes (Kokelj, Burn, 2005; Batchelor et al., 2013). Further, there is a distinct lack of geological mapping in the Mackenzie Uplands

areas in detail to accurately map small catchments characteristic of this landscape that can adequately include microtopography (Palmer et al, 2012); despite numerous papers studying what affects temperature at the top of permafrost (Morse et al., 2012; Palmer et al., 2012; Obu et al, 2019). Recent studies tend to focus on the variation of the organic layer between sites over the Mackenzie Delta rather than variations within a single catchment, and largely ignore the physical properties as it applies to hydrology and microtopography (Palmer et al., 2012; O'Connor et al., 2020).

According to Mackay (1980), the mineral earth hummocks in this area formed by freeze-thaw cycles at the top and bottom of the active layer, causing upwards and downwards movement – which over the period of many years creates these mineral earth hummocks (Mackay, 1980). The soil structure between hummocks and inter-hummocks has different compositions – primarily in the thickness of organic materials such as peat. The soil profiles over the mineral earth hummocks in many cases lack a layer of peat, whereas in the inter-hummock zones the thickness of the peat can vary (Quinton & Marsh, 1999). Being able to accurately map peat across a catchment is crucial for this study due to the ability of peat to convey both water and heat.

The mineral soil layer is predominately composed of clays and silts with sands and gravels intermittently (Quinton & Marsh, 1999). The mineral earth soil has a low potential for holding water and has a higher thermal conductivity. O'Connor et al., (2020) showed that these mineral soils have a higher thermal conductivity than the different layers of peat, and thus the active layer in these soils thaws at a different rate compared to the peat layers. For frost table depth studies, one could attribute changes in thaw rates to thaw depths and the transition to different layers of soil. One can label these two layers of peat the acrotelm and catotelm (even if the full definition of the catotelm being submerged is not met) – with the acrotelm being the living portion of peat and the catotelm being the thicker dead portion of peat lying underneath of the acrotelm (O'Connor et al., 2020). The transition from acrotelm to catotelm helps to explain the differences in the bulk density and other physical properties mentioned by Quinton & Marsh (1999).

The depth of active layer development differs greatly between the hummock and inter-hummock channels due to the thickness of the peat layer above. Where the peat layer is thicker,

the active layer depths tend to be thinner, and vice versa. Hummock mounds, which have the same composition as the mineral earth soils and have less peat overhead as it protrudes into the peat layer, tend to have deeper active layer depths than their inter-hummock counterparts (Figure 2.1). Active layer depths in these areas range from 0.3 to 0.8 m on average, with deeper depths associated with the hummocks and the shallower depths with the inter-hummocks (Endrizzi et al., 2011; Wilcox et al., 2019).

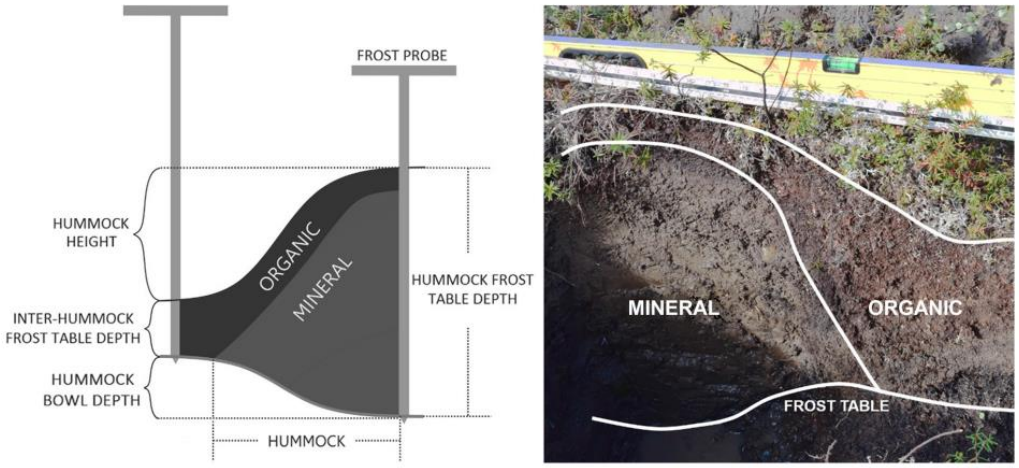

Figure 2.1 Sectional view of a hummock and inter-hummock zone with associated frost table depths. The figure is from Wilcox et al. (2019).

This study focuses on the summer (May to August) of 2021, which was an extremely dry and warm year, being the 7th warmest summer on record and driest July on record for Inuvik, NT (Environment and Climate Change Canada). Temperatures were above 30 °C at multiple points throughout the summer, with the average summer temperature around 11 °C. This is an incredible opportunity to analyze an extremely dry year in the Arctic tundra, a phenomenon that may become more common due to climate change and will act as a validation dataset for further studies seeking to research the drying of the arctic. The objectives of this chapter are twofold:

- To examine differences in active layer depths and peat thicknesses between hummocks and inter-hummocks - they are the primary obstacles groundwater is forced to flow through / around from the hillslopes to the creeks and are the primary driver of thaw spatial variability.
- Attempt to answer if warm and dry conditions represent a risk to permafrost degradation underneath hummocks / inter-hummocks.

2.2 Study Site

Siksik Creek is a sub-catchment of Trail Valley Creek (TVC) and is located approximately 50 km northeast of Inuvik (Figure 2.2). It is roughly 1 km^2 in area, with elevations in the basin ranging from 50 m a s l. to 100 m a s l. and is located within the continuous permafrost zone in the Western Canadian Arctic. The active layer depth typically ranges between 0.4 and 0.8m (Quinton & Marsh, 1999). Underneath the active layer the permafrost layer is estimated to be 100-150 m thick (National Resources Canada, 1995). The Inuvik region is characterized by short, cool summers, and long cold winters with a mean annual air temperature of -9.8°C, and an annual total precipitation of 266 mm (Quinton & Marsh, 1999). This catchment is representative of other catchments found in the uplands to the east of the Mackenzie Delta, and due to its size and location nearby the Trail Valley Creek Research Station, offers a unique ability to observe, record, and study the changes to this northern region.

There are two weather stations in Siksik Creek: the Trail Valley Main Meteorological station (TMM) and Environment Canada's Meteorological Service weather station (MSC). These were installed in 1991 and 1998 respectively. They are roughly 15 metres apart and contain a suite of meteorological equipment to monitor radiation fluxes, rainfall, temperature, humidity, wind, barometric pressure, and turbulent energy fluxes.

Siksik Creek is north of the forest-tundra transition and the vegetation ranges from smaller shrubs dominated by dwarf alder species to larger alder, willow, and birch shrub species that are found near the creek and on the hill slopes (Wilcox et al, 2019). Tussocks are also common within the riparian zone. Most of the surface is dominated by peat, moss, and lichens, as well as mineral and earth hummock terrain.

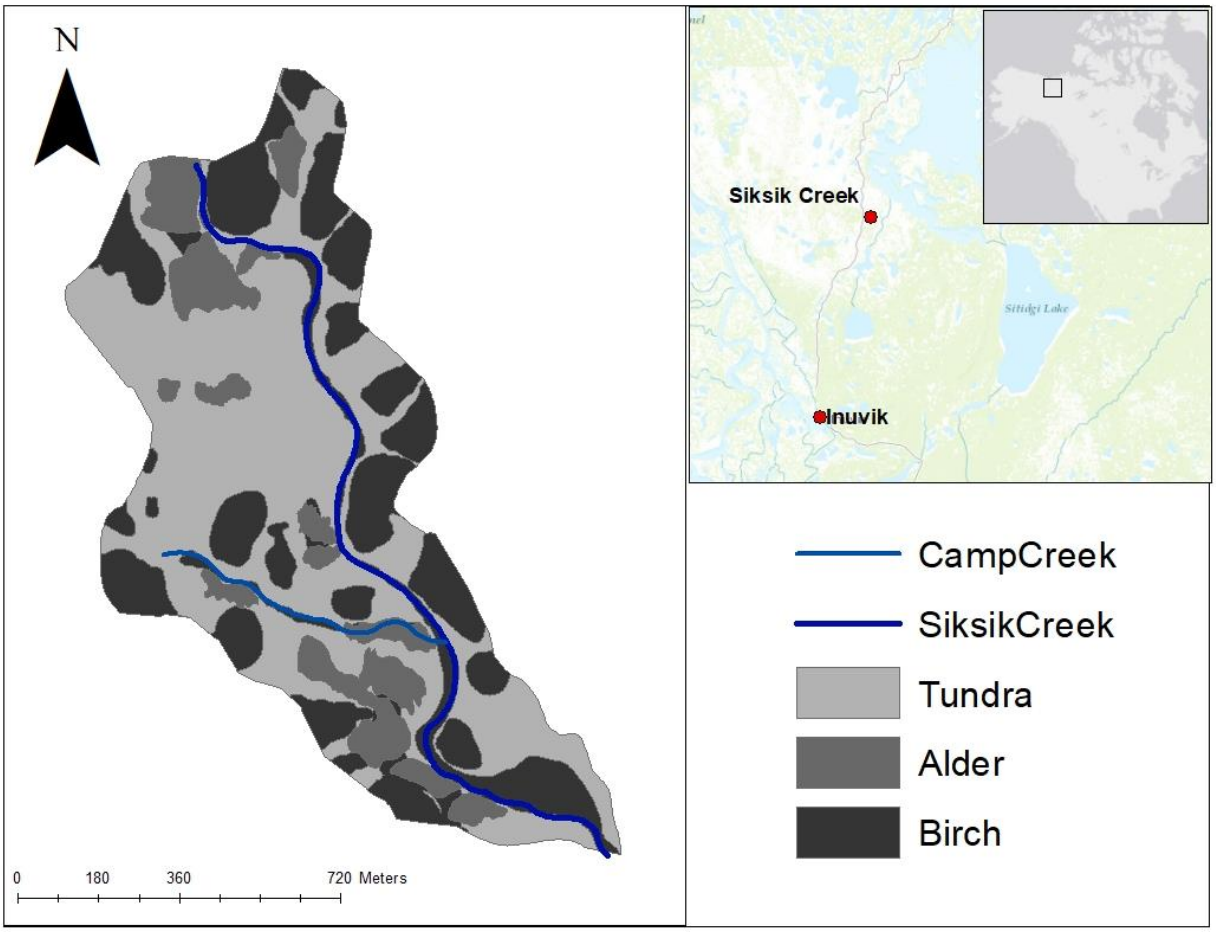

Figure 2.2: Siksik Creek, a 1 km^2 watershed located within Trail Valley Creek. The landscape is composed of tundra which has a variety of mosses, lichens, sedges, and tussocks, taller alder and birch shrub species, and is ubiquitously covered with hummocks.

In the uplands east of the Mackenzie Delta, hummocks and inter-hummock zones dominate the landscape and are incredibly important when examining microtopography and its influence on active layer development and sub-surface flow. The presence of mineral earth hummocks can be differentiated between two areas that are considered to be ubiquitous: that occupied by the hummocks, and an inter-hummock area (Figure 2.1 & Figure 2.3). Groundwater mostly flows through the inter-hummock areas, whereas the hummock areas have much lower hydraulic conductivities (by a magnitude of 3-6 times depending on the depth from the surface), forcing water to flow around them and creating a tortuous drainage network for flow downslope (Quinton & Marsh, 1998; Quinton et al., 2000). The inter-hummock channels have a thick layer of peat overtop of mineral soil and is typically overlaid by moss and lichens. This peat layer can

further be divided into an upper and a lower portion based on its bulk density and other physical properties. Underneath is a mineral earth soil composed predominately of clays and silts.

Previous studies have looked at the thickness of peat within Siksik Creek around the riparian zone with some distinction for the differences between hummock and inter-hummock zones (Quinton & Marsh, 1999; Endrizzi et al., 2011). These studies have also found that the bulk density of the peat layer increased with depth, and thus its physical properties change as well – specifically its thermal and hydraulic conductivities (Quinton & Marsh, 1999). Studies focused on Siksik Creek examined the soil properties for modelling that have been normalized for the whole catchment (Endrizzi et al, 2010; Endrizzi et al, 2011). These studies did not map out the spatial patterns and thickness of soil types outside of the riparian zone, nor did they account for vegetation other than hummock or inter-hummock zones. Rather, these were averaged together into one soil type rather than into several different soil types for the catchment (Quinton & Marsh, 1999).

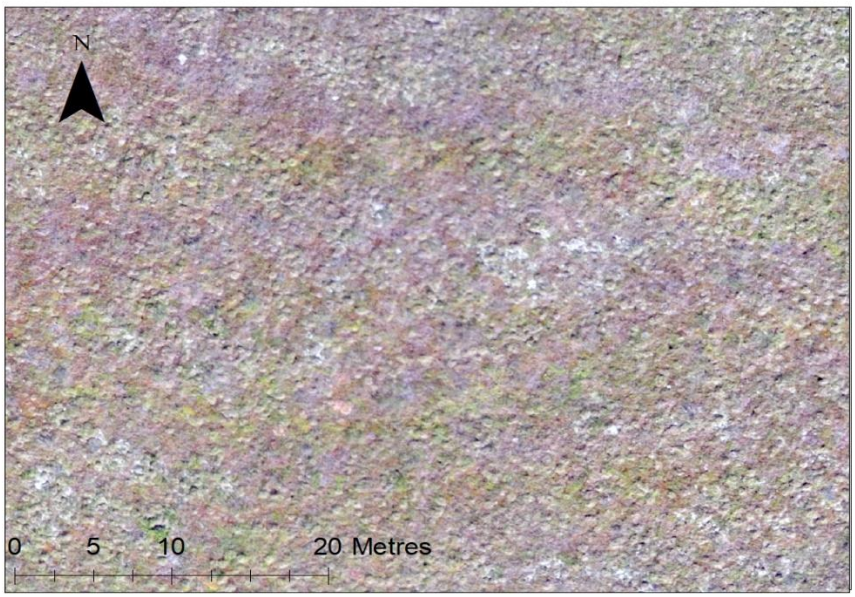

Figure 2.3: An image of a hummock field in Siksik Creek from above (the small mounds throughout the image), taken from UAV imagery over a tundra portion of the catchment..

2.3 Methods

During the summer of 2021 active layer depths were measured to capture the rate of frost table thaw and permafrost table depths across Siksik Creek. Further, coring was conducted to analyze the stratigraphy and spatial distribution of soils and peat in the basin. Further work involved identifying unique landforms such as peat, alder and birch shrub patches, and mosses and lichens. This was done to examine how the variability in the landscape will influence active layer thaw and will be explained in the sub-sections below.

2.3.1 - Active Layer Depths

To accomplish our tasks, 15 transects that ranged in length from 50 m to approximately 200 m were established to measure frost table depths every 5-10 m across Siksik Creek at the beginning of the 2021 summer (Figure 2.4). Three additional transects were added near the head of the catchment at the end of the summer to ensure all transects covered the full extent of the catchment. These measurements were done on a weekly basis beginning on May 25th until August 28th. The beginning and end of each transect were marked with a flag to remain consistent. There were slight variations in the location of these measurements over the season to avoid the compaction of the transect, which could have influenced measurements.

Frost table measurements were done primarily with a metal frost probe and ruler, which marked as deep as 120 cm (Figure 2.4). The general procedure was to push the frost probe into the ground until the frost table was reached, and then with a ruler measure how far from the 120 cm mark the rest of the probe was above the ground; subtracting this value from 120 cm to give the actual depth of the probe into the ground. Early into the thaw season, locating the frost table was identifiable when the frost probe produced a dull thud. However, near the end of the summer, and where frost table depths had dropped below the transition from peat to mineral soil – which was also a barrier to inserting the frost probe – a sledgehammer was used to ensure that the frost probe reached the frost table.

There was a heavy emphasis throughout this study on hummocks and inter-hummocks, and these measurements were defined as being in a hummocks or inter-hummock zone. As seen in figure 2.1 however, there can be a large degree of latitude in measurements when measuring around hummocks as these depths can be vastly different even in an area as small as 30-40 cm. To ensure that the measurements that were taken in hummocks or inter-hummock zones were

representative, care was taken to ensure that the frost probe was inserted into roughly the middle of each feature.

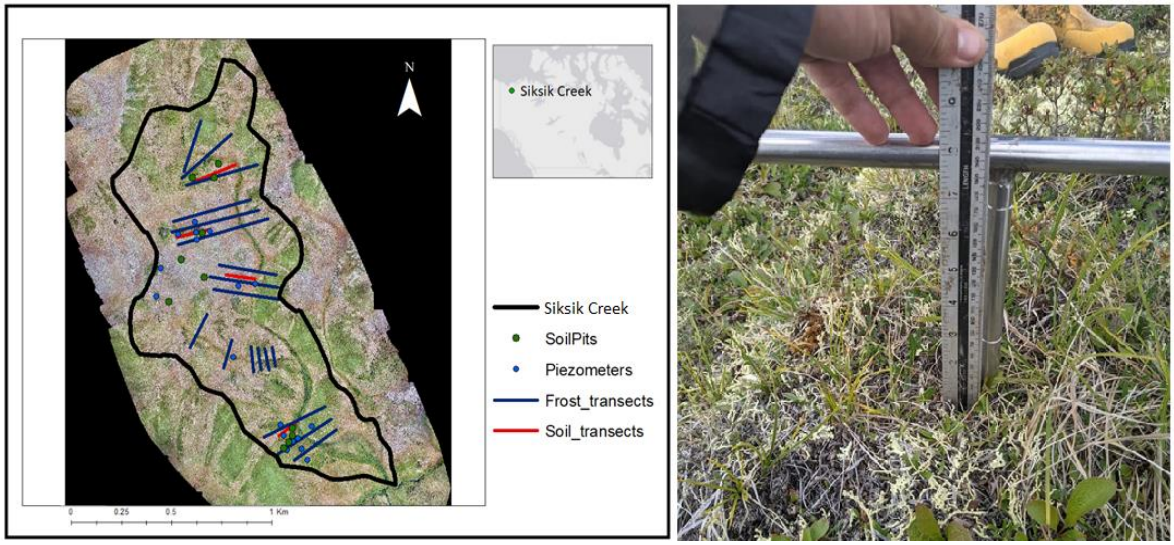

Figure 2.4: A map showing the location of the frost probing transects, soil pits and piezometer installation locations on the left, with the frost probe and ruler technique on the right.

2.3.2 – Soil Stratigraphy and Spatial Variability

There were three primary methods used to record soil stratigraphy and variability with respect to overburden and the vegetation that lay over top: coring, soil pits, and drill hole measurements taken along transects. Soil cores were collected from June of 2021 until the end of the field campaign on August 28th. An ABS Drill Max with a coring extension, which was 2” in diameter, was used to drill through the frost table and into the permafrost (Figure 2.5). There were 19 cores that were drilled and recorded. Typically, the depth to the permafrost throughout the summer ranged from 60 cm to just over 1 m, which was dependent on the soil properties and ice content. In some cases, reaching the permafrost was abrupt and produced a solid lens of ice. Coring stopped once the permafrost table was reached to save the drill bit from wear and tear, and as it met the requirements needed for the study necessary for the modelling efforts.

Figure 2.5: A photo of the coring extension used by the drill on the left, as well as how the cores were laid out in the field to be recorded.

There were 11 soil pits were dug in the second last week of the field campaign in order to capture differences in vegetation, elevation, position, and/or topography, from August 11th to the 18th, as the active layer thickness is at its maximum by the end of the summer season (Figure 2.6). The soil pits were measured length wise and at every 10 cm across the depth of the pit. The depths of transitions in vegetation, soil, and temperature were recorded at each point (Figure 2.6). For the overlying vegetation, the locations were chosen based on the transition from a decently sized patch of moss to a patch of lichen. This was based on a hypothesis formed during the summer that hummocks and inter-hummocks may correspond to the overlying vegetation. The modelling of flow through inter-hummock channels by Quinton et al. (2008) suggested that the hummocks typically lay at the ground surface or just below it, however, they did not correspond these features with the overlying vegetation.

Figure 2.6: A soil pit in the Siksik Creek catchment showing how soil depths and temperature were measured. To note, an inter-hummock zone marked by the redder mosses is surrounded by the lighter lichens, which happened to lay over top of the hummocks.

There were four soil transects across the catchment that were measured in the last week of the summer from August 11th to August 18th; three started from the edge of the creek and worked their way upslope away from the creek (Figure 2.4). This followed a similar study by Quinton et al. (1999) that examined the relationship of peat thickness regarding distance from the creek. These transects used the ABS drill and a drill bit to determine the different thicknesses of soil layers in each drilled hole. This was done by physically looking into the drilled hole and using a ruler to measure from the ground surface (Figure 2.7). This included a distinction of the overlying vegetation, the different components of the peat, as well as the depth of the mineral soil and the frost table. Their length ranged between 50 m and 100 m, with measurements taken every 3-5 m.

Figure 2.7: A soil transect example: drilled hole shown in the middle that shows a change in colour delineating the peat and mineral soil boundary.

2.4 Results

2.4.1 - The Dry Summer of 2021

The summer of 2021 was an exceptionally dry year for Siksik Creek and the Inuvik area. Using observations from TMM, maximum daily temperatures in the catchment passed 30°C several days throughout the summer, with an average temperature of 14.4°C in July; 4°C warmer than the average in camp for the summer months, and the 3rd warmest July recorded (Figure 2.9). Summer total precipitation was only 6 mm for the month of July, making it the driest July on record, and the third driest summer overall (Figure 2.8). Summer total rainfall recorded at TMM was also some of the lowest recorded at 64.7mm for the entirety of the summer, which is barely over half of the long-term average of 120mm (Figure 2.8). End of winter snow surveys for 2021 showed that the basin had only 75 mm of snow water equivalent (SWE) across the basin, half of the yearly average of 150 mm (Figure 2.10).

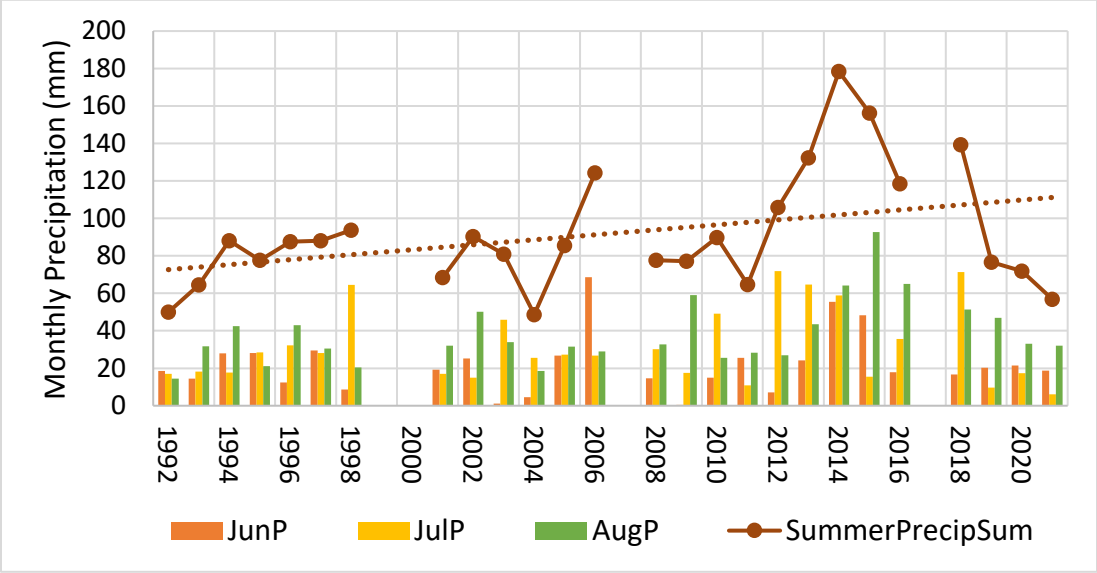

Figure 2.8: Monthly Precipitation for June / July / August from TMM observations.

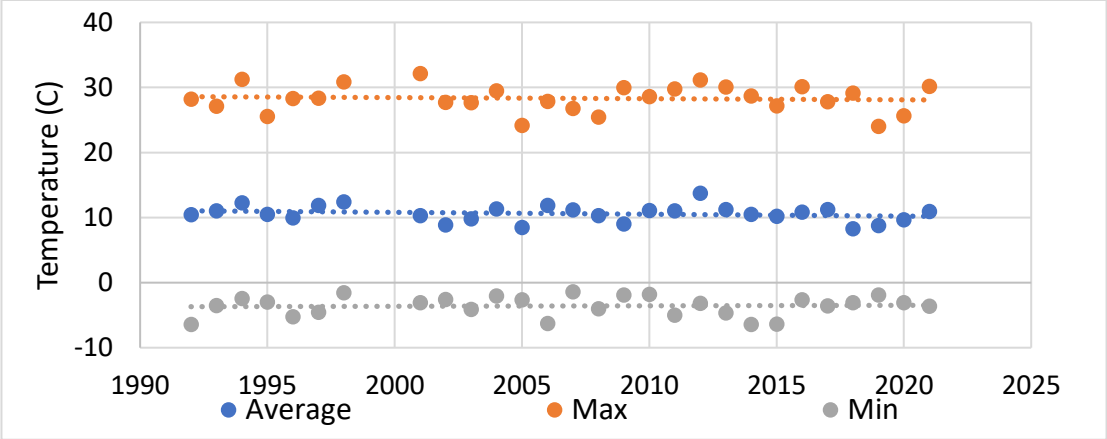

Figure 2.9: Averaged mean, minimum, and maximum summer temperatures from the TMM station.

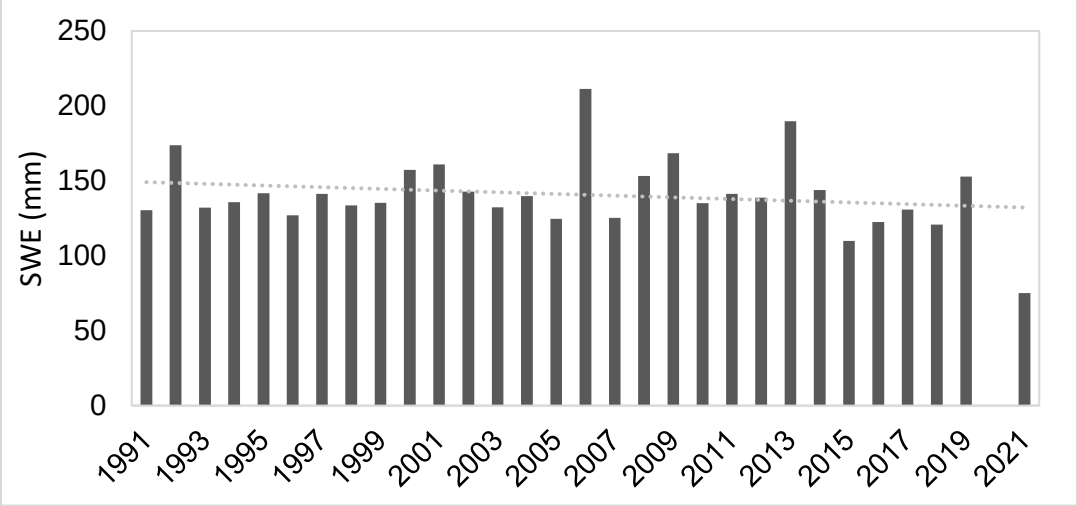

Figure 2.10: End of winter snow water equivalent for Siksik creek. No Data was collected in 2020 because of Covid-19.

2.4.2 - Peat Thicknesses & Active Layer Depths

Previous studies on peat depth variability in permafrost regions have shown that peat thicknesses can be highly variable spatially (Wilcox et al., 2019; Quinton et al.,2000). In Siksik Creek, there are a variety of topographical landforms that can influence this, including shrubs and trees, mosses, lichens, and hummocks/inter-hummocks. In the open tundra, which is dominated by mosses and lichens, a possible relationship between mosses, lichens, and peat thicknesses will be explored. To test this hypothesis, four peat transects were drilled across Siksik Creek, where acrotelm and catotelm thicknesses were recorded under both mosses and lichens, as well as the depth to the frost table. The acrotelm being the living portion of peat and the catotelm being the thicker dead portion of peat lying underneath of the acrotelm (O'Connor

et al., 2020). In total there were 124 samples in mossy locations, and 65 samples within lichen (Figure 2.11). It was found that for both acrotelm and catotelm, their thickness was deeper where mosses were found, and shallower where lichens were found. The average catotelm and acrotelm thicknesses underneath mosses were 27 cm and 11 cm; and for lichens 16 cm and 6 cm respectively. These values were consistent across the basin and the average peat thickness under mosses were 38 cm and 22 cm under lichens.

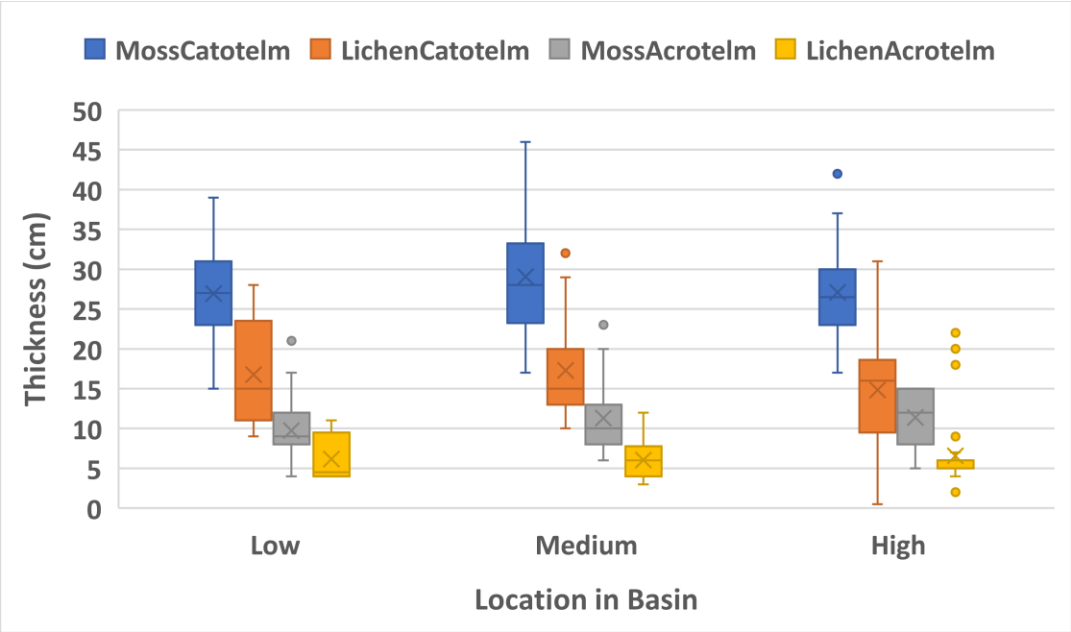

Figure 2.11: A comparison of catotelm and acrotelm thicknesses with either moss or lichen cover, separated by relative elevation in the basin.

End of summer frost table depths separated by lichens and mosses were also recorded. Taken from the last week of the summer (August 28th), the frost table depths for each series of transects were separated by moss or lichen coverage above the measurements (Figure 2.12). There were 131 and 125 observations for mosses and lichens respectively. Overall, the depth to the frost table underneath of mosses was much shallower than underneath of lichens across the entirety of the basin with the average around 36 cm. For lichens, the depths were much deeper and were typically around 60 cm. In some places this was much deeper, and it was noted that many of the deeper depths tended to be on the south-facing slopes underneath of lichens.

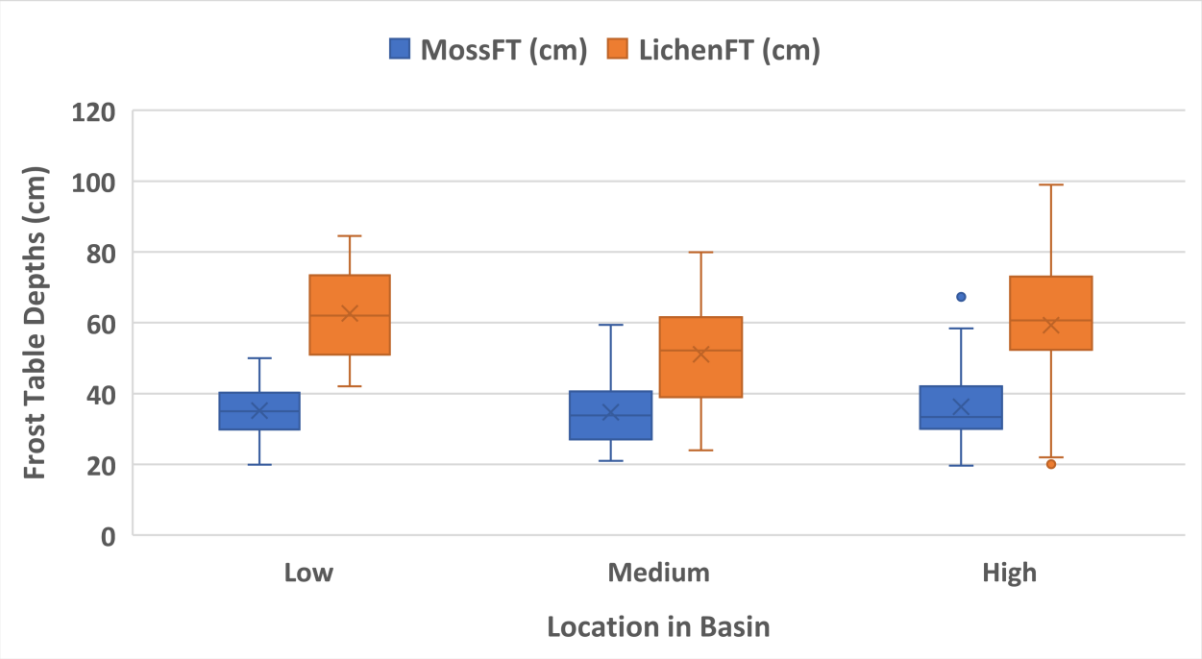

Figure 2.12: End of summer frost table depths separated by lichens and mosses and by location in the basin.

Throughout the summer there were 15 transects within Siksik Creek where active layer depths were continuously measured on a weekly basis; by the end of the summer there were 18 transects, as mentioned in Section 2.3.1. When compiling this data and separating it by elevation in the basin (i.e.., high, middle, and low elevation), and whether it was located in a hummock or inter-hummock zone, there was a distinct pattern: a separation in end of summer thaw depths between hummocks and inter-hummocks, as shown in Figure 2.13.

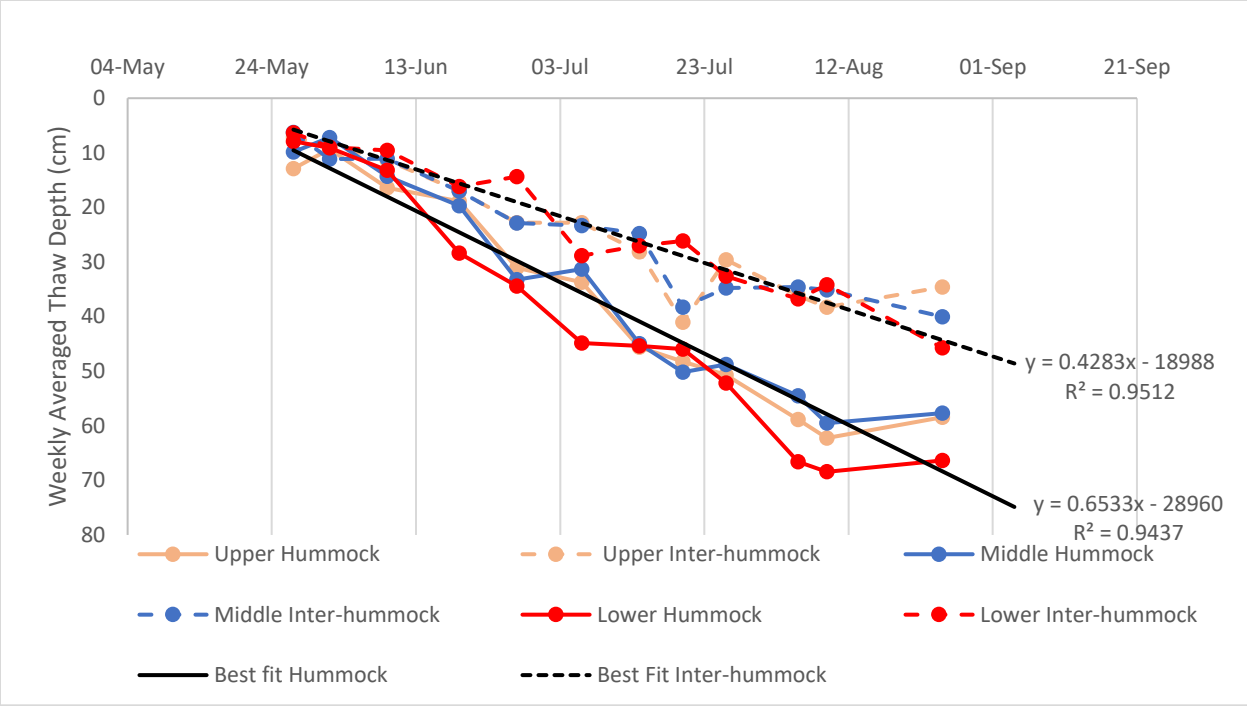

Figure 2.13: End of summer active layer thaw depths separated by location and elevation with a distinction between hummock features in the solid lines, and inter-hummock features with the dashed lines.

Nine soil pits were dug at the end of the summer that went across a hummock mound and an inter-hummock zone. Measurements confirmed that hummocks had deeper thaw depths than their inter-hummock counter parts. However, with the soil pits, it was also possible to distinctly measure peat thicknesses and frost table depths. The peat layer was broken into its catotelm and acrotelm components. The relationship between frost table depths and hummocks/inter-hummocks can also be broken down further based on the volume of peat found in each sample. A relationship between lichens and mosses and inter-hummocks was found, as shown in Figure 2.14.

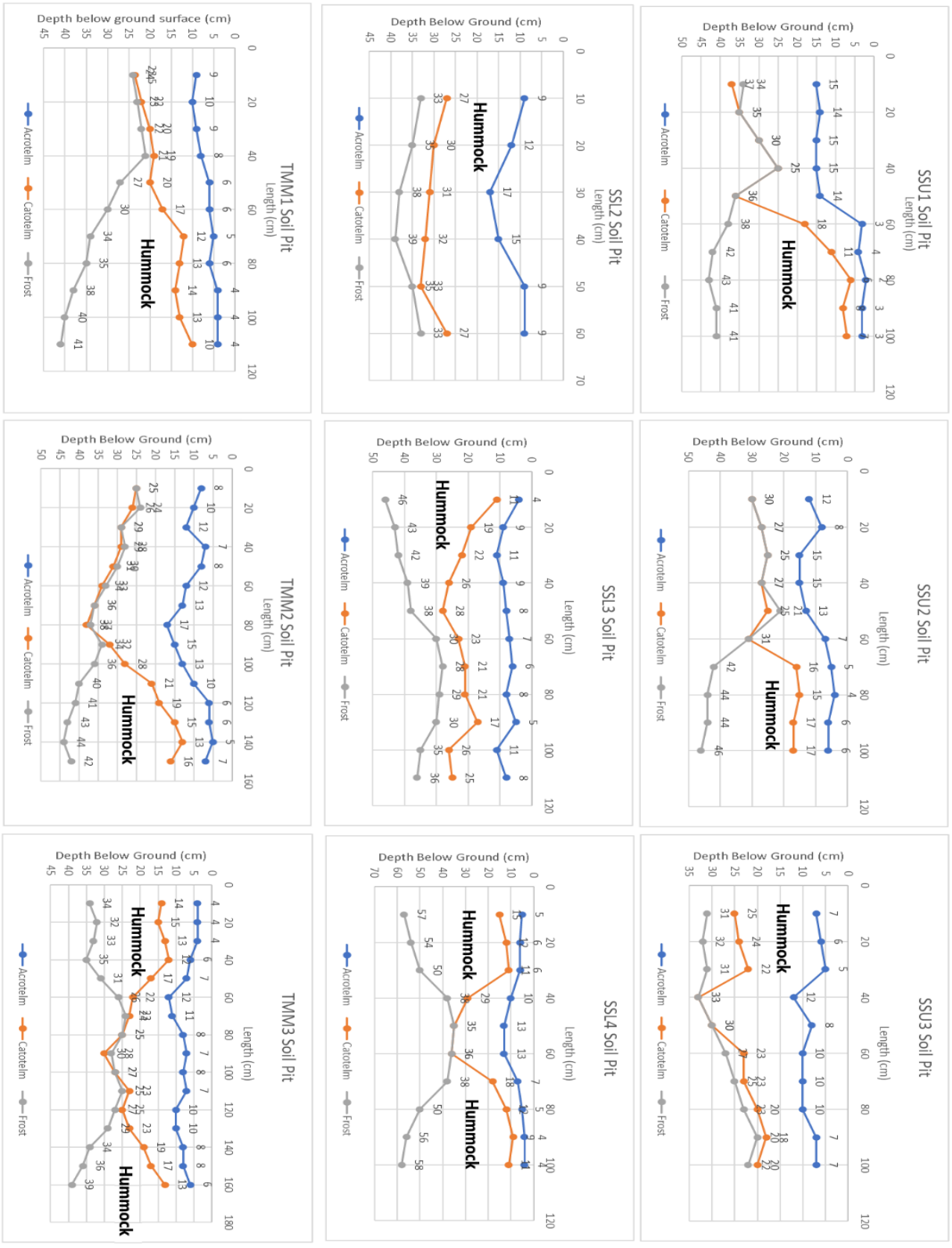

Figure 2.14: Measurements from nine soil pits showing that the depth of the acrotelm (blue), the catoltelm (orange), and frost table (grey). Where the hummocks exist there is a distinct thinning of the peat and a thickening of the frost table.

Lichens were mostly found to be overtop of hummocks, and mosses were primarily found in the inter-hummock zones. Collected data shows there is a disproportionate separation of mosses and lichens between hummocks and inter-hummocks. For the mosses there were 210 measurements in mossy materials - 176 were in moss covered terrain over identifiable inter-hummock materials, and 34 measurements had moss over hummocks. For lichen materials there were 166 measurements - 123 were found over hummocks and 43 samples over inter-hummock zones. From this we can establish a null hypothesis where we assume that mosses are not correlated with inter-hummocks, and lichens are not correlated with hummocks; our true hypothesis being the opposite. A Chi-square test was then calculated to reject the null hypothesis. The values and results, seen in Table 2.1 below, gives a p-value of 1.24E-28 and a chi-square value of 123.2. Thus, we can reject the null hypothesis.

Table 2.1: Chi-Square Test and p-value for the correlation of lichens, mosses, hummocks, and inter-hummocks

Observed				Expected		((o-e)^2)/e	
	Inter-hum	Hummock	Sum	Inter-hum	Hummock	Inter-hum	Hummock
Moss	174	36	210	121	89	23	31
Lichen	43	123	166	96	70	29	40
Sum	217	159	376				
Chi-sq	123.232						
DF	1						
CV	3.841459						
P	1.24E-28						

2.4.3 – Depths to Permafrost

The aim for collecting cores over the summer was three-fold: first, to learn about the surficial geology of the catchment; to determine the depth to permafrost throughout the catchment; and to install piezometers in the holes created by coring. There were 18 cores taken throughout the catchment, and their locations can be seen in Figure 2.4. Of these 18 cores, 13 reached the ice-rich permafrost that is typical of this area, as shown in Figure 2.15, where the core is rich in ice and the rest a mix of mineral soil and peat.

Figure 2.15: Ice-rich permafrost core taken from SSL-6 taken near the end of June of 2021.

The depths to permafrost from these 13 cores are shown in Table 2.2. The average depth to permafrost across these sites was 64.6 cm. Sampling was done to adequately cover the different landforms and vegetation in the basin. This included hummock, inter-hummocks, as well as below and around tall shrubs, within shorter shrub patches, and within Siksik Creek and Camp Creek. Some cores did not reach the permafrost table likely due to the cores being sampled in the stream bed or hummocky areas, where the highest thaw depths were typically observed (Endrizzi et al., 2011). In Table 2.2, the acronyms SSL, SSM, CC, SHR, and SSC stand for Siksik Lower, Siksik Middle, Camp Creek, Shrub, and Siksik Creek.

Table 2.2: Permafrost and Peat Depths for 18 cores throughout Siksik Creek. SSl, SSM, CC, SHR, and SSC stand for Siksik Lower, Siksik Middle, Camp Creek, Shrub, and Siksik Creek.

Core Site	Permafrost Depth (cm)	Peat Thickness (cm)	Landform
SSL-1	72	35	Inter-hummock
SSL-2	85	30	Inter-hummock
SSL-3	77	10	Hummock
SSL-4	50	70	Riparian / inter-hummock
SSL-5	NA	65	Riparian
SSL-6	55	30	Inter-hummock
SSL-7	55	45	Inter-hummock
SSL-8	NA	5	North-face slope
SSL-9	NA	37	North-face slope
SSM-1	84	18	Hummock
SSM-2	45	15	Inter-hummock
CC	61	41	Creek
SHR-1	62	16	Inter-hummock
SHR-2	43	12	Inter-hummock
SHR-3	90	67	Shrub
SHR-4	62	19	Inter-hummock
SHR-5	NA	39	Hummock
SSC-1	NA	66+	Creek

Core samples have shown that the thickness of peat varies throughout the catchment (Table 2.2). The core taken in Siksik Creek (SSC-1) was mostly peat, even with the sample being 70 cm in length, whereas SSL-3, and the cores taken in the middle of the catchment only had around 10-15 cm of organic material.

2.5 Discussion

The cornerstone of this chapter is the linking of mosses and lichens to inter-hummocks and hummock zones. It was discovered that underneath lichens, mineral earth hummocks were present along with soils composed of primarily clays and silts. The mosses were typically present in the inter-hummock zones composed primarily of peat. The presence of hummocks will have an influence on groundwater flow in the catchment and will impact active layer development. As Endrizzi et al. (2011) noted, the spatial variability of the depth of thaw is dominated by microtopography, as these hummock mounds control the distribution of soil moisture by creating a tortuous subsurface flow pattern, which is also reflected in thaw.

However, both Endrizzi and Marsh (2010) and the Endrizzi et al. (2011) studies that looked at active layer thaw within Siksik Creek used simplified versions of the catchment in conjunction with the hydrological model GEOtop to model end of summer thaw depths. They found that when lateral movement of water was turned off in the model, the spatial variability of peat was the primary influence on active layer thaw. This coincides with other studies showing the effectiveness of peat as an insulator (James et al., 1996; O'Connor et al., 2020). Its efficacy as an insulator is not always constant and depends on the amount of moisture content the peat contains (Farouki, 1981; Oke 1987). When the peat is dry it has relatively low thermal conductivities, and when it becomes wet this conductivity can drastically increase (Farouki, 1981; Oke, 1987). The first half of this statement is pertinent within the context of this study, where the summer of 2021 in a peat dominated Arctic catchment was extremely dry, where conditions at the beginning of the summer with the lack of snowmelt as well as the persistent lack of precipitation throughout the summer giving the catchment very little moisture. Due to this, the singular property of peat where its thermal conductivity decreases with decreasing soil moisture leading to the reduced conduction of heat vertically and laterally is important. In locations with a thicker peat layer we should expect that active layer thaw depths would be shallower than normal.

With the data collected over the summer of 2021, measured results show that the presence of peat affected the end of summer thaw depths (Figures 2.13). Results by Endrizzi et al. (2011) showed that the end of summer thaw depths (mid-September), with some spatial variability, ranged from 60 to 70 cm in depth in a relatively uniform layer of peat. The physically

measured active layer depths in Siksik Creek for the summer of 2021 showed roughly the same values, with a distinct separation between different soils and vegetation cover. Specifically, when separated into hummock and inter-hummock classifications, average physical measurements showed an end of August thaw depth between 30 and 40 cm for the inter-hummock zones, a decrease of 30 cm compared to Endrizzi et al. (2011), and depths that reached 70 cm on average for the hummocks. While this distinct difference of ground thaw between hummocks and inter-hummocks is not new (Wilcox et al., 2019), the conditions within which these were measured present a potential for different results. Further, it was expected based on previous literature (Endrizzi et al., 2011; Atchley, 2016; O'Connor et al., 2020) that active layer thaw would have an inverse relationship with peat thickness – where the thicker the layer of peat, the shallower the thaw. This holds true except for in the creeks where there is a thick layer of peat and yet even deeper ground thaw. This likely has to do with the constant flow of water both above and below the surface, and therefore the flow of heat as well.

Studies in similar areas, such as the Alaskan north slope (Walker et al., 2003), and even previous studies in Siksik Creek (Endrizzi et al., 2011; Wilcox et al., 2019; Grunberg et al., 2020) give us a few data sets to compare our measured active layer depths to. Walker et al. (2003) separated their measurements along the north slope in Alaska into three different zones based on NDVI maps. Siksik Creek, which is mostly open tundra with some larger shrubs, best fits into their subzone D classification. Their active layer thaw measurements were taken over the course of three years and were typically measured in August. Their average active layer thaw depth in this zone was 55 cm. Grunberg et al., (2020), in comparison measured active layer thicknesses across two years in Siksik Creek and analyzed how vegetation cover related to active layer thicknesses. This study specifically separated active layer thaw depths into six categories: underneath lichen, tussock, dwarf shrub, tall shrub, riparian shrub, and trees. They found that underneath of lichens active layer depths reached as deep as 90+ cm, with an average of 75 cm. Tussocks on the other hand had thaw depths reach 60 cm but had an average of 47 cm. Dwarf shrubs were slightly deeper with an average of 63 cm, and tall shrubs were similar to tussocks. The Endrizzi et al. (2011) study found that the average active layer depths in the catchment in early September were around the 40 cm mark.

Compared to the Grunberg et al., (2020), and Walker et al., (2003) studies, the measurements of active layer thaw during the summer of 2021 was significantly shallower. While Walker et al. (2003) is only approximately similar, there is a difference of nearly 20 cm of thaw depth in the open tundra areas. The Grunberg study on the other hand, assuming lichens are equivalent to the measurements in hummock areas and tussocks to inter-hummocks, is slightly closer. We still see a difference of ~10 cm for the inter-hummock zones, and 5 cm for the hummocks, but this is much more reflective of past conditions for the catchment. The Endrizzi et al., (2011) study had results similar to what was physically observed in our study, within 5 – 10 cm. However, they averaged together hummocks and inter-hummocks, and because of this should have on average deeper depths.

Of the 18 cores drilled in the catchment, five cores did not reach the permafrost layer. These were either located in hummocks or along the creek. Of the permafrost depths that were collected, they were primarily from inter-hummock, peat dominated areas. Unfortunately, while more drilling was planned for underneath of hummocks, part of the coring extension broke before this could be done and so the data underneath of these features is limited. From these cores, the average depth to permafrost from these cores was around 64 cm. This is a depth that is typically deeper than the depths that the peat normally reaches, where these depths across soil pits, cores, and transects were typically 30-40 cm deep in the inter-hummock zones. It should not come as much surprise that the permafrost was able to be recorded largely only where peat was located with the tools that were used to reach it. The average depth to permafrost across the inter-hummock cores (there were 9 cores) was 58.8 cm. Through measurements taken across the catchment, it was found that the top of the permafrost was variable and reflects the surrounding topography and vegetation (James et al., 1996).

The shallowest depth to permafrost recorded was 43 cm around a shrub patch, and the deepest depth to permafrost at 85 cm in the lower portions of the creek close to the riparian zone. Based on the core measurements and linear equation from Figure 2.15, and assuming a linear rate of thaw, estimates suggest that active layer could thaw to the average permafrost depth by October 1st. However, at this time air temperature within the basin would have begun to cool down during the autumn months. Previous literature suggests active layer thaw should still occur in inter-hummock zones in dry conditions even though its thermal conductivity decreases with

decreasing soil moisture, even later into these months – and even implies that the thinning of the active layer may be possible (Walker et al., 2003; O'Connor et al., 2020).

Given that thermal conductivities of the mineral earth soils associated with hummocks is higher than in peat, there does exist the possibility for thaw to be much deeper than usual in these locations. Walker et al. (2003) found that mineral soils like what exists in Siksik Creek could follow this. The deepest depth to permafrost recorded in the catchment during the summer of 2021 was 90 cm, even though this was not underneath a hummock. If we use this as a basis for potential depths to permafrost underneath hummocks, the linear relation suggests that this depth of thaw could be reached by September 27th. This date is within reason, as air temperatures were still positive at this time, but the rate of thaw would have drastically decreased by this point. If we consider the two data points collected underneath hummocks, with depths to permafrost of 77 cm, and 84cm this timing seems much more plausible. The potential for thaw underneath hummocks reaching into the permafrost layer exists. However, without the use of modelling to fill in the lack of data underneath hummocks, this cannot be answered any further than it already has as this study doesn't have enough measurements to make a statistical analysis of this.

2.6 Conclusions

This study found that hummocks and inter-hummocks seem to be statistically linked to lichens and mosses within Siksik Creek. This allowed measurements to be made in inter-hummocks and hummock zones even when these features were not readily apparent from the surface and has implications for the mapping of these features. Further, as the summer was on record as one of the driest, there was very little moisture available in the system, which affected the thawing of the active layer. Measurements of active layer depth where peat was found in the catchment were more shallow than previous studies by as much as 20 cm. This means that underneath mosses and inter-hummocks it is highly unlikely that thaw in the basin reached permafrost in these areas. It is possible however that underneath of hummocks, where mineral earth soil dominates the sub-surface, that thaw in the basin could thaw into permafrost; however, not enough information was gathered for permafrost underneath of hummocks to conclusively predict this. This study infers that the thinning of the active layer during a dry summer is possible on a local scale, and where the potential for thaw to be deeper underneath of hummocks exists as well.

Chapter 3

The Role of Microtopography, Shrubs, and Snow on Ground Thaw and Hydrology

3.1 Introduction

The use of numerical models is an invaluable tool in northern hydrological research due to the complexity of processes, in addition to the scarcity of long-term research stations in the Canadian Arctic (Tetzlaff et al., 2017). Several cyrohydrogeological models have been developed to include cold region processes, such as GEOtop (Rigon et al., 2006; Endrizzi et al., 2014), or the Advanced Terrestrial Simulator (Ahmad et al., 2020), and some are even receiving additions to properly model permafrost regions such as Hydrogeosphere (Lemieux et al., 2008). There are a variety of processes that need to be considered when modelling in cold regions, which range from surface energy balances, to snow dynamics and insulation, including processes in the ground with regards to groundwater flow as well as active layer dynamics, etc. Bui et al., (2020) gave as many as 11 processes that should be considered, and of the models that were compared only three contained the ability to simulate all of these processes: ATS, CryoGrid3, and GEOtop (Bui et al., 2020). Of these three, the authors note that only GEOtop was found to be suitable for small-scale catchments (Bui et al., 2020). This was reaffirmed by a similar study by Lamontagne-Halle et al. (2020) where GEOtop and ATS were the top two choices for modelling in cold regions, but where GEOtop had the advantage for smaller scale features, such as microtopography (Lamontagne-Halle et al., 2020).

GEOtop (V2.1) can calculate in 3D the exchange of various fluxes, including heat and water, at small scale grids that range in size from metres to tens of metres. GEOtop can also compute surface energy balances in both snow-covered, and snow-free terrain. A blowing snow module based on Pomeroy et al., (1993) is used to redistribute snowfall throughout the domain to accurately represent the distribution of snow in Arctic catchments typical of the Mackenzie uplands – specifically snow build up in drifts along north facing slopes and in taller shrub patches. Within this context, GEOtop is also capable of representing vegetation and its influence on snow and snowmelt with a module that represents turbulent fluxes in vegetated terrain (Endrizzi et al., 2010). Further, the coupled water and heat transport equations allow

consideration of active layer and frost table depths throughout the summer seasons. This makes GEOtop a very useful tool for this study that will focus on active layer thaw, which includes a heavy focus on hummock and inter-hummock terrain, as well as snow-and-shrub patches, where these features are typically around 1 m in areal extent. Because of these reasons, GEOtop is the numerical model that was chosen for this study.

The discretization of initial conditions, use of saturated states, and simplified boundary conditions over heterogeneous terrain can produce large uncertainties in numerical modelling. (Ajami et al., 2015; Way & Lewkowicz, 2017; O'Connor et al., 2020). Initializing these parameters across a basin relies on many assumptions and estimations. As an example, the use of saturated states and boundary conditions tend to be simplified from what would be expected in nature and can lead to results that could be unrealistic (McKenzie & Voss, 2013). For Siksik Creek many of these parameters have been previously measured in past studies, such as peat thicknesses, calculations of thermal and hydraulic conductivities, and even water balance studies that have looked at many of the components necessary for model initialization such as stream flow, soil moisture contents and SWE. Despite these previous studies, there will still be estimations needed for modelling in Siksik Creek and issues with scaling. However, some of this is mitigated due to the small size of the catchment, as it is easier to physically measure these variables across the whole basin which can allow for a much denser dataset with higher spatial and temporal resolutions, rare for catchments this far north (Way & Lewkowicz, 2017).

In past studies, coarse resolution data were only available for modelling in Arctic regions, and thus made it difficult to validate against field observations (Zhang et al., 2012). Where finer resolutions were considered, most still chose to ignore topographical influences, especially regarding the impacts that these may have on the ground receiving solar radiation (Zhang et al., 2012). Given that GEOtop can use discretized maps as part of the initialization process, its design and initialization process can reduce some of the uncertainties addressed by Ajami et al. (2015).

Advances in UAV technology and photogrammetry have allowed for higher imagery resolutions than with any current publicly available satellite imagery. For example, Sentinel-2 satellite imagery has a spatial resolution of 10 m, whereas UAV imagery can produce accurate local spatial resolutions on the scale of several centimetres. Using UAV technology at this scale

will help to improve the mapping of microtopography, and to map hydrological variables when combined with GEOtop. Most modelling studies deal with microtopography by having an assimilation of processes averaged over larger resolutions (Endrizzi et al., 2011; McKenzie & Voss, 2013). UAV imagery will be used in this study to map the catchment at a hyper-resolution to allow GEOtop to better model the highly variable terrain (such as patches of lichen, mosses, and hummocks) in Siksik Creek.

GEOtop has been utilized in the past by Endrizzi et al (2011), and Endrizzi & Marsh (2010) to simulate different permafrost processes in a 3D manner for the entirety of Siksik Creek, which itself is built upon the work of Quinton et al., (1999; 2000). Endrizzi et al. (2011) and Endrizzi & Marsh (2010) modelled processes controlling active layer development across the Siksik Creek domain using an earlier version of GEOtop (v 0.9375). In these studies, GEOtop was run for the entirety of the summer months in 1993 and was able to output specific heat fluxes, water table depths, and active layer depths across the catchment at the end of the summer. The authors were able to isolate specific processes such as lateral subsurface flow, flow in only partially frozen soil, uniform and variable ground heat fluxes, as well as uniform and variable thermal conductivities to assess their impact on active layer thaw depths. There was only a focus on analyzing the topographical influences on these processes and did not include snow or vegetation in any capacity. This thesis will expand upon their modelling approach to include snow, vegetation, and microtopography, previously excluded while using more recent and higher resolution data. The science objectives of this chapter are twofold:

- To simulate hummocks and inter-hummocks as well as snow and vegetation to properly establish if GEOtop, a high resolution, physics-based model, can capture these observed changes.
- To assess the differences that each of these when added to the model affect active layer thaw, water table depths, and the hydrology of the catchment during a dry summer.

3.2 Study Site

This study examines Siksik Creek, a small sub-catchment found within Trail Valley Creek and is home to the Trail Valley Creek Research Station. Siksik Creek can be found approximately 50 km northeast of Inuvik, NT, and it lies ~2 km to the east of the Inuvik to Tuktoyaktuk highway. The catchment itself is roughly 1 km^2 in size and represents topographical features that are common to this region. Siksik Creek is north of the forest-tundra transition, with vegetation ranging in sizes from mosses and lichens to smaller shrubs like dwarf alder, to larger alder, willow, and birch shrub species found near the creek and on the hillslopes (Wilcox et al., 2019). Most of the surface is dominated by peat, moss, and lichens, as well as mineral and earth hummock terrain. The peat rests overtop of a mineral earth soil that is composed of silt and clays. The basin is within the continuous permafrost zone and spatially variable permafrost does exist ubiquitously throughout the catchment reaching depths of up to 150 m below the surface. The annual freeze-thaw cycle that the region experiences mean that much of the ground close to the surface has undergone cryogenic frost heaving processes, which has left the basin covered nearly ubiquitously in topographical features called hummocks, which are composed of small mounds < 1 m of this mineral earth soil; inter-hummock zones surround these and are typically composed of thicker layers of peat. Long, cold winters, and short, cool summers means that this region has an annual average air temperature of -8.2 °C, and is arid in nature with typically only 241 mm of precipitation for the whole year at the main meteorological station (TMM).

Siksik Creek is a smaller catchment, but it is well representative of the kind of landscapes that exist to the east of the Mackenzie River in its upland area. This stretches from North of Inuvik all the way to Tuktoyaktuk and the coastal plains there. It is also similar to other landscapes in Alaska, specifically the north slope, and to other regions in Siberia. This is due to this site largely being north of the tree line, where most of the landscape is tundra. Sedges tussocks, and hummocks dominate the surface vegetation along with mosses and lichens. Shrubs are largely confined to the stream channels and hillslopes. Lastly, these streams are largely characterized by snowmelt and freshet, and are most often ephemeral in nature.

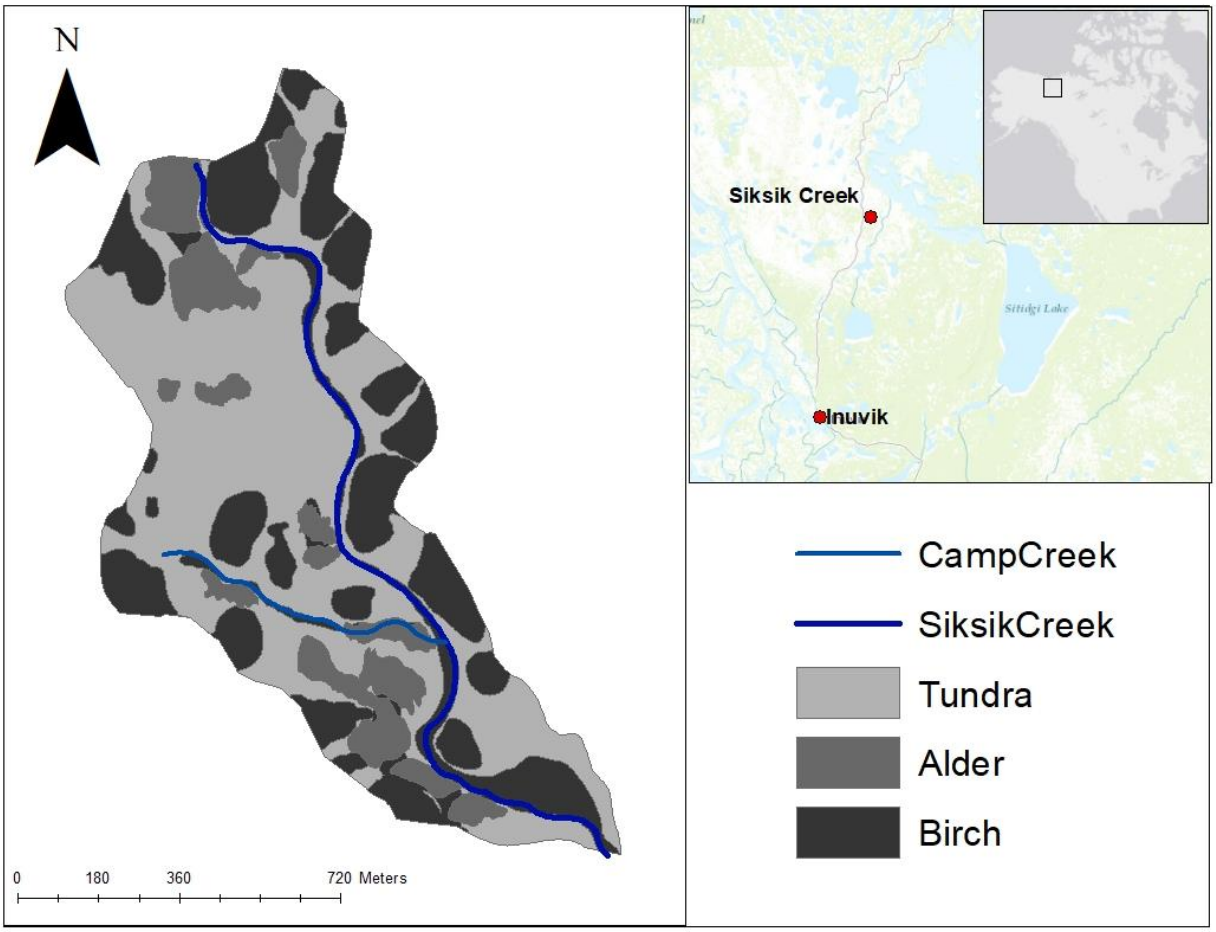

Figure 3.1: Siksik Creek, a 1 km^2 watershed located within Trail Valley Creek. The catchment is largely open tundra, with the occasion alder and birch shrub species on the hillslopes and within the creeks.

3.3 Methods

The following sub-sections describe the various data and the methods that went into calculating and measuring these values that were input into GEOtop. This data was used to simulate a 1-soil simulation based off of Endrizzi et al., 2011, as well as a 2-soil simulation that specifically discretized hummocks and inter-hummocks (seen in section 3.3.3); as well as simulations that covered the addition of shrubs and snow both individually and together to build a more complete simulation of Siksik Creek. Understanding the importance shrubs, active layer thaw, and snow have on the basin hydrology under dry conditions is necessary to understanding the changes that we may begin to expect to see as the Arctic warms. Five simulations were run in Siksik Creek, where the 2-soil domain was used as the base for each except for one which was the 1-soil domain simulation. The four simulations were: shrubs with no snow, snow with no

shrubs, neither snow and shrubs, and finally a simulation where both were included. These results were then compared to one another and the physically measured ET and Discharge data to produce the results seen in 4.0 onwards.

3.3.1 – Field Data Collection

There was a wide range of data that was collected and measured during the summer of 2021. This included active layer depths throughout the summer, as well as soil properties underneath of hummocks and inter-hummocks; UAV imagery was used to create a classification map of the catchment; as well as stream discharge, evapotranspiration, snow water equivalent, and the other meteorological variables that were necessary for GEOtop to run. The collection of active layer depths and the measuring of soil properties can be seen in Chapter Two in sections 2.3.1 and 2.3.2. The UAV imagery and its classification is described in section 3.3.4, and the meteorological data and evapotranspiration in section 3.3.3.

Stream discharge was measured from May 25th, 2021, until the creek dried up in mid-June using both a Sontek logger instrument, as well as a handheld sonic anemometer. The Sontek provided continuous measurements of stream flow for the entirety of the summer at a half hourly rate. The handheld sonic anemometer was used once a day and the measurement was typically taken later into the day, as historical data between mid-day temperatures and discharge has shown that discharge tends to peak later during the day at 8-10 pm.

3.3.2 - Pre-processing & Initialization for GEOtop

GEOtop (V2.1) is a physically based, distributed hydrological model, discretized into a finite regular grid where the heat and groundwater equations are solved with finite difference schemes (Endrizzi et al, 2011). To run GEOtop for Siksik Creek, several input maps needed to be developed alongside defining the soil properties, providing meteorological data, and the other necessary coding parameters. The maps used in this study include maps at the surface of aspect, slope, river network delineation, sky view factor, a digital elevation model (DEM), soil type, and landcover type (GEOtop User's Manual). Sky view factor is an assessment of each pixel in the raster and its ability to view the horizon compared to its surrounding pixels, and is used to measure the amount of radiation received at the surface (GEOtop User's Manual). Most of the input maps were produced using ArcGIS with internal functions, however the sky view factor

was produced in QGis. Other inputs required the specific properties of the soil in layers by depth, as well as meteorological forcing data. The soil data was collected with field work near the end of the summer of 2021 through a mix of coring and soil pits, as seen in Chapter 2. Meteorological data was collected at TMM, where air temperature, relative humidity, incoming and outgoing shortwave and longwave radiation, and precipitation were measured.

Model simulations began right at freshet in mid-May – where the snow on the landscape was beginning to rapidly melt and contribute to creek streamflow. This value of snow water equivalent (SWE) was manually measured with snow surveys in and around TMM before and during snowmelt where the weight and density of the snowpack was measured to calculate a value of SWE from. While snowmelt was occurring and freshet began, stream gauging began and measured stream velocities every 10 cm along the creek to create a discharge measurement. Stream gauging stopped in mid-June once the creek had stopped flowing.

The input maps used in GEOtop came from two sources: with the DEM, aspect, slope, and sky view factor maps all being produced from the 2008 LIDAR imagery flown by Chris Hopkinson (2011); the soil and land cover classifications were all produced from UAV imagery flown throughout the entirety of Siksik Creek. The DEM was the original data received from the LIDAR flight at a 1 m resolution. The aspect, slope, and sky-view factor maps were calculated with ArcGIS and QGis internal functions from this singular map. We flew the UAV in mid-June of 2021 where the whole catchment was imaged and gave a resolution of 13 cm. An unsupervised classification of this imagery was then done in ArcMap where mosses, lichens, and shrubs were given a value corresponding to one of these three classes in this UAV imagery (Figure 3.4). These classifications were produced primarily because of their spectral wavelengths in the RGB spectrum. Because of the time of year, the lichens were predominately white, the mosses predominately red, and both the taller and shorter shrubs, tussocks, etc., were green. The shrub component of this map has been simplified to cover all of these based on their colour. As will be discussed in section 3.4, this was enough to satisfy the soil and landcover maps. However, all of the input maps were upscaled to a 10 m resolution to reduce processing time and because GEOtop has been proven to work at this scale in past research (Endrizzi et al., 2011). The initialization scheme and the equations GEOtop uses to solve these problems can be seen in

sections 3.3.3 and 3.3.4, as well as the values that were input by the user to simulate these conditions.

3.3.3 - Meteorological Forcing

There are two meteorological stations located in the Trail Valley Creek watershed that were used for the study: TMM and MSC (Figure 3.2). Half hourly data was used from TMM, except when there was missing data due to power interruptions or instrument malfunctions, then MSC data was used to gap fill.

Figure 3.2: TMM on the left, and a view of, the eddy covariance tower on the right

The meteorological data that GEOtop requires, and which is measured at TMM, or can use as an input is (GEOtop Users Manual):

1. Precipitation intensity (mm h^{-1})
2. Wind velocity (M s^{-1})
3. Wind direction (°N)
4. Relative humidity (%)
5. Air temperature (°C)
6. Dew temperature (°C)
7. Air pressure (bar)
8. Short waver solar global radiation (W m^{-2})
9. Short wave solar direct radiation (W m^{-2})
10. Short wave solar diffuse radiation (W m^{-2})
11. Short wave solar net radiation (W m^{-2})
12. Long wave incoming radiation (W m^{-2})

It should be noted that one of the variables not listed as accepted is evapotranspiration (ET) which is measured by a nearby eddy covariance tower at TMM in the upper tundra portions of Siksik Creek. The post-processed data was provided by Oliver Sonnentag and Gabriel Hould-Gosselin. This data can be used as a validation data set for the simulated values from GEOtop. GEOtop estimates evapotranspiration based on the other meteorological variables that are provided from TMM such as windspeed and direction, temperature, and relative humidity. Both will be used in this study.

3.3.4 - Soil Initialization State

The presence of microtopography, such as earth mineral hummocks, can significantly influence different processes in this catchment. Additionally, the physical properties of both energy and water flow need to be accounted for within the soil. With consideration of water flow, coupling vertical and horizontal hydraulic conductivities is required, as well as the pressures, porosities, and water saturations. The energy and heat flow equation requires the thermal conductivity of the soil and its specific heat capacity, as well as the initial temperatures. This is because GEOtop works in a grid-based manner, where it seeks the solution to this flow of heat and water in the sub-surface (Endrizzi et al., 2011). The soils consist of volumes specified by depths, and their extent spatially via the input maps, and discretized into a finite difference regular grid. The heat and ground water flow are then solved (Endrizzi et al., 2011). The Richards equation is used to describe groundwater flow and is solved in a 3D form using the hydraulic head (H) as the unknown variable (Endrizzi et al., 2011):

$$\frac{\partial \theta w}{\partial t} = \nabla * (\mathrm{K}\nabla \mathrm{H}) + S \qquad (3.1)$$

where K [m s^{-1}] is the hydraulic conductivity, S [s^{-1}] is a source term, and θw is the soil moisture content. The Van Genuchten model (Van Genuchten, 1976) is used by GEOtop to relate the volumetric water content with the pressure head in unsaturated soils. The Mualem model (Mualem, 1976) gives the relationship between pressure head and hydraulic conductivity in unsaturated soil. In partially frozen soils, the hydraulic conductivity decreases as the ice content increases, as seen in Hansson et al. (2004), and this is incorporated into GEOtop (Endrizzi et al., 2011).

It can further be written, as seen in Zanotti et al. (2004), where assumptions of stationary conditions in subsurface flow are removed, with an emphasis placed on describing the movement of water and infiltration. This can be written according to Paniconi and Putti (1994), as seen in (Rigon et al., 2006):

$$qsub = -KsKr(Sw)\nabla(nz + \varphi), \tag{3.2}$$

$$\sigma(Sw)\left(\frac{\partial\varphi}{\partial t}\right) = \nabla * [Ks(T)Kr(Sw)\nabla(\varphi + nz)] - S \tag{3.3}$$

where Sw is the relative water saturation, Ss is the specific storativity coefficient (m^{-1}), φ is the pressure hydraulic head [m], Ks(T) is the saturated hydraulic conductivity, which can be further broken into lateral and vertical conductivities [m s^{-1}], T is the temperature (K), Kr is the relative hydraulic conductivity, and S is the modulus of the source or sink terms (Rigon et al., 2006). The relation between the pressure hydraulic head and soil volume water content is done via the van Genuchten schematization (Rigon et al., 2006).

Overland flow uses the continuity equation to calculate the conservation of water on the surface:

$$\frac{\partial qsup(x,t)}{\partial t} + c(x,t)\nabla * qsup(x,t) = c(x,t)Ql(x,t) \tag{3.4}$$

where x is the position, qsup is the runoff discharge on the surface [m^3s^{-1}], c(x) is the spatially varying kinematic wave celerity [m s^{-1}], and Ql [T^{-1}] is the volumetric flow exchange with the soil (Rigon et al., 2006). The vertical infiltration of water in GEOtop accounts for the fraction of the surface covered in water, as well as microrelief that is defined by surface roughness (Rigon et al., 2006):

$$I = Io \quad if \quad d \geq ho, \tag{3.5}$$

$$I = Io\frac{d}{ho} \quad if \quad d < ho, \tag{3.6}$$

Where I is the effective infiltration rate, Io is the infiltration with no microrelief, d is the depth of water on the surface, and ho is the height of microrelief (Rigon et al., 2006). Overland flow of water eventually leads to the stream channel, and this streamflow can be characterized by the volume of water that leaves the outlet. GEOtop can further have a channel defined within the model domain, and thus there is channel specific routing within the model that is separate from

hillslope runoff. Channel flow in GEOtop is described by the incoming streamflow using a constant celerity for the creek network. This is based on the solution of the de Saint-Venant parabolic equation as seen in Rinaldo et al. (1991), and D'Odorico & Rigon (2003) (Rigon et al., 2006):

$$Qc(t) = A_T \int_0^t \int_0^{Lmax} \left(\frac{sW(\tau,S)}{\sqrt{4\pi D(t-\tau)^3}} \right) \exp\left[- \frac{(\mathrm{s-uc(t-\tau)})^2}{(4\mathrm{D(t-\tau)})} \right] ds\, d\tau \quad (3.7)$$

where Qc(t) is the discharge of water at the outlet of the catchment [$m^3\ s^{-1}$], A_T is the basin area, $W(\tau, S)$ [s^{-1}] is the inflow of water from the hillslopes into the stream network from distance s[m], Uc is mean celerity [m s-1], D is the hydrodynamic dispersion coefficient [m2s-1] and Lmax is the maximum distance from the outlet from the stream network (Rigon et al., 2006).

The heat equation is solved in its 1D form perpendicular to the surface at the surface-atmosphere boundary, which is then coupled with the Richards equation to solve in a 3D manner to describe the vertical movements of both heat and water in the ground (Endrizzi et al., 2011). The surface energy balance requires an accurate description of the surface fluxes, and in GEOtop the fluxes of sensible and latent heat are calculated with a flux-gradient relationship (Endrizzi et al., 2011):

$$H = \rho * cp * u \frac{(Ta-Ts)}{ra};\ LE = \beta * Le * \rho * u \left(\frac{Qa - \alpha Q*s}{ra} \right) \quad (3.8)$$

where ρ is the air density, Cp is the specific heat at constant pressure, u is the wind speed, Ts is the temperature above the surface, Ta is the air temperature, Le is the specific heat of vaporization, Q*s is the saturated specific humidity at the surface, Qa is the specific humidity of the air, ra is the aerodynamic resistance, and α and β are coefficients that account for the resistance of the soil to evaporation, calculated according to the scheme seen in Ye and Pielke (1993) (Endrizzi et al., 2011).

The transfer of heat, or the heat flux, into the ground and as used in GEOtop, is given by the sum of shortwave radiation, longwave radiation, and the fluxes of sensible and latent heat (Endrizzi et al., 2011). Its 1D form can be written as:

$$\frac{\partial U(T)}{\partial t} = \left(\frac{\partial}{\partial z} \right) \left(k * \left(\frac{\partial T}{\partial z} \right) \right) \quad (3.9)$$

where t[s] is time, z[m] is the coordinate normal to the surface, T[K] is the soil temperature, U[Jm^{-2}] is the internal energy of the soil, and k [$Wm^{-1}s^{-1}$] is the thermal conductivity of the soil (Endrizzi et al., 2011). This can then be integrated after the assumption that the surface boundary condition is defined by the surface heat flux, where the bottom boundary condition at some depth has no fluctuation (Endrizzi et al., 2011). This can be written as:

$$U = C\ (T - Tf) + Lf * \rho w \theta w \tag{3.10}$$

where C is the soil thermal capacity [$Jm^{-2}K^{-1}$], Tf is the freezing temperature (273.15K), Lf is the thermal heat of fusion ($3.34*10^6$ J kg^{-1}), ρw is the density of water when a liquid (1000 kg m^{-3}), and θw is the volumetric water content [-] (Endrizzi et al., 2011).

Evapotranspiration within GEOtop is handled as a sink term for the overall water balance equation and is broken into three components that are calculated separately (Rigon et al., 2006). These three components are: the sum of evaporation and/or sublimation from snow and/or the soil surface (E_G), transpiration from vegetation (E_{TC}), and evaporation of precipitation intercepted by the vegetation and of water on the ground (E_{VC}). Together these give E_T (Rigon et al., 2006):

$$E_T = E_{TC} + E_G + E_{VC} \tag{3.11}$$

The computation of total evaporation is calculated as a function of potential evapotranspiration E_p, which is a function of saturation specific moisture at surface temperatures $q^*(T_s)$ and atmosphere specific moistures $q(T_a)$ (Rigon et al., 2006). It is calculated as:

$$\lambda E_p = \lambda p C_E u_w [q * (T_s) - q(T_a)] \tag{3.12}$$

where Ce is a bulk turbulent transfer coefficient, p is the density of air, uw is windspeed, Ta is air temperature, and Ts is surface temperature. Eg is defined by the water content of the first soil layer via the soil resistance similarity seen in (Bonan, 1996). It can be calculated as:

$$E_G = (1 - S_v) E_P \left(\frac{r_a}{r_a + r_s}\right) \tag{3.13}$$

where S_v [-] is the portion of soil at the surface covered by vegetation and ra is its aerodynamic resistance where $r_a = 1/(p\ C_e\ u_w)$. The resistance, r_s, is defined by the water content of the first

layer of soil (Rigon et al., 2006). The evaporation of water intercepted by vegetation is calculated as:

$$E_{vc} = S_v E_p \delta_w \tag{3.14}$$

where δ_w is the wet vegetation fraction. Transpiration is calculated as:

$$E_{TC} = s_v E_p (1 - \delta_w) \sum_i^n (f^l_{root}\, r_a)/(r_a + r_c^l) \tag{3.15}$$

where f^l_{root} is the root fraction of each soil layer defined the model inputs calculated from the surface linearly to the maximum root depth; r_c is the canopy resistance, where it depends on solar radiation (Rigon et al., 2006).

This all comes together to form a water balance equation that is separated into surficial and sub-surface components:

$$\frac{\partial q_{sup}(X,t)}{\partial t} + c(x,t)\nabla * q_{sup}(x,t) = c(x,t) q_l(x,t) \tag{3.16}$$

and in the soil:

$$\frac{\partial \theta(x,t)}{\partial t} + \nabla * q_{sub}(x,t) = -S(x,t) \tag{3.17}$$

where x is a vector delineating the position, t is time, q_{sup} is the runoff discharge on the surface and qsub is in the soil. C(x) is the spatially varying kinematic wave celerity and q_l is the volume exchange with the soil. S is the exchange between atmosphere and soil (Rigon et al., 2006).

Endrizzi et al. (2011) and Endrizzi & Marsh (2010), set their soil columns to a depth of 10 m and the 8 m mark was set to the depth of zero amplitude temperature – a depth at which temperatures were constant year-round and did not fluctuate. Endrizzi & Marsh (2010). Endrizzi et al. (2011) used a 1-soil type that was designed to average both hummock and inter-hummock zones and two soil types into one. To do this they reduced the thickness of the peat layer, as well as the hydraulic conductivities, to represent both the lesser volume of peat as well as the lower conductivities associated with the hummock mounds. One aim of this project is to improve on their simplified profile and introduce separate soil columns for both hummocks and their inter-hummock zones, as shown in Figure 3.3 with a 2-soil type design. The 2-soil design would incorporate hummocks as the first soil type, and inter-hummocks as the second soil type.

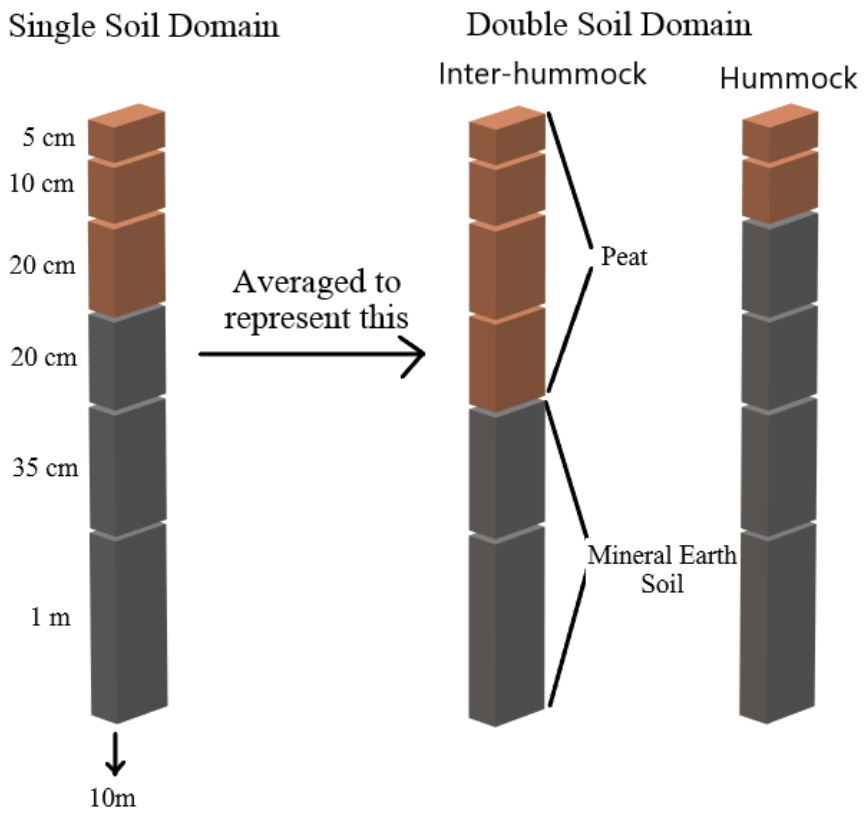

Figure 3.3: On the left is the simplified version of the soil column that was used in Endrizzi et al (2011) and for the 1-soil simulations in this study, and on the right is the separate 2-soil version that will be used in this study to represent hummocks and inter-hummocks.

It should be noted that the 1-soil simulation by Endrizzi et al. (2011) does incorporate hummocks in its own way by decreasing the overall thickness of peat in the catchment and reducing the hydraulic conductivity of the soils to average the properties of hummocks and the inter-hummocks into the 1-soil layer simulation. The 2-soil simulation has a shallow peat layer to represent the hummock mounds, and the second deeper layer of peat layer to represent the inter-hummocks; the conductivities and soil properties were also changed to represent both the peat over top, as well as the mineral earth soil underneath for each of these zones.

Mosses and lichens can act as important identifiers for the location of hummocks and inter-hummocks, as seen in Chapter 2. A land classification map was created with the use of UAV imagery taken from an EBee fixed wing drone, where the images had a spatial resolution as small as 13 cm covering the whole of Siksik Creek over the summer period. A series of flights were flown in late June to early July when the basin was in full bloom – where the green

vegetation had sprouted, and where the colours between mosses, lichens, and other shrubs and vegetation were immediately apparent. This imagery was used to produce a map of mosses, lichens, and shrubs, which was turned into a format that GEOtop could read in the form of an ascii map, where each pixel was given a number representing a certain soil/landcover type (Figure 3.4). These classified pixels were then assigned a soil type with hummock characteristics for lichens, and inter-hummock properties for mosses and shrubs.

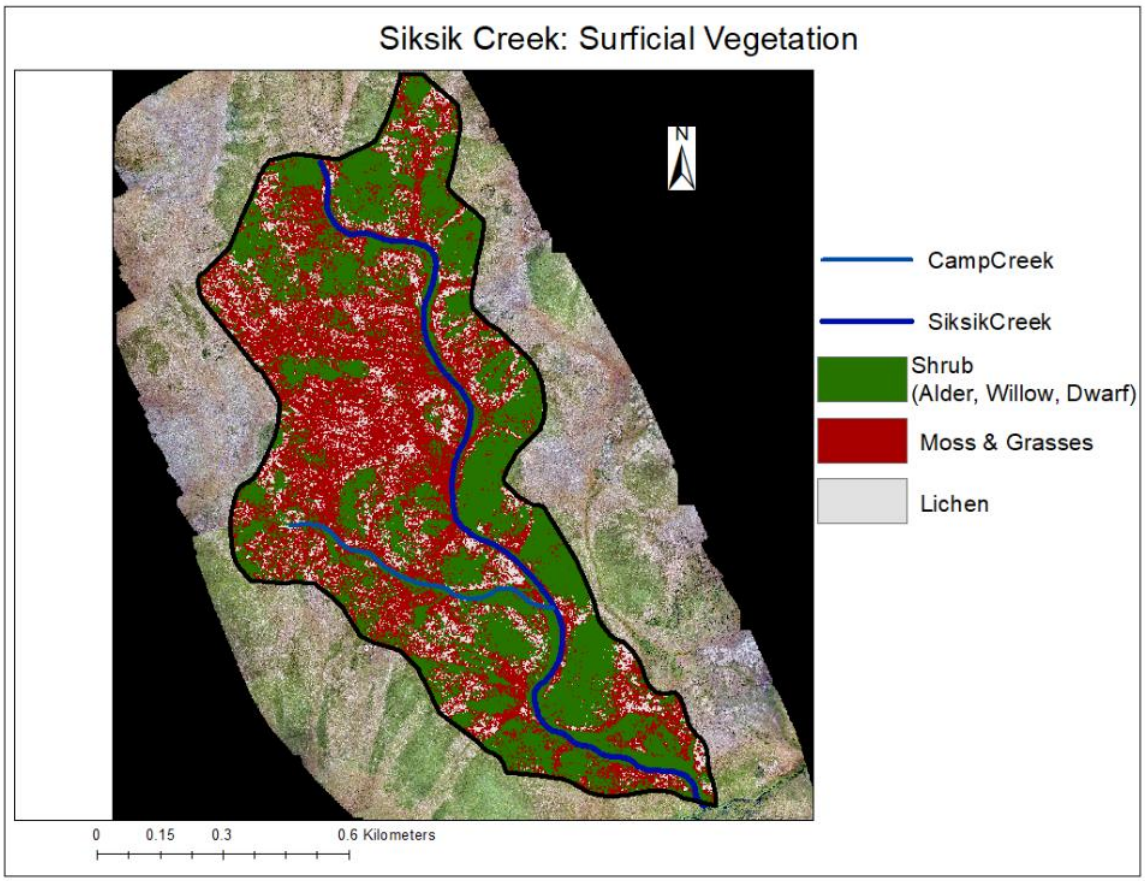

Figure 3.4: Unsupervised classification of surficial vegetation into mosses, lichens, and shrubs in Siksik Creek by UAV imagery which shows the true colour of the vegetation in the basin.

Soil parameters for the three different vegetation types (Tables 3.1, 3.2, and 3.3) include:

Dz [mm] the thickness of a soil unit, *Kh* and *Kv* [mm s^{-1}] are the lateral and vertical hydraulic conductivities of this soil layer, *res* and *sat* [-] are the residual and saturated water contents for the soil, *a* [mm^{-1}] and *n* [-] are the Van Genuchten parameters, and *Ss* is the specific storativity of the soil. The depths are taken from field work and the physical attributes from Endrizzi et al., (2011), who based these values on measurements from Carey et al. (2007) for Granger Creek, and from Quinton et al., (2005) for Scotty Creek, as well as Quinton and Gray (2003) who measured porosity and the other parameters in Siksik Creek.

Table 3.1 Soil parameters used in GEOtop for the lichen land classification, denoted as soil type 1.

Dz	Kh	Kv	res	sat	a	n	Ss
50	1.751	1.751	0.45	0.9	0.0044	2.1	1.00E-07
100	1.642	1.642	0.45	0.9	0.0025	1.95	1.00E-07
200	1.107	1.107	0.45	0.9	0.0015	1.6	1.00E-07
200	0.64	0.64	0.45	0.9	0.0008	1.35	1.00E-07
350	0.138	0.138	0.45	0.9	0.0008	1.35	1.00E-07
1000	0.0138	0.0138	0.45	0.9	0.0008	1.35	1.00E-07
2000	0.0132	0.0132	0.45	0.9	0.0008	1.35	1.00E-07
3000	0.0131	0.0131	0.45	0.9	0.0008	1.35	1.00E-07

Table 3.2: Soil parameters used in GEOtop for the moss classification, denoted as soil type 2.

Dz	Kh	Kv	res	sat	a	n	Ss
50	1.751	1.751	0.45	0.9	0.0044	2.1	1.00E-07
100	1.721	1.721	0.45	0.9	0.0035	1.95	1.00E-07
200	1.642	1.642	0.45	0.9	0.0025	1.8	1.00E-07
200	1.107	1.107	0.45	0.9	0.0015	1.6	1.00E-07
350	0.0036	0.0036	0.45	0.9	0.0008	1.35	1.00E-07
1000	0.00138	0.00138	0.45	0.9	0.0008	1.35	1.00E-07
2000	0.00132	0.00132	0.45	0.9	0.0008	1.35	1.00E-07
3000	0.00131	0.00131	0.45	0.9	0.0008	1.35	1.00E-07

Table 3.3: Soil parameters used in GEOtop for the shrub land classification, denoted as soil type 3.

Dz	Kh	Kv	res	sat	a	n	Ss
50	1.751	1.751	0.45	0.9	0.0044	2.1	1.00E-07
100	1.721	1.721	0.45	0.9	0.0035	1.95	1.00E-07
200	1.642	1.642	0.45	0.9	0.0025	1.8	1.00E-07
200	1.107	1.107	0.45	0.9	0.0015	1.6	1.00E-07
350	0.0036	0.0036	0.45	0.9	0.0008	1.35	1.00E-07
1000	0.00138	0.00138	0.45	0.9	0.0008	1.35	1.00E-07
2000	0.00132	0.00132	0.45	0.9	0.0008	1.35	1.00E-07
3000	0.00131	0.00131	0.45	0.9	0.0008	1.35	1.00E-07

3.3.5 - Vegetation and Landcover Initialization State

In their study, Endrizzi et al (2011) ignored vegetation within Siksik Creek for their simulation. These previous simulations had vegetation treated as a single mass that was continuous throughout the domain only to represent mosses / lichens; shrubs of any variety were completely ignored. GEOtop (v2.1) used for this study is able to calculate the energy balance at the surface for a variety of vegetation types that cover the domain, and which are able to absorb and reflect shortwave radiation, emit longwave radiation, and can even allow air to transfer heat and vapor within vegetative canopies (Endrizzi et al., 2010). Key processes for this version of GEOtop includes root depths, vegetation reflectivity and transmissivity, density of the canopy, and leaf surface area indexes (LSAI).

GEOtop solves the vegetation energy balance with the calculation:

$$C_v\left(\frac{dT_v}{dt}\right) = SW_v + LW_v - H_v - LE_v \tag{3.18}$$

where T is time, Cv is the thermal capacity of the specified vegetative type, SWv and LWv the incoming shortwave and longwave radiation absorbed by the vegetation, and Hv and LEv are the sensible and latent heat fluxes emitted from the vegetation within the canopy (Endrizzi et al., 2010). There are several assumptions: first, longwave radiation that is emitted is spread equally towards both the soil and the atmosphere, and that emissivity increases with density (Endrizzi et al., 2010). Secondly, the air within the canopy is negligible regarding storing heat and water vapor, and that they are balanced by the fluxes above the vegetation (H and E). This leads to calculations that separate these fluxes into canopy fluxes (Hv and Ev) and under-canopy fluxes (Hs and Es) (Endrizzi et al., 2010):

$$H_v = p\left(\frac{q_v - q_{ca}}{r_v}\right);\ H_s = pC_p\left(\frac{T_s - T_{ca}}{r_{uc}}\right);\ H = pC_p\left(\frac{T_{ca} - T_a}{r_{aH}}\right) \tag{3.19}$$

$$E_v = p\left(\frac{q_v - q_{ca}}{r_c}\right);\ E_s = p\left(\frac{q_s - q_{ca}}{r_{uc}}\right);\ E = p\left(\frac{q_{ca} - q_a}{r_{aE}}\right) \tag{3.20}$$

where p is the air density, and C_p the specific heat at constant pressure; T_{ca} is the temperature of the air within the canopy and q_{ca} the specific humidity of air within the canopy; T_s is the temperature at the ground surface, and where q_s is the specific humidity at the ground surface; T_a is the temperature of the air above the canopy, and q_v is the specific humidity at the canopy

surface; r_{aH} is above canopy aerodynamic resistance for heat transfer, and r_{aE} is aerodynamic resistance for water vapor transfer; r_v is the aerodynamic resistance of turbulent exchange of heat between the canopy and air, and r_c is the aerodynamic resistance of turbulent transfer of water vapor between the canopy and air within it; r_{uc} is the aerodynamic resistance of exchange for both heat and water vapor between the ground surface and the volume of air within the canopy (Endrizzi et al., 2010).

GEOtop uses the Monin-Obukhov similarity theory to determine the above canopy resistances. However, there is much more uncertainty with the under-canopy resistances as turbulence within the canopy is quite complex. Aerodynamic resistances to momentum (r), sensible heat fluxes, and evaporation between heights must be defined (Endrizzi et al., 2010). GEOtop does this according to Choudhury & Monteith (1988) (Endrizzi et al., 2010):

$$r = \int_{z1}^{z2} \left(\frac{dz}{K(z)}\right) \tag{3.21}$$

where z is the vertical heights at two locations (1,2), and K is the eddy diffusivity. Assuming an exponential decay of the eddy diffusivity, GEOtop calculates K(z) as:

$$K(z) = K(H_c) * \exp\left[-n\left(1 - \frac{z}{H_c}\right)\right] \tag{3.22}$$

where Hc is the height of the vegetated canopy, and n is its decay coefficient. Eddy diffusivity at the canopy height is calculated by the Monin-Obukhov theory (Endrizzi et al., 2011). At the surface however, the r length of surface roughness (Z0g) and the height of momentum that the canopy influences must be considered (Endrizzi et al., 2010). This results in the equation:

$$r_{uc} = \left(\frac{H_c}{nK(H_c)}\right)\left\{\exp\left[n\left(1 - \left(\frac{z_{0v}}{H_c}\right)\right] - \exp\left[n\left(1 - \left(d + \frac{z_{0v}}{H_c}\right)\right)\right]\right\} \tag{3.23}$$

where z_{0v} is the roughness length of vegetation at the surface. Vegetation and landcover parameters for each landcover type are listed in Table 3.4. LSAI, VegHeight, Snow depth thresholds, decay coefficient of eddy diffusivity, momentum roughness lengths of vegetation, and stomatal resistance are from Endrizzi & Marsh (2010), which is based on similar studies of shrub tundra from Sturm et al., (2001) and Marsh et al., (2010). Albedo values are taken from Pomeroy & Dion (1999) and Gubler et al. (2013).

Table 3.4: Landcover and vegetation parameters used for each simulation run in GEOtop.

	Lichen	Moss	Shrub
SoilRoughness	10	20	20
ThresSnowSoilRough	10	20	20
VegHeight	200	200	1500
ThresSnowVegUp	200	200	1500
ThresSnowVegDown	200	200	1500
LSAI	0.6	0.9	0.7
CanopyFraction	1	1	1
DecayCoeffCanopy	2.5	2.5	2.5
VegSnowBurying	1	1	1
RootDepth	30	100	500
MinStomatalRes	1.00E+04	1.00E+04	1.00E+04
VegReflectVis	0.15	0.15	0.15
VegReflNIR	0.58	0.58	0.58
VegTransVis	0.07	0.07	0.07
VegTransNIR	0.25	0.25	0.25
LeafAngles	0.3	0.3	0.3
CanDensSurface	0.4	0.4	0.7
SoilAlbVisDry	0.16	0.16	0.16
SoilAlbNIRDry	0.33	0.33	0.33
SoilAlbVisWet	0.08	0.08	0.08
SoilAlbNIRWet	0.16	0.16	0.16
SoilEmissiv	0.99	0.99	0.99

3.3.6 - Hydraulic and Thermal Boundary Conditions

Surface boundary conditions are given by atmospheric forcing, derived from Bixio et al (2000), which allows for surface flow and heat to infiltrate, and for subsurface flow and heat to return to the surface. The lateral borders follow the same concept as the surface boundary conditions where water is allowed to drain at the outlet. Both the lateral and surface boundary conditions are Neumann in nature. In contrast, the lower boundary condition is given by a constant temperature at some depth and follows a Dirichlet boundary condition scheme where the depth and the temperature at this depth is defined as constant as well as a zero flux of water.

3.4 Results & Discussion

This study seeks to answer how microtopography, shrubs, and snow when added to the domain affects ground thaw, water table depths, and the general hydrology of the Siksik Creek basin.

The over-arching research question that this chapter attempts to answer is:

- How do simulated active layer thaw and water balance components change when hummocks and inter-hummocks, shrubs and vegetation, and snow are added to GEOtop individually during a dry year?

The following results and discussion will be centered on answering these questions and on the elements that were found to influence these processes.

3.4.1 - GEOtop and Sensitivity to Soil Types: Comparison Between 1 & 2-Soil Simulations

The previous study by Endrizzi et al. (2011) used a single soil that averaged hummocks and inter-hummock zones into one. This study has discreetly defined both within the simulated domain by comparing the 1-soil to a 2-soil simulation. The 1-soil to 2-soil comparison is important for trying to understand how hummocks affect the hydrology of these small Arctic catchments. Within Siksik Creek these hummocks are composed of mineral earth soil that is dominated by clays and finer sediments left from the last glacial period (Mackay, 1980). They are essentially small mounds that dominate the landscape and are impermeable compared to the surrounding peat. There is typically very little peat that lies overtop of these features, and instead the space between these mounds, called the inter-hummock zone, is where the majority of the peat can be found in the basin (Quinton et al., 1999; Wilcox et al., 2019). It is within the inter-hummock zone that water will flow through after freshet, and the presence of these impermeable hummocks means that the path water is forced to take downhill is tortuous in nature (Quinton et al., 1999).

Figures 3.5 and 3.6 show the comparison of daily and cumulative discharge, and evapotranspiration between these two simulations, where both shrubs and snow are accounted for in the model initialization. For both the daily and cumulative discharge, the 2-soil simulations have streamflow occurring a day sooner than the 1-soil simulation, a trend that causes a

persistent lag between the two model runs. This lag is also found with the daily and cumulative evapotranspiration graphs. Further, the 2-soil simulation has a slightly higher peak flow on the daily graph, but a slightly lower cumulative discharge. Both simulations fail to recognize streamflow later into the summer and lack response to rainfall events. For ET (Figure 3.6), the peaks between observed and modelled are consistent, but with cumulative modelled ET being 5 mm higher for most of the summer, despite ending the summer with similar volumes.

The general pattern of discharge barely changes between the 1-soil and 2-soil simulations. The peak volumes of water are roughly the same in both the daily and cumulative, and both do not respond to precipitation events after freshet. The main difference between the two simulations is the timing of freshet, where the 2-soil simulation starts two days before the 1-soil simulation. This is likely to do with the lower conductivities of the soil in the 1-soil simulation, as well as the presence of peat being ubiquitous throughout the catchment rather than intermittent as in the 2-soil simulation. For the whole of the basin, this layer of peat needs to become saturated before flow downslope and into the creek can begin. For the 2-soil simulation, the peat layer has a higher conductivity and with the presence of hummocks, snowmelt will move to the inter-hummock zones. This means that these zones will become saturated more quickly, and there will be more water moving through less space than the 1-soil simulation.

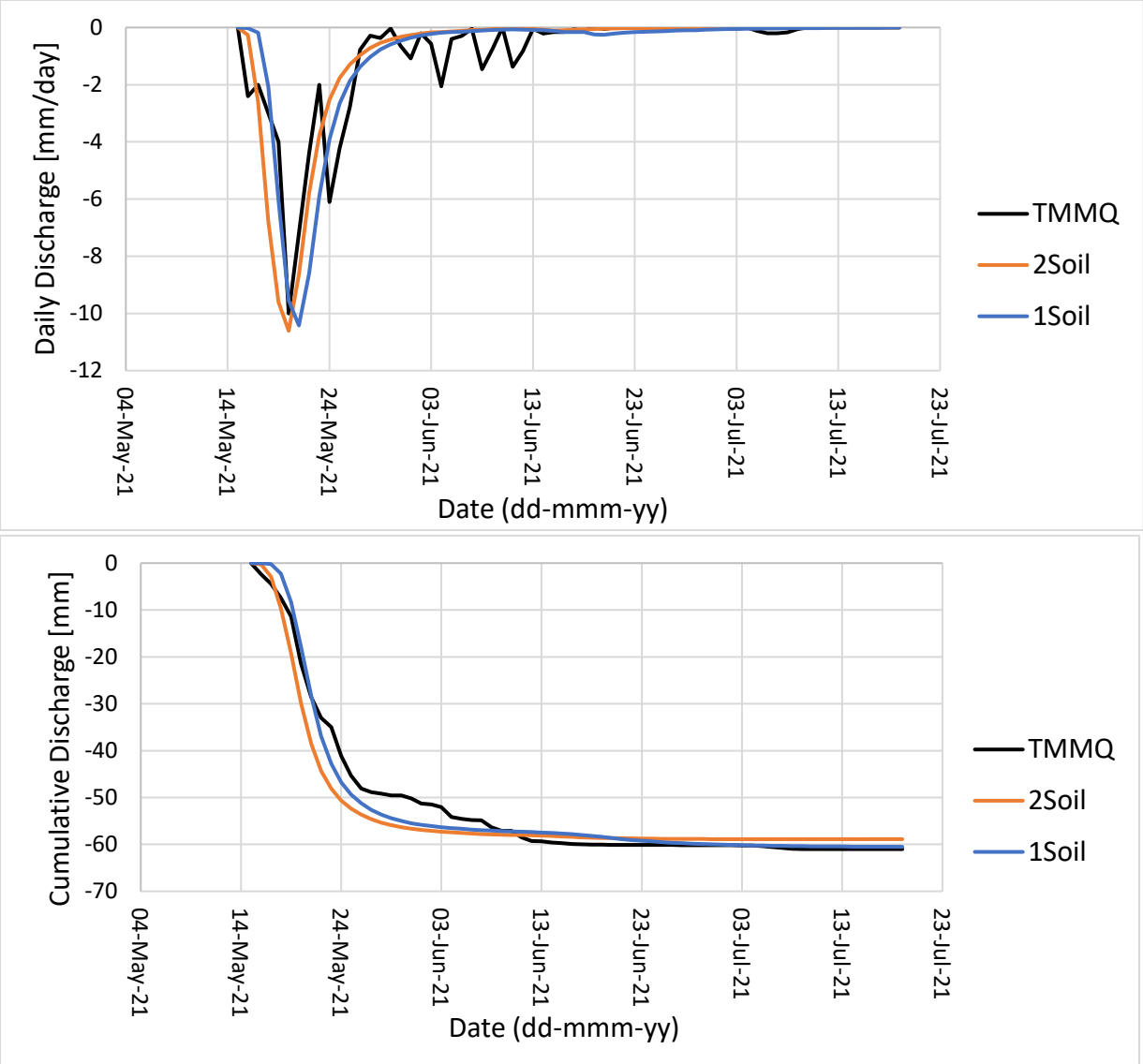

Figure 3.5: Comparison of the 1-soil simulation in blue to the 2-soil simulation in orange, with the physically measured values in black for daily and cumulative discharge. TMMQ is the physically measured discharge. Both use daily data that has been summed from hourly data.

The delay in flow and evapotranspiration is likely due to the ground not being thawed at the period when freshet starts. Additionally, the snowpack has not been fully melted, and while temperatures at the bottom of the snowpack may be near 0°C, very little of the ground under the snowpack will have received the energy necessary to thaw it past several centimetres (Wilcox et al, 2019; O'Connor et al., 2020). Because of this, much of the flow will be overland rather than in the ground surface and thus avoiding the issue that hummocks pose. Further, once the snow begins to melt, freshet tends to be quite rapid, where as much as 80% of streamflow for the year in these catchments can occur in just a period of 2-3 weeks (Marsh & Woo, 1981).

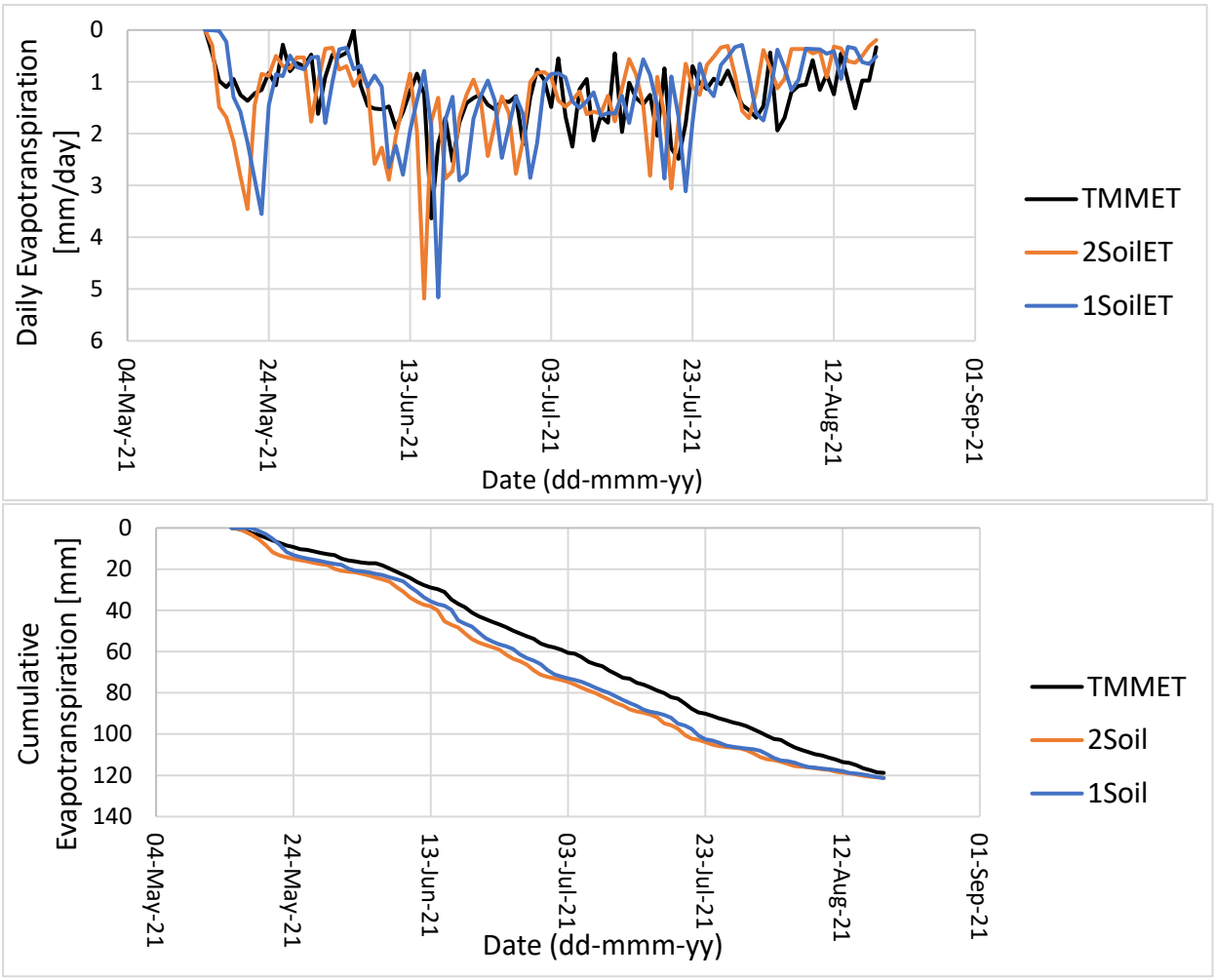

Figure 3.6: Comparison of the 1-soil simulation in blue to the 2-soil simulation in orange, with the physically measured values in black for daily and cumulative ET. TMMET is the physically measured eddy covariance data from TMM. Both use the daily data that has been summed from hourly data.

Simulated active layer thaw depths between the two simulation runs were quite different. As seen in Figure 3.7, there is a higher degree of spatial variability for the 2-soil simulation. This corresponds to the discretization of the hummocks and inter-hummocks, which we know from Chapter 2 have different rates of thaw, as well as shrubs. Figure 3.8 shows the distribution of active layer thaw depths throughout the catchment for the 1- and 2-soil simulation. We see a shift in the distributions where we go from a three-modal distribution for the 2-soil simulation to a two-modal distribution in the 1-soil. The mean and median active layer thaw depths for the 1-soil map are also lower by about 2 cm, with a mean of 500 mm, and a median of 478 mm compared to a mean of 522 mm and a median of 494 mm for the 2-soil map. Both the 2-soil and 1-soil simulations reside within the range of what was physically measured in Chapter 2.

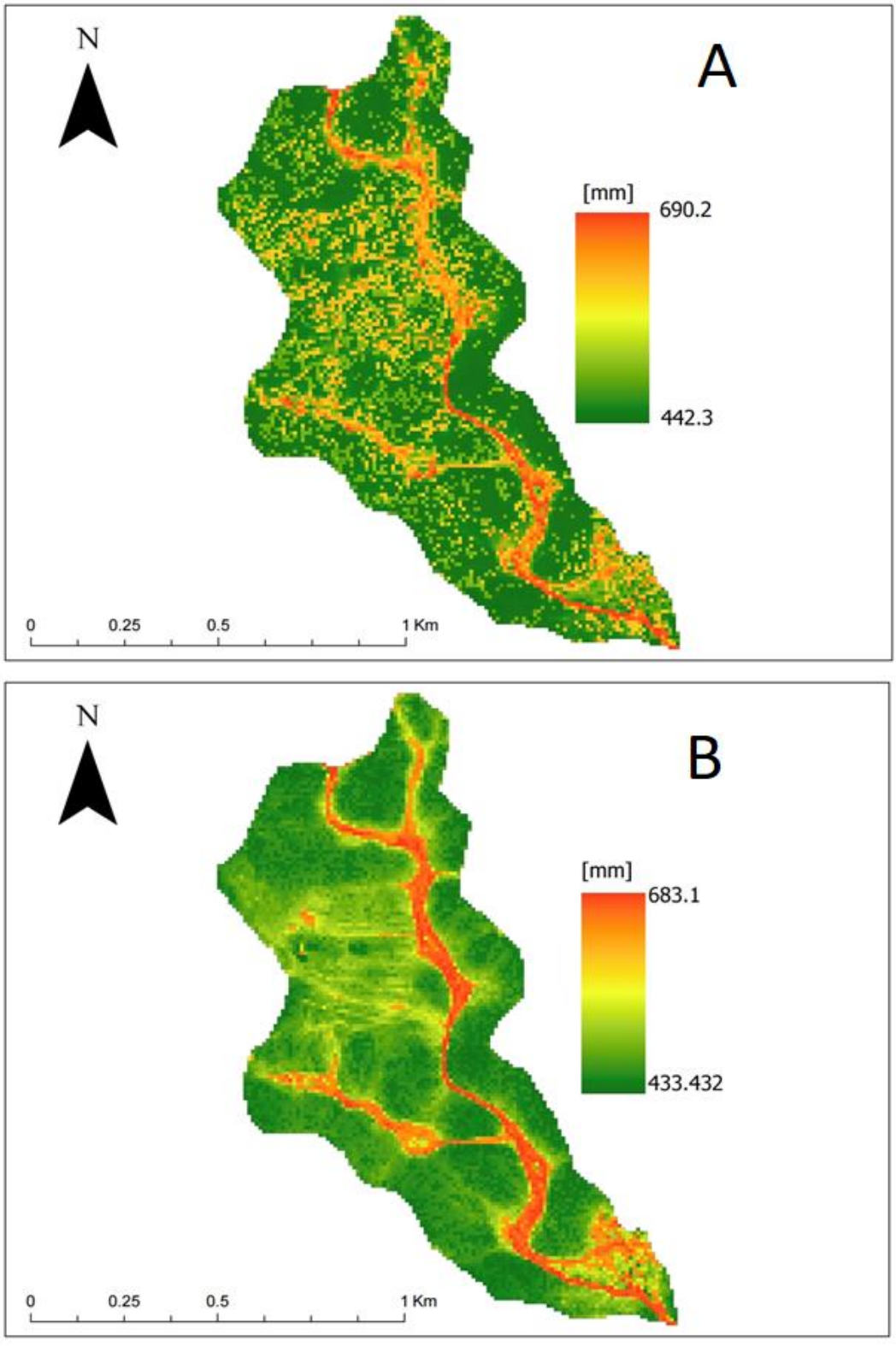

Figure 3.7: Comparison of the 2-soil to 1-soil simulation for active layer depths at the end of the summer. A is the 2-soil, B is the 1-soil. The more red and yellow colours are the deepest depths of thaw in the catchment where this is further into the ground relative to the ground surface

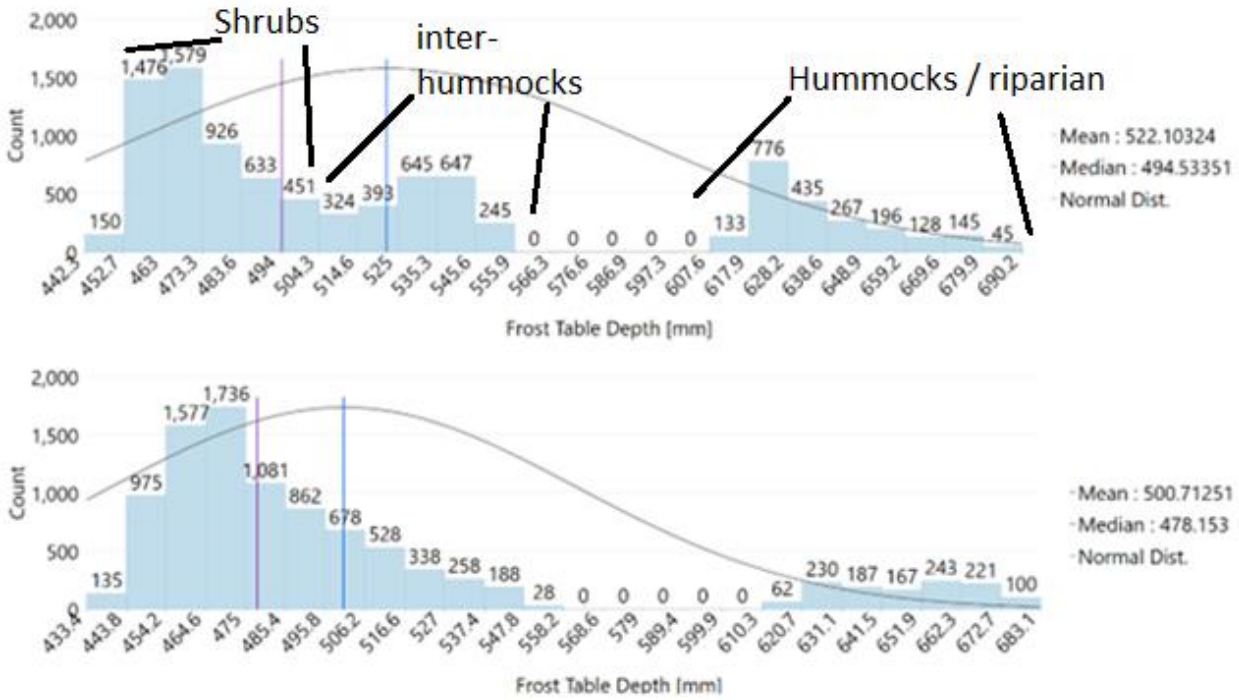

Figure 3.8: Distribution of thaw depths comparing the 1-soil to the 2-soil simulation. The top figure is the 2-soil, and the bottom is the 1-soil. The thawed depths have been roughly interpreted into three different areas, that match the depths that were recorded in the catchment for shrubs, inter-hummocks, and hummocks and the riparian zone. The 1-soil simulation has no distinction. The mean value is the blue vertical line, the median value the purple vertical line, and the normal distribution is the curved line.

The water table depths between the two simulation runs were similar in contrast to the active layer depths. The maximum depth between the 1-soil and 2-soil simulations only has a difference of 10 mm (Figure 3.9). The mean depth of the water table is 196 mm for both, where the median differs by only 5 mm from 221 mm to 226 mm (Figure 3.9). The average depth to the water table across piezometers was 376 mm, and where the riparian zone is ignored, the average depth is 299 mm – this is based on the ten piezometers that had water in them at the end of the summer. The model seems to underestimate the depth to the water table by 60 mm.

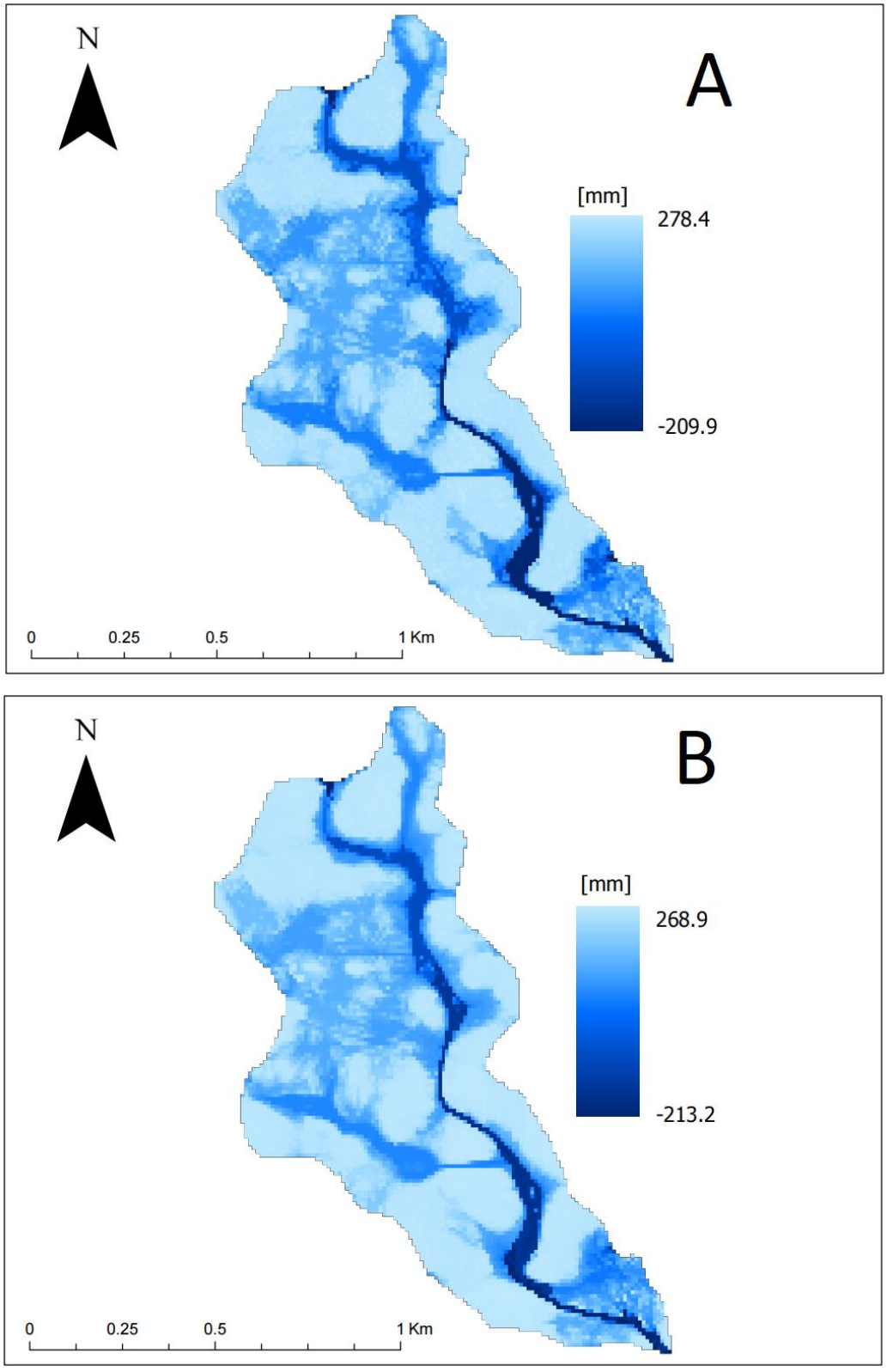

Figure 3.9: Comparison of the (A) 2-soil to (B) 1-soil simulation for water table depths. Positive is down, and negative is up relative to the ground surface. The lightest colours have the deepest depths to the water table and the darkest is the shallowest depths, in some cases this even results in the ponding of water.

The active layer depths output from GEOtop showed that the deepest thaw depths reached were typically within the creek, and that thaw depths became shallower with distance from the creek (Figure 3.7A). Similar results can be seen in Figure 3.7B with hummocks and inter-hummocks, as well as when shrubs are physically accounted for in the domain, although the output looks rather more chaotic in comparison. The distribution of thaw depths, as seen in Figure 3.8, shows the distinct separation of thaw into three separate peaks. The distributions on these peaks roughly line up with the depths measured for shrubs, inter-hummocks, and hummocks. The average thaw depth in the catchment is 522 mm, where the median depth is 494 mm. The separation of the graph into the three different land classes is apparent, but it is likely that there is some co-mingling of these values between classes. Our interpretation of the graph, based on field results, would have the average thaw for the shrubs in the 463-473mm range, inter-hummocks in the 535-545mm range, and the hummocks as well as the creek in the 628 mm+ range. The creeks having deeper active layer thaw depths is consistent with the findings in Endrizzi et al. (2011).

While thaw was recorded throughout the summer, because of the coring tool breaking halfway through the sampling program, it was not possible to fully understand permafrost depths underneath of hummocks. We know the permafrost table is not even, because thaw itself in the basin is not even; further, because peat thicknesses control the rate and extent of thaw in the catchment, it is very possible that since hummocks have very little peat overtop of them that thaw underneath of these features is actually amplified in a dry year, whereas it is mitigated in the inter-hummocks where peat is thicker. Without knowing what permafrost depths are underneath of hummocks though, it is difficult if not impossible to tell what these depths underneath of these features mean for permafrost degradation. Therefore, there is room for improvement in understanding how dry summers may degrade or aggrade permafrost in relation to hummocks.

The influence of topography is very much apparent in the 1-soil frost table map, where depressions and the creeks are clearly defined as having deeper thaw than the hillslopes, and where the open tundra areas in the middle of the catchment can also be identified by slightly deeper thaw than the hillslopes. The 2-soil map has a wide range of seemingly random deeper thaw depths around shallower thaw depths and vice versa. These represent the hummocks and

inter-hummock zones and have a stronger influence than the topography of the basin. Thaw is not uniform in the basin, and deeper thaws in the basin can be found elsewhere than just in the creeks. Further, the shallower depths have a bimodal distribution rather than a modal – fitting of the hummocks, and inter-hummocks.

In comparison, while using the same domain discretization, the water table depths are more consistent when compared to frost table depths. Where the active layer depths had the deepest thaw in the creeks, the corresponding water table depths are shallow, although in and around the creeks this would be expected most of the year. However, some areas of the basin show the presence of ponded water. The average water table depth in the catchment is 196 mm below the surface, and the median is 221 mm. This falls in line with what was seen in the Endrizzi et al. (2011) study where the water table depths never really left the layer of peat that was defined for the domain. In this case there are two different thicknesses of peat in the catchment – that below lichens representing hummocks and a thinner layer of peat, and that underneath of mosses representing the inter-hummocks and a thicker layer of peat. The water table depths are quite similar, despite the frost table maps showing a clear differentiation between the two soils. While the maximum depth to the water table between the two differs by 10 mm, the average depth in each figure is both 196 mm, and the median is only different by 5 mm. Spatially, there is little difference in the extent of depths throughout the basin. Because the distributions as well as the 2-D maps are similar, we can assume that microtopography does not influence the water table depths as much as larger topographical features of the basin such as hillslopes. When you view water tables as a pressure boundary rather than as a physical boundary though this makes sense that it would be flatter.

Overall, the 2-soil simulations did not prove to be much better than the 1-soil simulation for most of the metrics that were analyzed. Specifically, discharge and ET while having a small lag between the two simulations of two days, had the same patterns over time and reached the same cumulative volumes by the end of the summer. The water table depths did not change much, although this could be because of the lack of moisture. What this did influence was the active layer depth maps, with a remarkable difference between the two simulations.

3.4.2 – Sensitivity to Snow-and-Shrubs

Snow is an important component for streamflow in the Arctic (Marsh and Woo, 1981). When snowmelt contribution is omitted from simulations, it is not surprising that low levels of discharge are generated, especially during a dry summer. A comparison of the snow-only simulation to the snow-and-shrub simulation shows that there is a lag of two days, where the snow-only simulation had a rise in streamflow two days after the snow-and-shrub simulation. This lag is persistent through most of the snowmelt period and consistent in both the daily and cumulative charts, as shown in Figure 3.10.

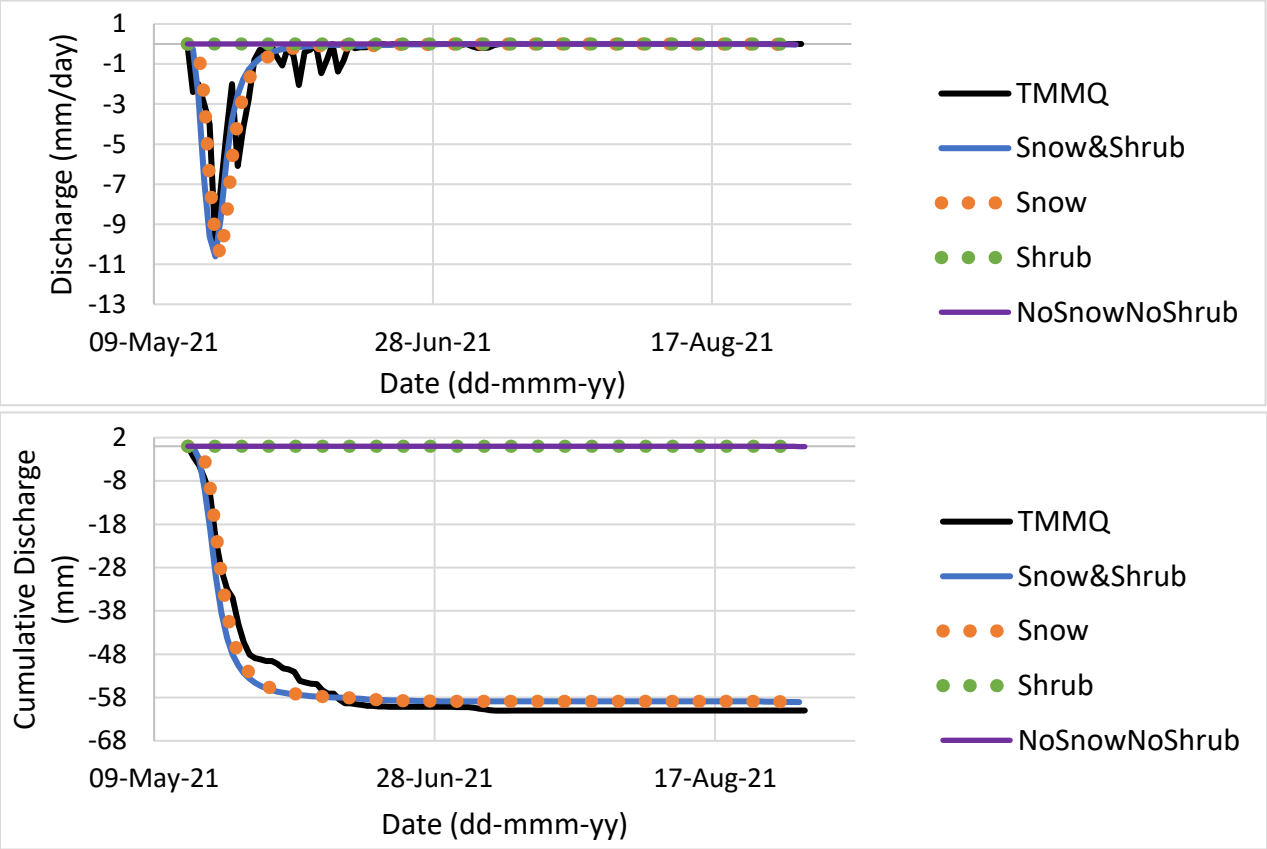

Figure 3.10: Comparison of both daily and cumulative discharge for snow-only (blue), shrub-only (green), no snow or shrub (dotted grey), and snow an shrub (orange) simulations in the 2-soil domain for Siksik Creek with physically measured values in black.

The two simulations that had no snow generated very little discharge – a total of 2-3 mm total for the summer. This is lower than what might have been expected as the summer was persistently warm and dry. When shrubs are added though, the snow-only simulation had a later date of streamflow than the snow-and-shrub simulation. It has been noted in recent studies that

taller shrubs that stick above the snowpack may help accelerate the timing of freshet (Wilcox et al., 2019), and it is possible that this is what GEOtop is picking up.

Comparison of evapotranspiration values between simulation runs show there is no lag between them at the beginning of the summer, however, when transpiration begins, a lag does develop within twenty days of the start of the simulations (Figure 3.11). The simulation runs with shrub-only and no snow and no shrubs show no difference and are similar to the measured values. In contrast, the snow-only and the snow-and-shrub simulations follow the general trend of the physically measured values but are slightly higher through the summer, ending with the same cumulative volume.

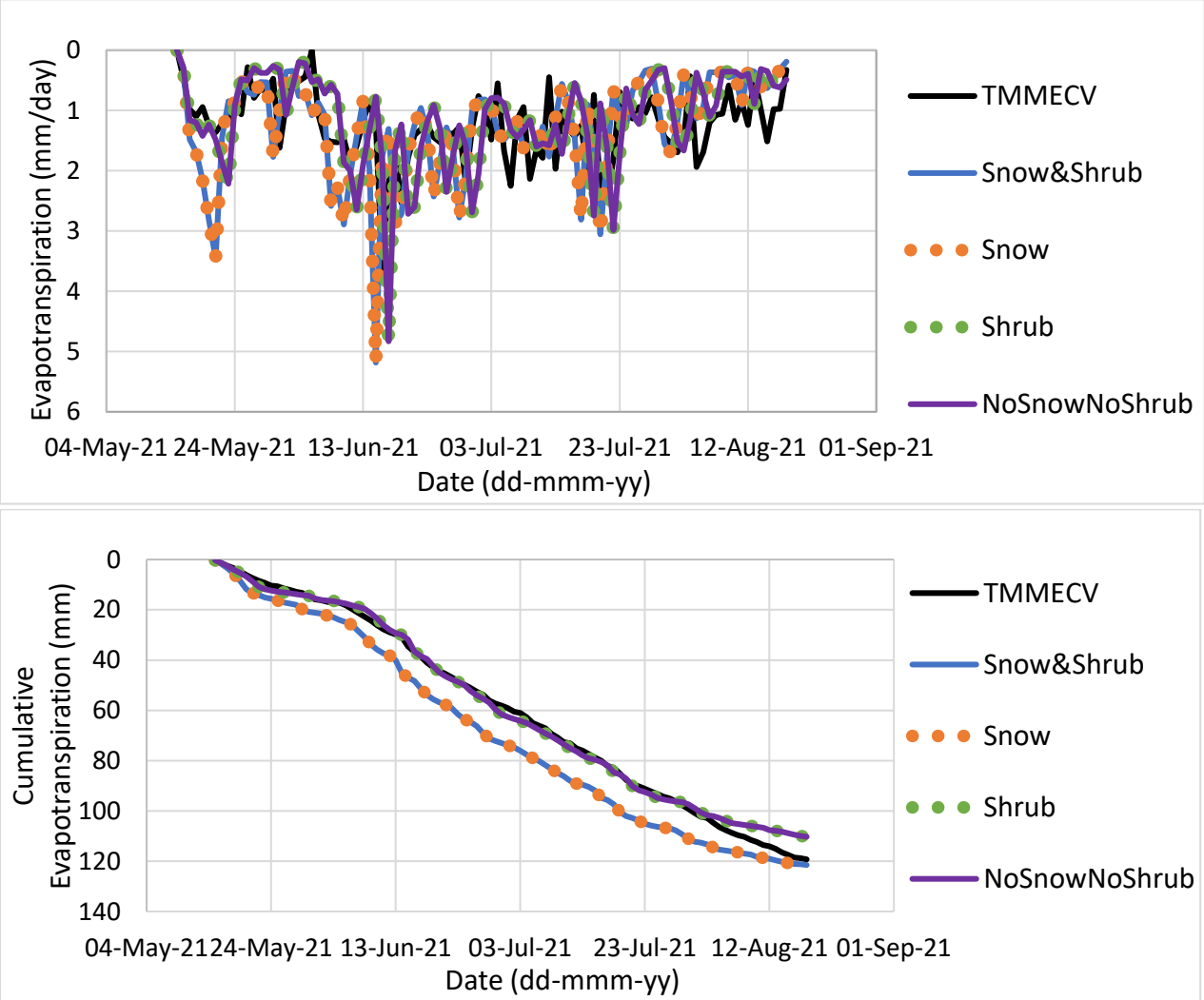

Figure 3.11: Comparison of both daily and cumulative ET for snow-only (blue), shrub-only (green), no snow or shrub (dotted grey), and snow&shrub (orange) simulations in the 2-soil domain for Siksik with measured values in black.

The eddy covariance tower in Siksik has a footprint that varies with wind speed and direction. The tower is placed in the upper middle of the catchment and is primarily surrounded by open tundra. Errors in the eddy covariance data could be due to the size of its footprint, as it could be capturing only the tundra portions of the catchment, and not the hillslopes or creeks. It is also possible that at the 10 m resolution the combination of snow-and-shrubs causes the model to simulate values that are slightly too high. At a 10 m resolution most of the pixels that were classified into shrub, mosses, or lichens, is really a pixel displaying what the most dominant landform in those 10 m is, not that it is purely moss, lichen, or shrub. Because of this, the model is likely interpreting there to be more shrubs in the catchment than there really are, and thus more ET.

Comparing the frost and water table depths for the snow-only and shrub-only simulations, the shrub-only simulation had shallower thaw depths than the snow-only simulation by 7 mm for the deepest thaw depths (Figure 3.12). The overall basin for the shrub-only simulation also appears to have less thaw depth than the snow-only simulation. The average thaw depths between the two are 8 mm apart, and the median only 5 mm. The water table depths are largely unaffected, where the average water table depths differ by 3 mm, and the median by 2 mm.

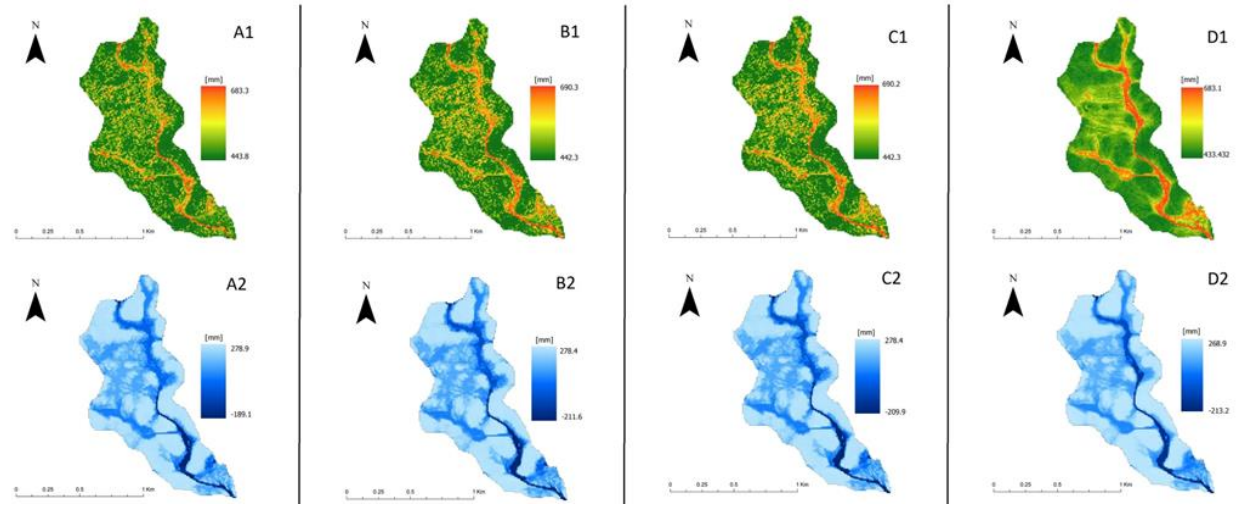

Figure 3.12: Distribution of frost table and water table depths for: A is the Shrub-only, B is the Snow-only, C is the Snow-and-shrub, and D is the 1-soil Snow-and-shrub

We see that thaw in the basin is slightly deeper than the shrub-only for the other 2-soil simulations. Peat can hold a great deal of water, and it also acts as a great insulator when saturated (Mustamo et al., 2019). It is possible that the initial conditions could produce

simulation errors, along with little infiltrating water from a dry summer. When we consider that much of the ground surface around freshet and snowmelt is still mostly frozen, and with a shallow active layer, there is not very much volume for water to infiltrate into, and thus only a limited amount of water from snowmelt can be stored in the soil. The reduced thermal conductivity of the peat because of the lower soil moisture content would help to explain the similar results from both simulations.

3.4.3 - GEOtop Comparison with Field Data

For daily discharge, the modelled results match well the observed peak discharge and spring freshet (Figure 3.13). The simulation used for this comparison is the 2-soil simulation that included both snow and shrubs. The model correctly predicted both the timing, as well as the volume of water that left the basin. For the cumulative discharge, the general pattern is simulated well, although the modelled cumulative discharge tapers off sooner than measured values by a few days (Figure 3.14). The modelled cumulative discharge was 59 mm, similar to the measured value of 61 mm.

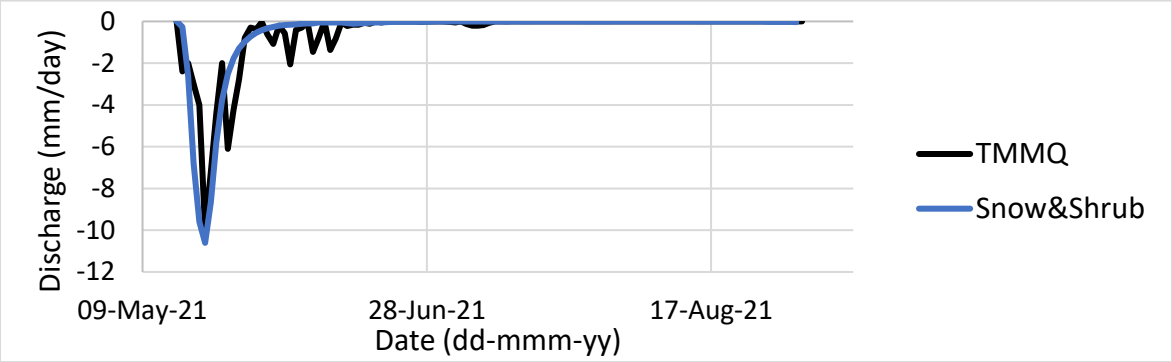

Figure 3.13: Comparison of modelled (blue) and observed (black) daily discharge at Siksik Creek.

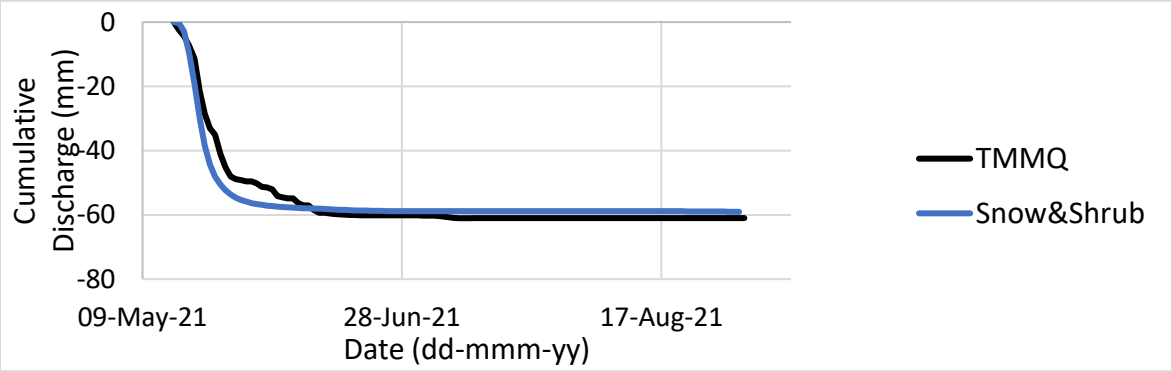

Figure 3.14: Comparison of cumulative modelled (blue) and observed (black) discharge across the summer for Siksik Creek.

Evapotranspiration measured at TMM, with the eddy covariance system, matches relatively well with the modelled daily values, where the timing of the peaks in ET are particularly close. Seen in Figure 3.15, the modelled values were higher than those observed. For the cumulative ET, the model simulates higher values throughout most of the season (Figure 3.16). However, the rate at which ET increases in the catchment occurs at the same time, and overall, the final volume for ET between the modelled and measured are within 2 mm (121 mm and 119 mm respectively). Considering that ET at TMM is a point measurement, and we're applying this to the whole of catchment with the results from GEOtop, it makes sense that there would be some differences, especially since the ET measurements are highly influenced by windspeed and direction. Further, that even without windspeed, the natural footprint of the tower would not normally cover the whole of the catchment anyways. These simulated values match very well and are within the same magnitude as the physically measured values.

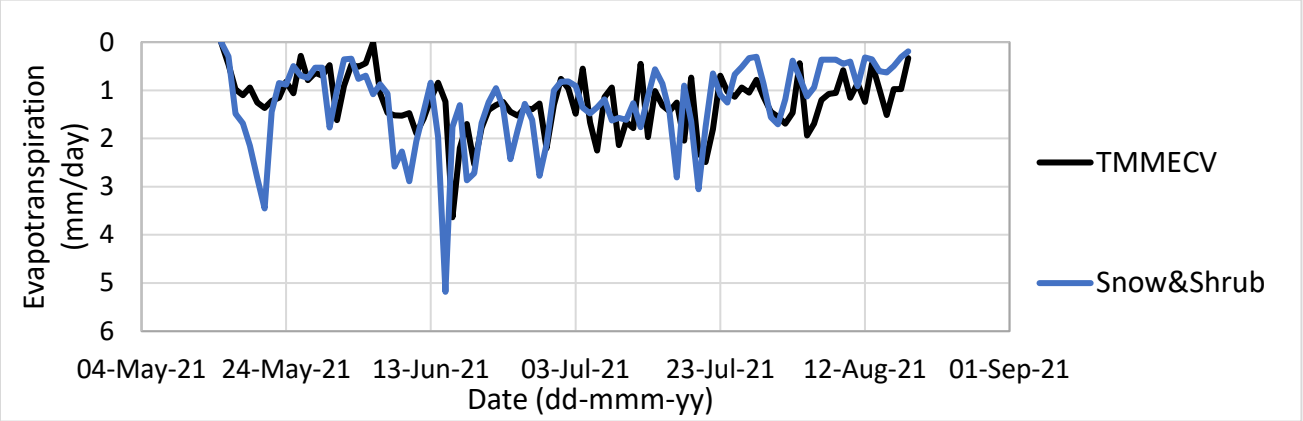

Figure 3.15: Comparison of daily ET values – blue is the modelled and black is the physically measured.

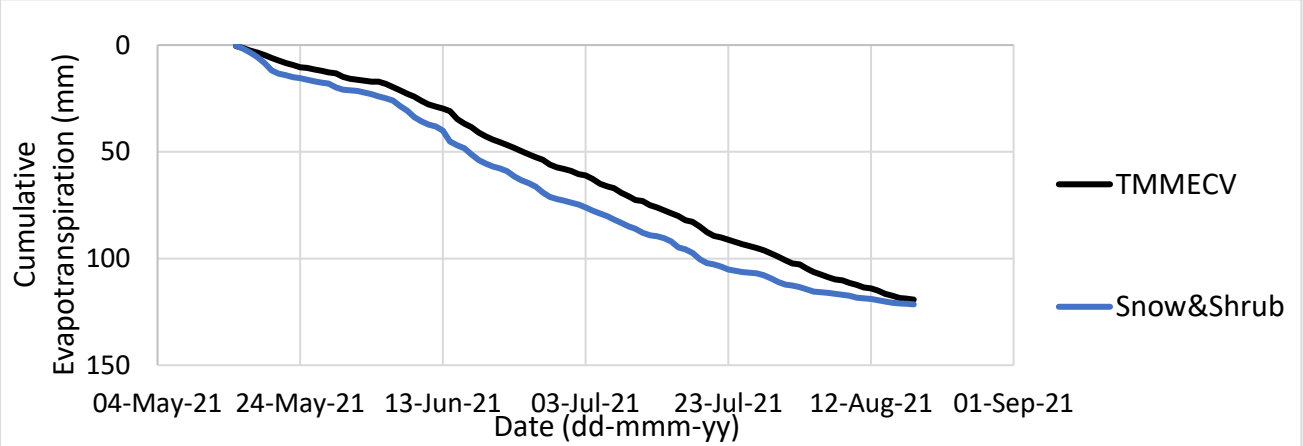

Figure 3.16: Comparison of cumulative ET values – blue is the modelled and black is the physically measured.

Figure 3.17 shows the discrete rates of active layer thaw for hummocks and inter-hummocks, as measured across a variety of landscape types throughout the catchment. The average weekly thawed depths can be separated into two different rates of thaw based on the presence, or lack of, hummocks. The model run simulating 2-soils, and which separates hummocks and inter-hummock zones, simulated the observed rate of active layer thaw fairly well (Figure 3.17).

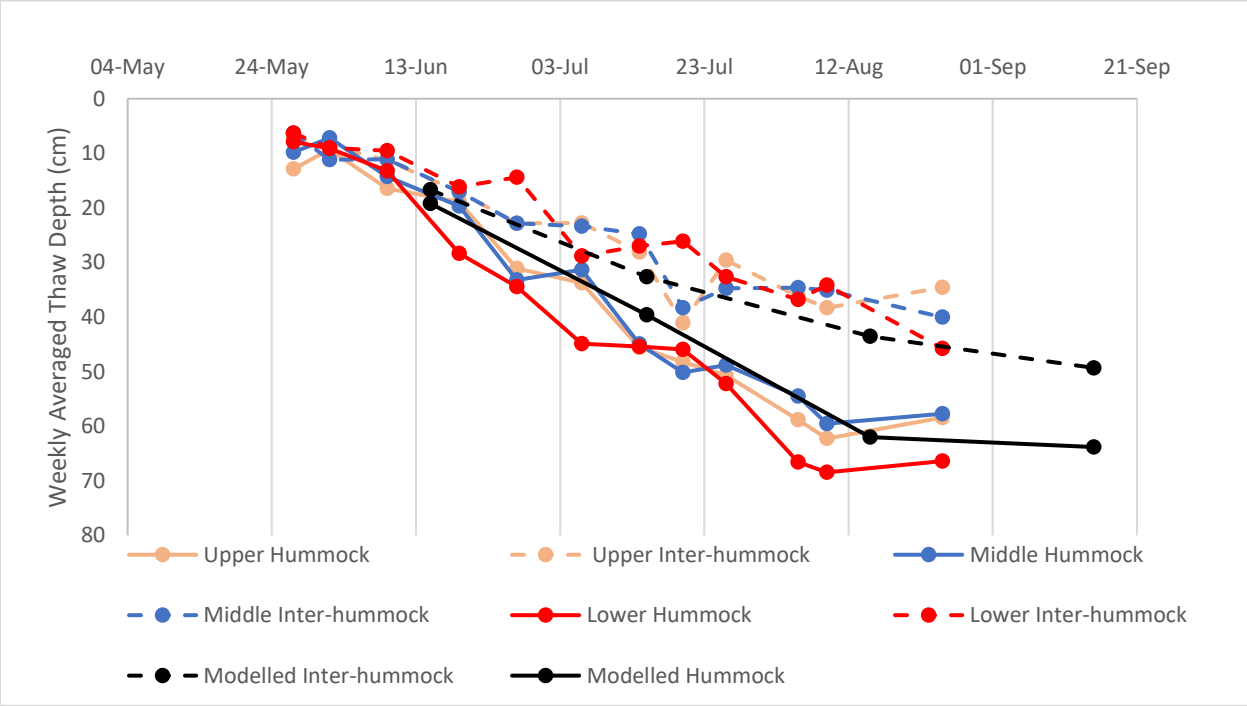

Figure 3.17: Comparison of thaw depths across landscape types for both modelled and physically measured. The black lines, solid and dotted, are the modelled results.

When comparing modelled to measured discharge data, we see that the model was able to correctly simulate the timing of snowmelt as well as the volume of water leaving the catchment during freshet. There are some discrepancies during the summer, especially the response to precipitation events. This could be related to the dry state of the catchment over the summer period. Despite this, the model simulations that incorporated the two-soil domain with shrubs and snow still simulated closely the cumulative volume of water that left the catchment during the summer.

Evapotranspiration in the catchment was also adequately simulated, where the comparison between the measured eddy covariance and modelled daily values are roughly accurate in both timing of peak ET, as well as the volume of ET. The model does simulate

slightly higher values at the beginning of the summer than what was measured, but both cumulative volumes were similar.

Lastly, simulated thaw depths in the catchment closely followed the discrete rates seen during fieldwork for both hummocks and inter-hummock zones throughout the summer. It was possible to look at the distribution of thaw depths every week to isolate the separate signals for hummocks and inter-hummocks and use those values to chart thaw in the basin across these landforms. There was a distinguished difference in thaw between hummocks and inter-hummocks, and where GEOtop was able to successfully simulate this.

Measurements and modelled results have shown that the deepest thaw tends to be in and around the creeks, and underneath hummocks (Endrizzi et al., 2011). Further, the model also shows adequately how thaw around the creek rapidly decreases with distance from it – something that was seen during field work; and where underneath of shrubs had the shallowest thaw, similar to the modelled results in Endrizzi et al. (2011), as well as the physically measured thicknesses seen in Quinton and Marsh (1999) and Quinton et al. (2000).

Differences in thaw between north-facing and south-facing slopes due to the lack of direct insolation are not represented well in the model. The north-facing slopes should have noticeably shallower thaw than the south facing slopes which receive more insolation (Jiang et al., 2012). This is in part because of the angle of the sun in the sky, even during the time of the year when the sun is above the horizon 24/7, whereas the sunlight is not as direct as in the southern latitudes. As seen in Jiang et al., (2012) this difference in thaw can be as large as a metre between the two different facing slopes.

Water table depths were shallow around the creeks and the depth of the water table largely stayed within the peat thicknesses defined for the domain. Underneath of the peat is a near uniform layer of mineral soil that is dominated by clays – making it near impossible for water to permeate into this layer in just the space of time that a single summer provides because of the low hydraulic conductivities typically seen in clay dominated soils (Mustamo et al., 2019; O'Connor et al, 2020). With the largest depth to the water table at 278 mm, these depths were primarily found on the hillslopes. Where the tundra is more low-lying in the middle of the catchment, the water table depths are shallower. Results suggest that the water table depths are not as heavily influenced by microtopography. The lack of distribution in water table depths

across these areas, as seen in Figures 3.9 and 3.12 confirm this as there is no clear distinction between landscape types. Total precipitation for the summer, as well as SWE stored on the land were historically low, and we suggest that this lack of variability between the simulations is because of a lack of moisture available in the system.

3.5.0 Conclusions

Overall, the model was able to adequately simulate the hydrological components of the basin affecting discharge and ET, and produced thaw maps that discretely followed the measured rates of thaw for hummocks and inter-hummocks. At a 10 m resolution, GEOtop can distinguish between hummocks, inter-hummocks, and shrub patches in its output. GEOtop showed that microtopography in the catchment influenced both discharge and evapotranspiration in the basin but had little influence on water table depths. A 1-soil to 2-soil comparison showed that the 2-soil simulations responded to freshet quicker by two days and created a delay in ET. Active layer thaw in the basin seems to show a stronger influence from microtopography than larger topographical features such as slope, aspect, and elevation, which is consistent with Endrizzi et al. (2011). The simulations with only shrubs had freshet begin a day earlier than the snow-only model and had smaller values for ET for most of the summer. These values did match measurements in the field. Active layer thaw for the shrub-only simulation was slightly shallower than the other simulations. This is likely limited because of how dry the catchment was for the summer and how thermal conductivities of peat decrease with decreasing soil moisture. As snow was only on the ground when the active layer was very shallow, very little of this water infiltrated into the ground.

Chapter 4

Assessing Ground Thaw Variability and Hydrological Regime Changes Between a Normal and Dry year for a Small Arctic watershed

4.1 Introduction

The rates of Arctic warming are 2-3x higher than those of the global average (Tetzlaf et al., 2018; Burn & Kokelj, 2009). The consequences of this are widespread, with the increased thawing of permafrost a common theme in these changing ecosystems; precipitation over the Arctic has increased by almost 8% (Young et al., 2006); and the expansion northward of the tree line (Wilcox et al., 2019). Webb et al. (2022) showed how many Arctic lowlands in lake dominated landscapes are becoming drier, despite increases in air temperature and precipitation. However, Olthof & Rainville (2022) compared Google Earth imagery to the National Hydrographic Network and found that wetting trends were more common than drying trends. In the area close to this study, in the Tuktoyaktuk peninsula, Olthof et al. (2015) found that lakes are expanding, a trend that is consistent across the pan Arctic (Olthof et al., 2015). The spatial and temporal distribution of wetter or drier conditions in the Arctic is a concern for northern ecosystems and communities (Olthof et al., 2015).

A persistent problem in Canada is the declining number of long-standing research stations which can monitor long-term changes (Tetzlaff, et al., 2017). To determine if catchments are becoming drier or wetter, there needs to be sufficient coverage of data temporally to determine trends. Webb et al. (2022) suggests that increasing air temperatures as well as autumn rains will lead to a decrease in surface water through two methods: permafrost thaw, or evapotranspiration. Of these two, permafrost thaw is much more responsible for this than evapotranspiration (Webb et al., 2022). As Webb et al. (2022) showed, despite the increase in precipitation and temperature, it is still possible for a catchment to become drier. While Webb et al. (2002) found that precipitation-evapotranspiration changes due to air temperature increases were negligible for affecting surface water decline, this makes other variables such as soil moisture studies and those that affect this and are linked directly to active layer thaw more important.

One of the best ways to observe and detect widespread change is through landscape change analysis, typically via satellite detection. Landscape change using satellite imagery has been a popular method for change detection, NDVI analysis, as well as for observing land surface temperatures (Muster et al., 2015; Jorgenson et al., 2018). This is because of its ability to cover vast areas with little effort. However, spatial heterogeneity is a common problem and results from one site are not consistent for all sites (Jorgenson et al., 2018).

One downside to using satellite imagery is the coarse resolution that these typically offer. Even today, some of the best publicly available imagery is only 10 m (Sentinel-2). Interpretation of these images for features that are smaller than this resolution can be incredibly difficult, and as Endrizzi et al. (2011) showed, microtopography is the primary driver of spatial variability in ground thaw. Features such as hummocks and inter-hummocks, sedges, tussocks, and shrubs are typically all around 1 m in size and are difficult to distinguish in satellite imagery. This can lead to many assumptions and estimations having to be used to analyze imagery and to incorporate these in modelling efforts (Ajami et al., 2015). There have been advances in the use of UAV imagery, which can produce hyper-scale images with resolutions that are centimetres in scale (Walker et al., 2020). Making it possible to capture and analyze microtopography in Arctic ecosystems.

In the upland region to the east of the Mackenzie Valley, microtopography can consist of hummocks and inter-hummocks (Quinton et al., 1999). The hummocks in this area are made of mineral earth soils composed of silts and clays (Quinton et al., 1999; Quinton et al., 2000). The inter-hummocks areas are largely dominated by thicker layers of peat, which are highly conducive to allowing water to flow through them. Hummocks are one of the driving factors of spatial variability of soil moisture in the sub-surface, and thus of thaw (Endrizzi et al., 2011). They essentially act as an impermeable boundary on the open tundra and the hillslopes, creating a tortuous network through the inter-hummock zone that water must follow to reach the streams.

This has direct implications on ground thaw, as well as the hydrology of these catchments. For example, as peat is dominant in the inter-hummock zones, we should expect shallower active layer thaw (Oke, 1987; Farouki, 1981). Chapter 2 of this thesis explored the relationship between peat thickness and thaw during a dry summer and found this to hold true.

Which should also mean that the opposite should hold true for a more normal to wet year where thaw is deeper than normal.

For comparison, the summer of 2016 compared to the average was a normal year for the TVC area, where precipitation was recorded to be 283 mm, and where the average from 1992 to now is 240 mm. Snow water-equivalent (SWE) stored on the ground before freshet was just over the average (1992 to 2021) of 150 mm, at 159 mm. Seasonal summer temperatures were found to be similar to the long-term average of 11°C. In conjunction with 2021, this provides a unique opportunity to analyze how dry vs. normal conditions over the course of a summer can influence a small Arctic catchment typical of the Mackenzie Uplands.

This chapter seeks to explore the differences in ground thaw, as well as water balance components, for a small Arctic catchment between a dry year and a normal year. To do this, the numerical model GEOtop will be used as it can adequately include microtopography, shrubs, and snow, and it is able to couple the heat equation with the Richard's equation in the subsurface (Endrizzi et al, 2011). GEOtop will allow us to analyze both the hydrology of the catchment under different climate conditions, as well as how each affects the development of the active layer and water table depths. The objectives of this chapter are twofold:

- To analyze how a wet and dry year influenced ground thaw in a small Arctic catchment, and
- To understand how these different types of years can impact the catchment should these wetting or drying phenomena become persistent.
-

4.2 Study Site

This study occurs across the entirety of Siksik Creek, a 1 km^2 sub-catchment of Trail Valley Creek (Figure 4.1). Siksik Creek is representative of catchments in the Mackenzie Uplands (Quinton and Marsh, 1999; Quinton et al., 2000). Being north of the Arctic tree line, taller shrubs are largely confined to the riparian zone and south-face slopes of the catchment; hummocks and inter-hummocks are ubiquitous throughout the catchment; it lies within the continuous permafrost zone and is dominated by open tundra (Wilcox et al., 2019). The catchment is dominated by mosses and lichens, where peat typically underlies these (Wilcox et al., 2019). Stratigraphically, mineral earth soils underly the layer of peat, and where its thickness

is spatially heterogeneous and depends on many of the topographical features of the basin (Quinton et al., 2000). The summer of 2021 was warm and incredibly dry. It was the 7th warmest summer, and the 3rd driest, with the driest July ever recorded (Environment and Climate Change Canada).

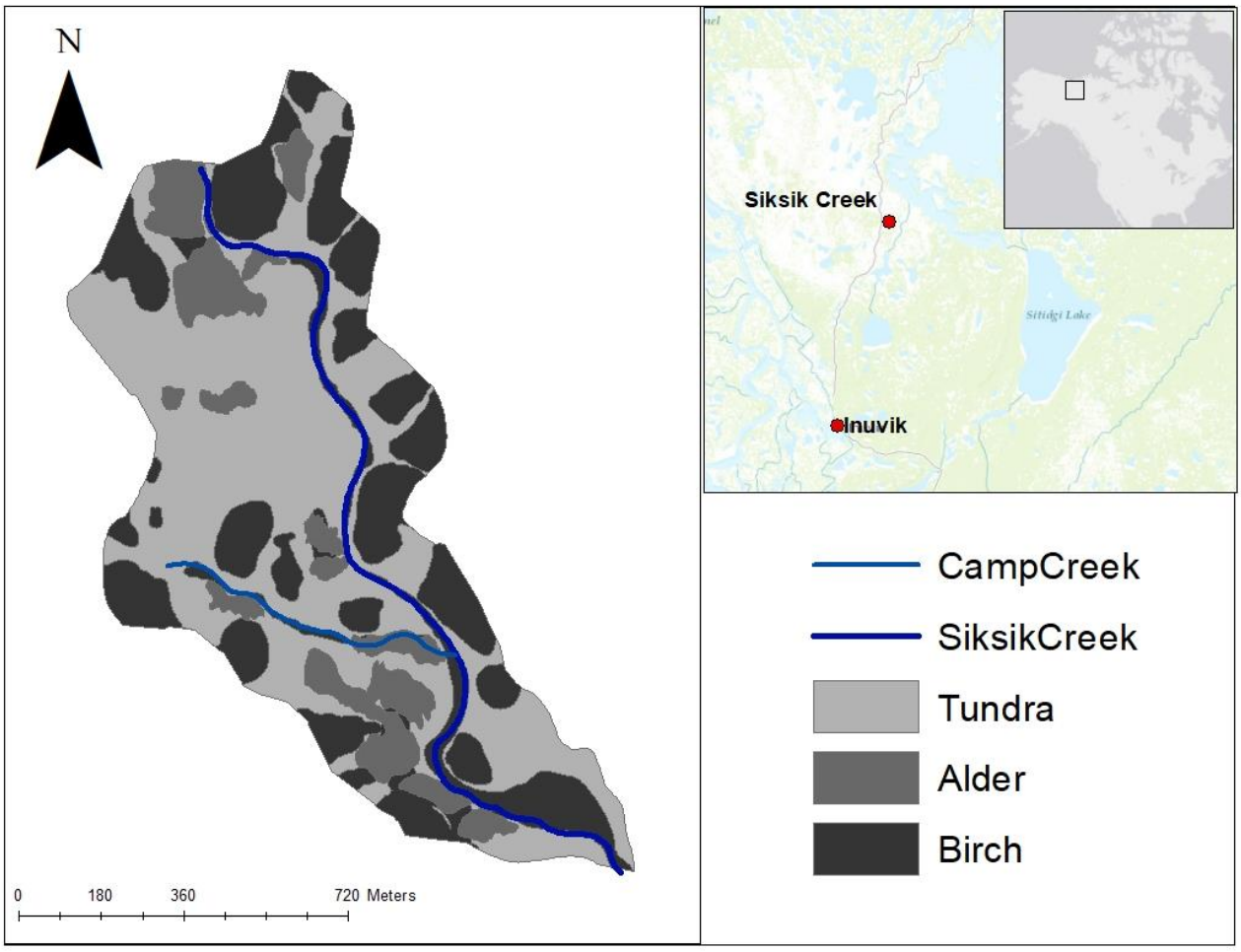

Figure 4.1: Siksik Creek, a 1 km² watershed located within Trail Valley Creek. The catchment is largely open tundra with the occasional alder and birch shrub patches on the hillslopes and within the creeks.

4.3 Methods

The following sub-sections describe the various ways in which data was collected in the field during the summer of 2021, as well as the postprocessing of this data into a format that could be used by GEOtop (V2.1). The data collected included peat thicknesses used to define hummock and inter-hummock zones, snow surveys to provide estimates of SWE, UAV imagery that provided a classified map of mosses, lichens, and shrubs; as well as stream discharge, evapotranspiration via an eddy covariance tower, and the other meteorological data measured at TMM. This data was then used to simulate Siksik Creek for two summers: 2021 and 2016. The results for 2021 are the same as those seen in Chapter Three for the 2-soil Snow and Shrub simulation. The results for 2016 only change the initial snow stored on the ground before melt as well as precipitation throughout the summer.

4.3.1 - Peat Thicknesses & Mapping Hummocks

The peat thicknesses that were measured in situ and used in GEOtop for the entirety of Siksik Creek were measured as seen in Chapter 2. Both hummocks and inter-hummocks will be included in the following simulations along with peat and mineral earth soil layers underneath. Soil pits, coring, and drilling were used to determine spatial variability in peat thicknesses across mosses, lichens, hummocks, and inter-hummocks, as described in Chapter Two, section 2.3. These measurements were taken at the end of the summer of 2021, when the active layer was at its thickest. It was found in Chapter Two that there was a relationship between mosses, lichens, hummocks, and inter-hummocks, where mosses tended to lay overtop of inter-hummocks, and lichens overtop of hummocks.

This relationship found between hummocks & lichen, and inter-hummocks & moss, allowed us to use UAV imagery to determine the location of hummocks and inter-hummocks across Siksik Creek. The UAV imagery was taken in mid-June, when all of the snow in the catchment had melted, and where the tundra had fully bloomed creating a vibrant vista of reds, greens, and whites. The imagery was taken in the RGB spectrum, and an unsupervised classification was run to separate the catchment into three segments: reds to represent the mosses, and thus inter-hummocks; whites to represent lichens and thus the hummocks; and green to represent sedges, tussocks, and both smaller and taller varieties of shrubs. This was done at the centimetre scale before being scaled up to 10 m to be used as an input map for GEOtop. This classified map can be seen in Chapter Three, section 3.3.4.

4.3.2 - Water Balances

The data used to calculate the water balance for the summers of 2016 and 2021 were physically collected throughout the summer for each year. The variables measured continuously include stream flow, snowmelt, evapotranspiration, and precipitation. Snowmelt was collected throughout the melt period with snow surveys in and around TMM measuring the changing SWE in the snowpack. Evapotranspiration was measured at an eddy covariance tower next to TMM at an hourly rate. Streamflow was measured in-situ at a weir and with handheld anemometers for the summer of 2016, and just with the anemometer for 2021. Precipitation was measured with a GEONOR sensor at TMM.

This balance is typically calculated as seen in Marsh et al., (2002) with the equation:

$$P_s \pm (T\text{-}S_b) - S_s + M + P_r - E - Q = \Delta S \pm e \quad (4.1)$$

Where P_s and P_r refer to precipitation as snow or rainfall, T is blowing snow into or out of the catchment, S is sublimation during these events, M is snowmelt of snow-covered areas, E is evapotranspiration, Q is stream discharge, and ΔS is a change in storage with e as the error term. However, this thesis uses a revised version of this equation where a snowmelt variable is introduced to account for changes in SWE during the winter and right before the melt period, as measured right before snowmelt. This changes the equation to:

$$\Delta S \pm e = Sm + Ps + \mathrm{Pr} - Et - Q \quad (4.2)$$

Where ΔS is the change in storage with e as the error term, Sm is the snowmelt variable, Pr and Ps are precipitation as rain or snowfall, Et is evapotranspiration, and Q is discharge.

4.3.3 - GEOtop Initialization

GEOtop (V2.1) is a physically based, distributed hydrological model, discretized into a finite regular grid where the heat and groundwater equations are solved with finite difference schemes (Endrizzi et al, 2011). The model domain for both the wet and dry simulations had the same initializations as that seen in Chapter Three, with snow present on top of the ground surface (although in different amounts) at a constant depth; the lateral boundaries and top boundary allowed for precipitation and energy balances at the surface and to infiltrate into the subsurface,

as well as the flow of water out of the catchment at the outlet. The top and lateral boundary conditions are Neuman in nature. The bottom layer boundary condition was closed at the 8 m mark, where Endrizzi et al. (2011) suggests that the exchange of heat and or water is zero. This boundary was set to a constant -6 °C, is Dirichlet in nature, and is known as the depth of zero amplitude.

The inputs necessary for GEOtop to run in 3D require a digital elevation model, as well as models of slope, aspect, and sky view factor. GEOtop also requires that the different soils and landscape types be distinguished in a similar fashion. These maps were produced from two sources: the first was from LIDAR imagery flown by Chris Hopkinson (2011) which provided the DEM, which in turn provided aspect, sky view factor, and slope maps; secondly, UAV imagery from June of 2021 provided the landscape and soil type maps were produced using unclassified RGB imagery. This provided a DEM of the area at a 1 m resolution, and the UAV imagery produced maps at a scale of 13 cm; these were both upscaled into 10 m imagery to facilitate the modelling of the catchment.

The soil parameters that GEOtop requires are the lateral and vertical hydraulic conductivities, the depth of each soil layer, where porosity, specific storativity, and the van Genuchten and Mualem parameters are defined for each soil type. The values used in this chapter and their description can be seen in Chapter Three in sections 3.3.4 and 3.3.5.

Meteorological inputs included precipitation, wind speed and direction, relative humidity, air temperature; air pressure, cloud cover, and both short wave and long wave incoming/outgoing radiation. These are all collected from the main meteorological station (TMM) located in Siksik Creek, where data provided by the Meteorological Service Canada's (MSC) met station, which is 15 m away from TMM, is used to gap fill. Evapotranspiration in the catchment is measured at an eddy covariance tower, roughly 10 m distant from TMM. A better example of how GEOtop uses these to calculate heat transfer into the ground, ground water flow, and vegetative shading can be seen in Chapter Three in sections 3.3.4 and 3.3.5.

4.3.4 - Wet vs. Dry Simulations

Precipitation and SWE data from 2016 will be used in GEOtop to simulate the catchment during an average year and compare it to a dry year (2021). The summer of 2021 was the 7th warmest, and 3rd driest summer recorded in the catchment with a wide range of data collected

over the summer. This can also be seen in Figure 4.2 where monthly precipitation across June, July and August are shown as well as the sum of summer precipitation with a trend line from 1992 to 2021; and in Figure 4.3 where the maximum, minimum, and mean temperatures for each summer are plotted against a line of best fit. The summer of 2016 was chosen for several reasons: First, we can see from Figure 4.2 that precipitation over the summer for the 2016 year was just above the summer average of 92 mm at 118 mm, whereas 2021 was far below the average at 57 mm. In Figure 4.3, 2016 was about as warm as 2021 with the average and maximum temperature being similar. Figure 4.4 shows the end of winter snow water equivalent (SWE) for each year, which is the amount of snow stored over the course of the winter on the landscape, and can provide as much as 80% of the yearly streamflow (Marsh and Woo, 1981). We can see from this figure that 2016 and 2021 differ, with 2016 near to the average amount of SWE at 159 mm, whereas 2021 has far less than the average at 84 mm. These two years have comparable summer temperatures but differ greatly in the amount of water each year has available in the basin, allowing us to test singularly the role that moisture has on active layer thaw and how water balances change. Both simulations will use the same soil and vegetation parameters and input maps. Each simulation will use the recorded meteorological data for 2021, where the wet simulations for 2016 will change only the initial snow stored on the ground before melt and the precipitation received in the catchment throughout the summer. Active layer thaw, water table depths, and water balance components will be analyzed to assess the differences that a wet and dry year will have on a small Arctic catchment.

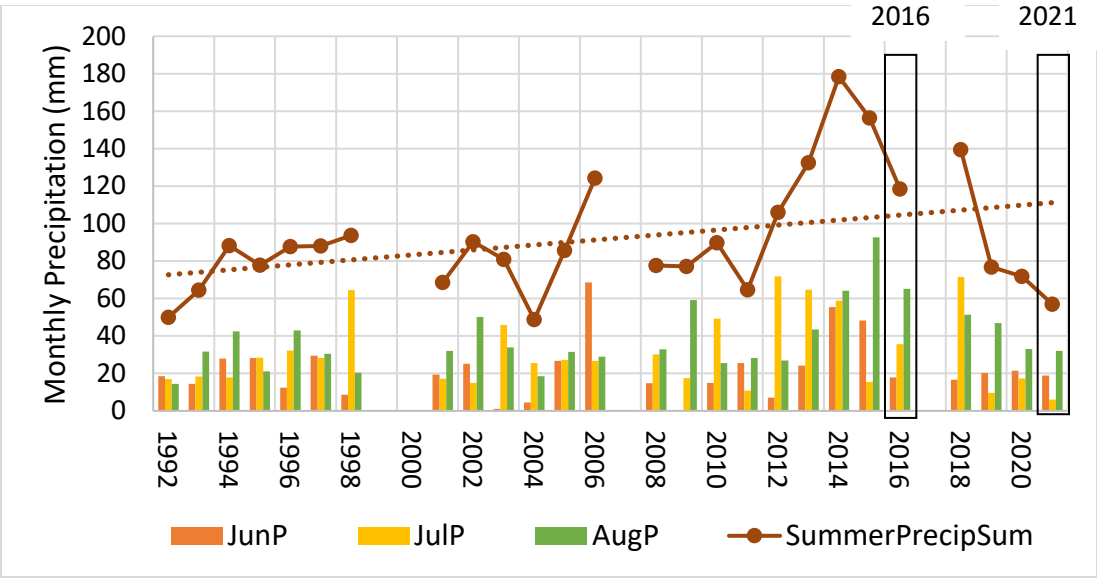

Figure 4.2: Monthly and monthly total Precipitation for June / July / August, as well as their cumulative sum for the summer seen in the red line from 1992 to 2021. 2016 and 2021 had vastly different amounts of precipitation over the summer, with 2016 receiving nearly double the precipitation over the summer than 2021 did.

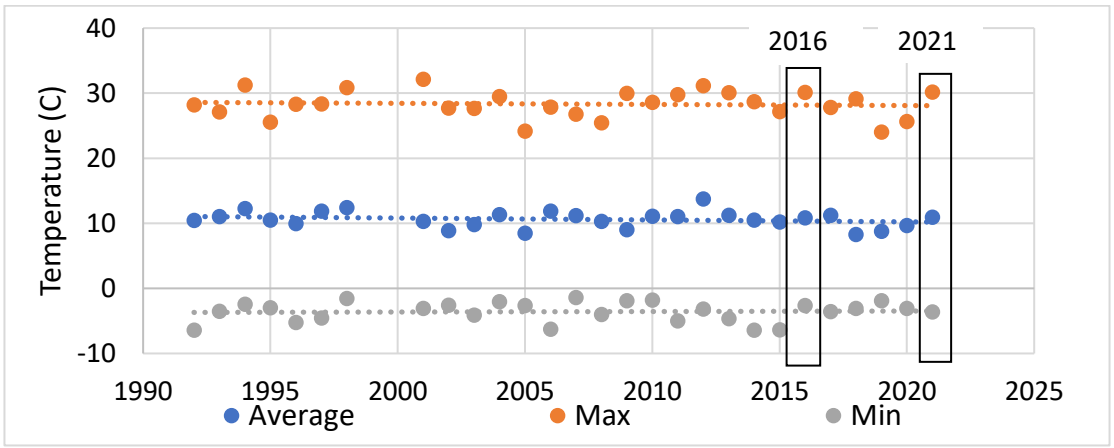

Figure 4.3: Averaged mean, minimum and maximum summer temperatures from 1992 to 2021, showing that both 2016 and 2021 were warmer than the average. As well, both their minimum and maximum temperatures were above average as well, indicating that they were both warm years.

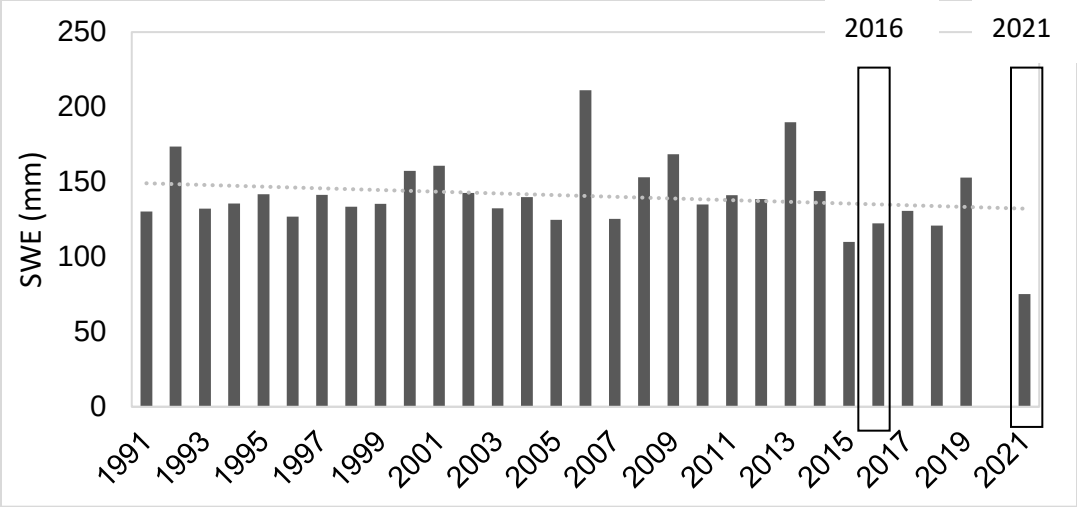

Figure 4.4: End of winter snow water equivalent (SWE)t for Siksik Creek from 1992 to 2021. No Data was collected in 2020 because of Covid-19. 2021 had barely half of the long term average whereas 2016 was similar to the average SWE.

4.4 Results

This chapter seeks to investigate any differences in modelled ground thaw for wet and dry conditions in a small Arctic catchment – Siksik Creek. This continues from the results and methods seen in Chapter 3, where a two-soil domain was discretized to include both hummocks and inter-hummocks. The following is a comparison of simulation runs for 2016 and 2021.

4.4.1 - Water Balances

These two years were drastically different, as 2016 had nearly double the precipitation and SWE stored on the ground than 2021, which led to higher amounts of streamflow (Figure 4.5). However, there was little difference in evapotranspiration between the two years. The summer of 2021 had a negative net balance of -38 mm of water whereas 2016 had a net gain of 28 mm of water. Simply put, 2021 lost 25% of the total contributions to the basin, and 2016 gained 13 % of its contributions.

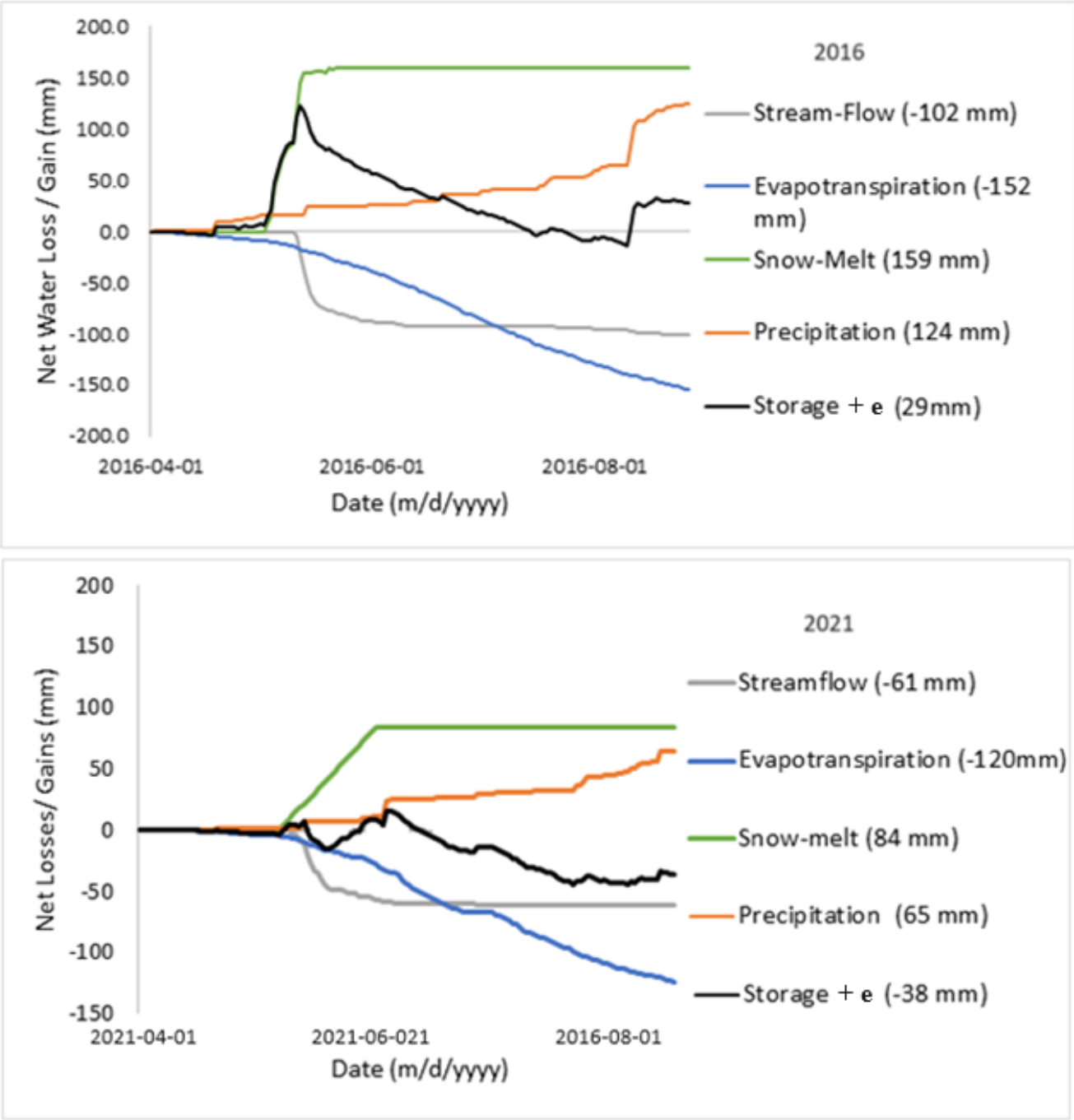

Figure 4.5: Water balances for 2016 and 2021 based on measurements taken throughout the catchment for each summer, as described in the methods section. Note that the storage term also encompasses the errors.

4.4.2 - Frost Table and Water Table Depths

A comparison of active layer thaw depths, and water table depths, as modelled by GEOtop, are shown in Figure 4.6 for 2016 and 2021. Similar to what was seen in Chapter 3, both simulations show active layer thaw variability due to the presence of microtopography. The 2016 simulation has a deeper active layer thaw than that for 2021, as shown by the red colours, as well as a shallower water table, as shown by the darker blue colours. Both the maximum and minimum thaw depths shifted by at least 3 cm, and both the mean and median shifted by as much as 5 cm (Figure 4.7). There are some common themes between the two, where in and around the creeks still hold the highest active layer thaw depths, and where the hillslopes typically have the smallest thaw depths; further, for both simulations, microtopography can be seen to influence the spatial variability of thaw.

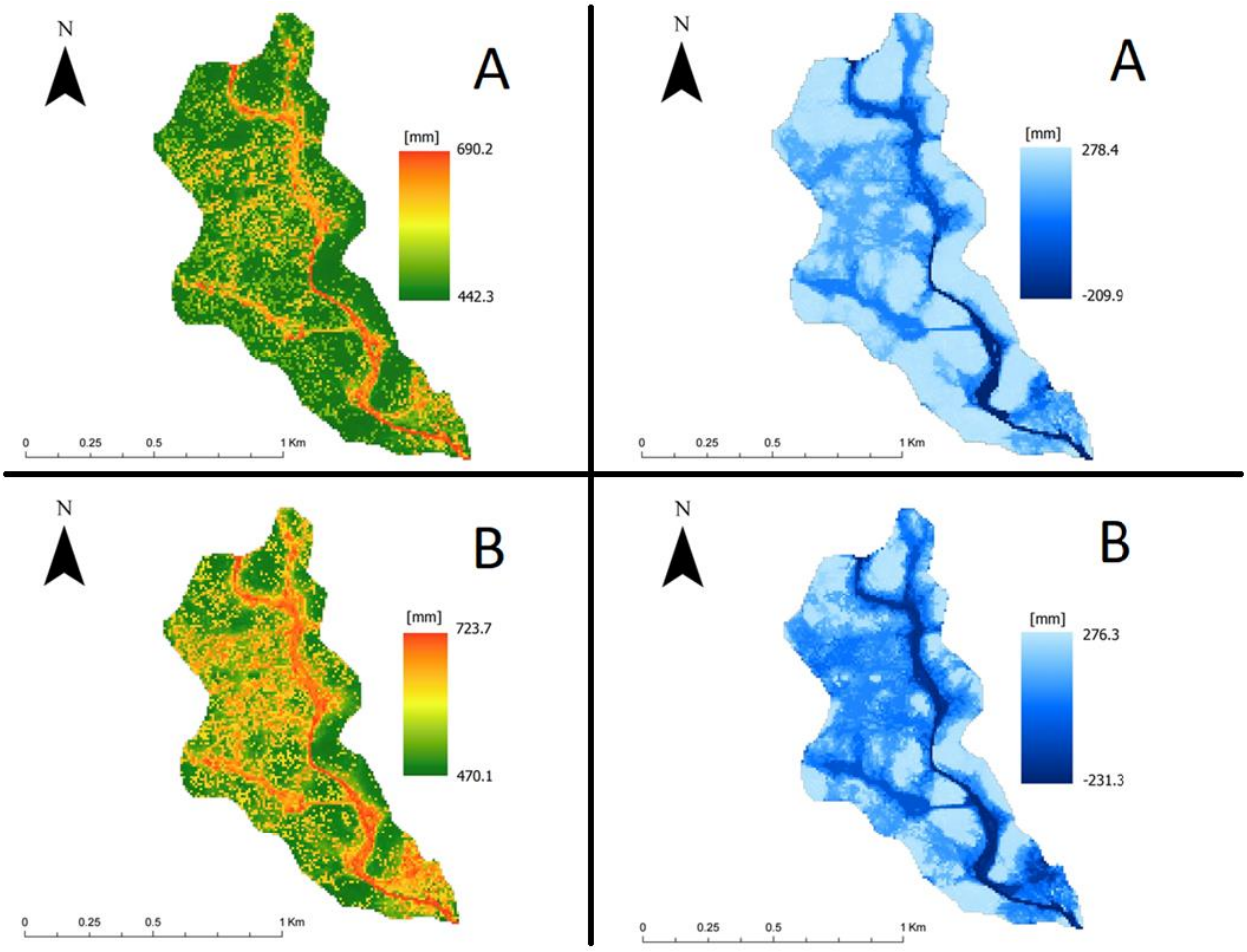

Figure 4.6: A is 2021, B is 2016. The left side is active layer thaw and on the right are water table depths at the end of summer. 2016 has more of the catchment thawed, with deeper depths overall. This is true for the water table depths as well where more of the subsurface is inundated with water.

Using a Chisquare test we can try to determine if these thaw depths are dependent or independent of the year. Our null hypothesis stated that the thaw depths were independent of the year, and our true hypothesis was that they were dependent on the year. The degrees of freedom for the test was 19, and at a 5% significance our CV is 30.1. When tested in this manner our X^2 is 859, thus we can reject the null hypothesis and state that these two data sets are dependent on the year, and thus are significantly different.

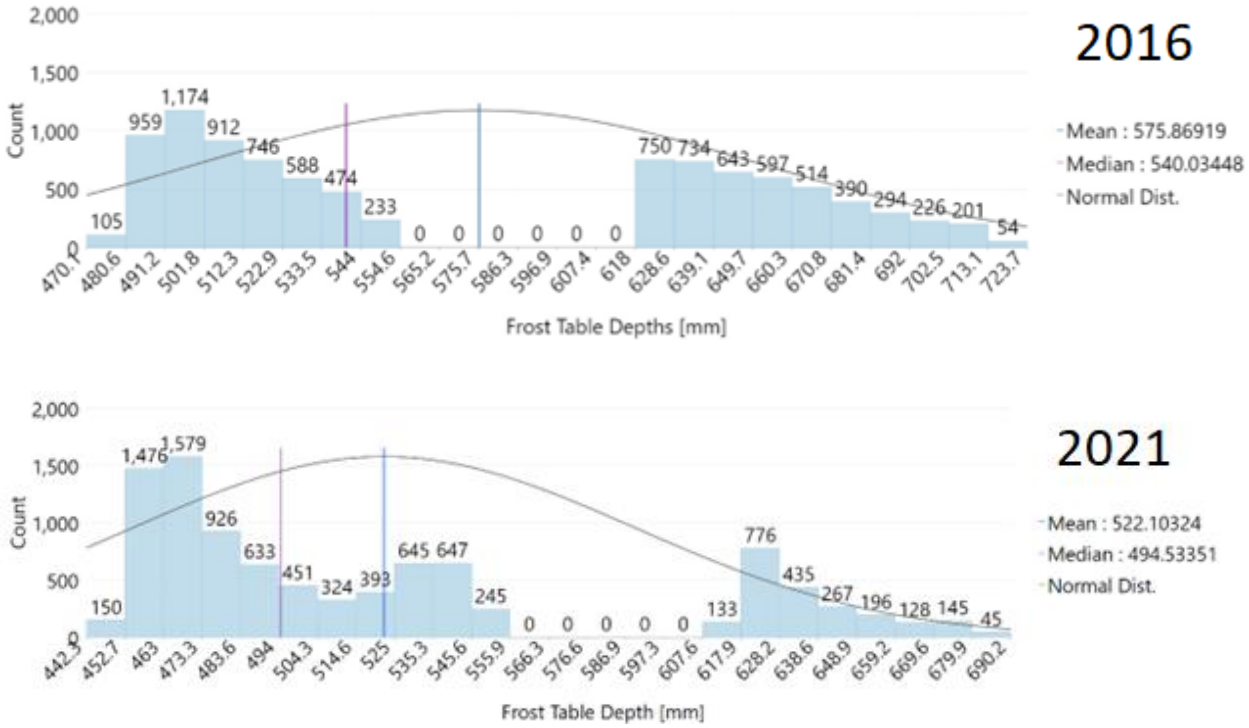

Figure 4.7: Distribution of active layer depths for both the summer of 2021 and 2016. The curved line shows the normal distribution, the purple the median value, and the blue line the mean depths. The depths for 2016 are much deeper than for 2021, with more of the distribution lying within the deeper portions of the graph.

The water table depths show a differrence between the wet and dry simulations, however the maximum and minimum depths between the two simulations are similar (Figure 4.6). Between the two, both the mean and median decreased by 4 and 7 cm respectively (Figure 4.8). The water table for 2016 for the majority of the catchment moved closer to the surface, which signifies that there was more water stored in the subsurface during the wet simulation than there was during the dry simulation. Compared to 2016, there are still patches throughout the basin that have a deeper depth than 2021. These patches correspond quite well with the locations of

shrub patches in the catchment that were discretized into the model, seen in Figure 4.11. The only difference is near the mouth of the catchment where the elevation is flatter and presumably where there is more ponding of water as suggested by the simulation.

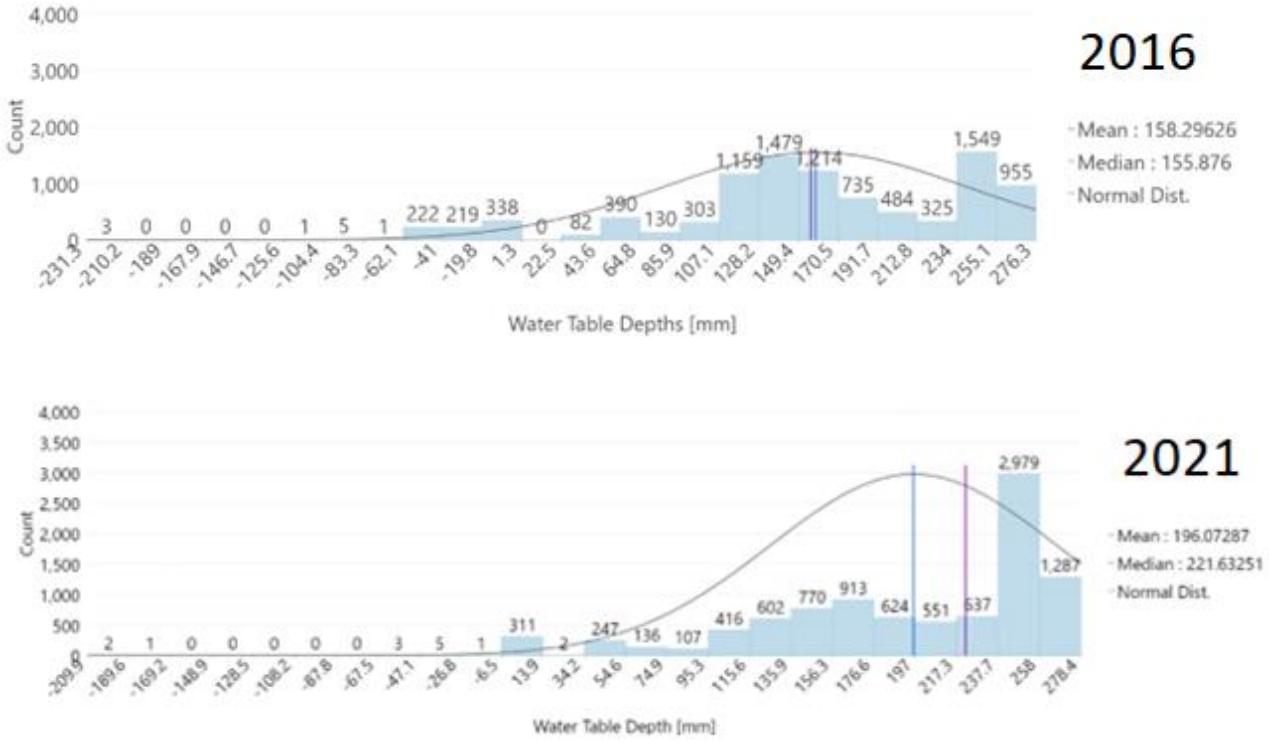

Figure 4.8: Water table depths, top is 2016, bottom is 2021. The curved line shows the normal distribution, the purple line is the median value, and the blue line is the mean depths. 2016 has shallower water table depths with more of the distribution lying to the left.

4.4.3 - Comparison of Hydrological Components

A comparison of the daily and cumulative modelled discharge between the wet and dry simulations (Figure 4.9), and the daily and cumulative modelled evapotranspiration (Figure 4.10), shows that while the timing of snow melt and peak discharge occur at the same time, the volume of water flowing out of the basin is different. The peak discharge for the summer in the daily discharge graph was over double the peak of the dry year, and the cumulative discharge for the summer tripled. The daily evapotranspiration values were typically just slightly higher for the wet simulation than the dry by less than 1 mm, and cumulatively by the end of the summer there was only 5 mm of difference between the two, but this separation maintained itself for most of the summer.

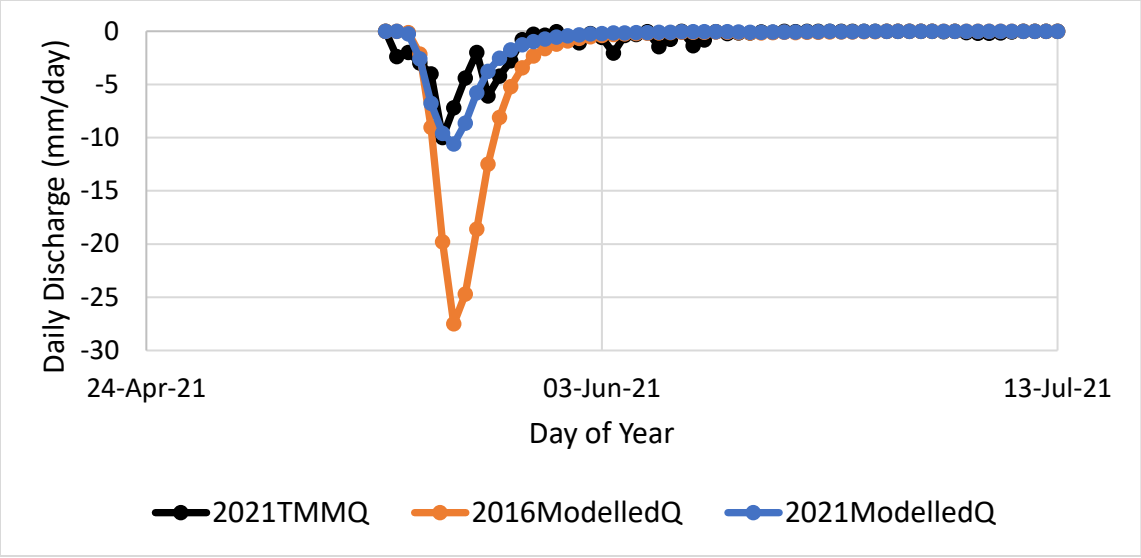

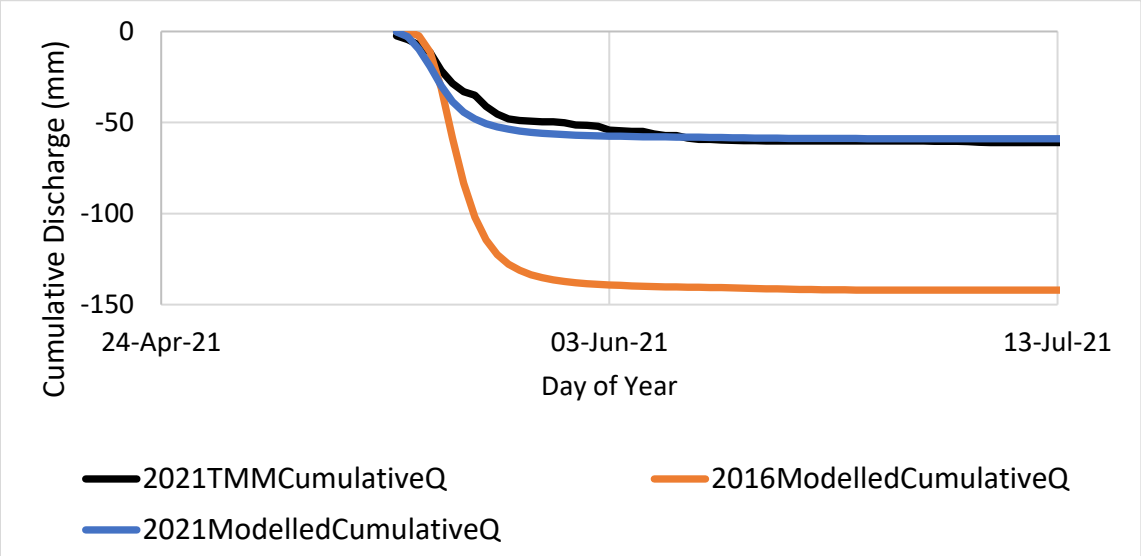

Figure 4.9: Comparison of daily and cumulative simulated and observed discharge for 2016 and 2021. 2016 in both images nearly triples the measured and simulated values for 2021.

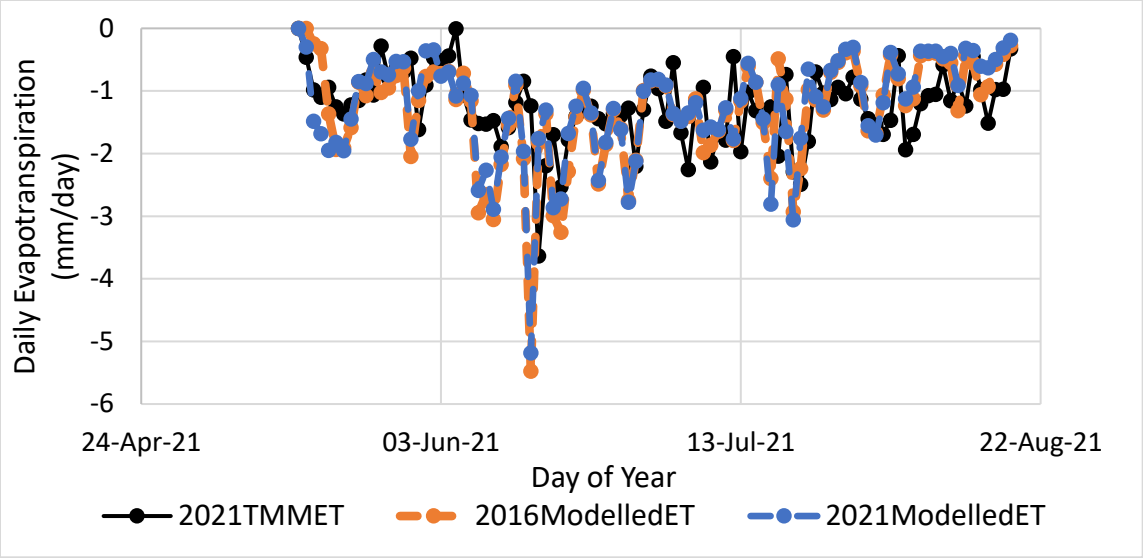

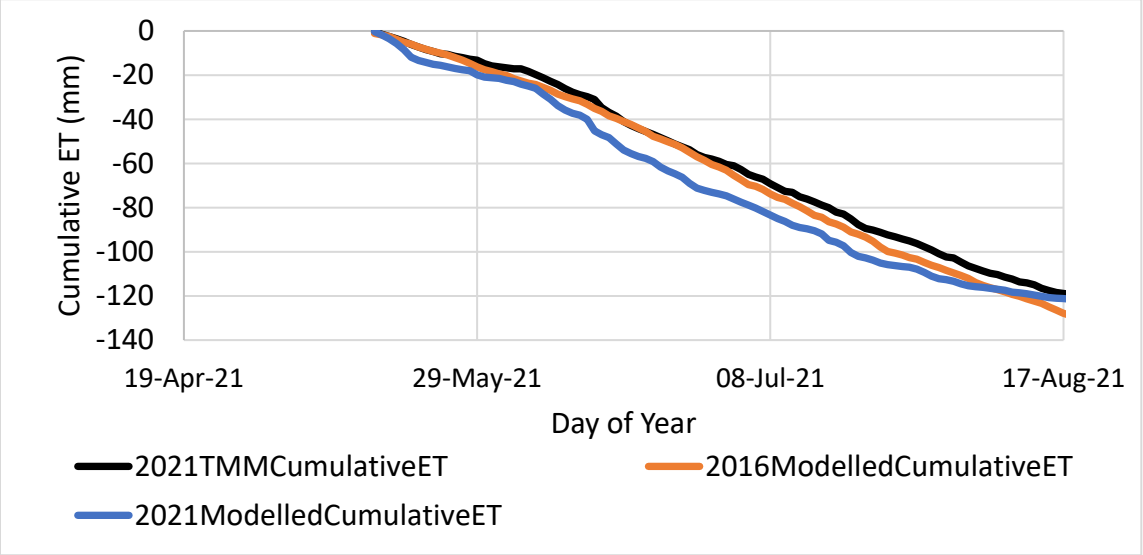

Figure 4.10: Comparison of daily and cumulative simulated and observed evapotranspiration for 2016 and 2021. There is little difference seen between the two simulations.

4.4.4 – The Importance of Soil Moisture

A comparison of soil moisture contents in the first two layers of soil are shown in Figure 4.11 from the 2016 and 2021 simulations. The first layer of soil is from 0-5 cm in depth, and the second layer of soil is from 5 – 15 cm in depth. Depths below these two layers were part of the water table and water table depth maps were used for this in later figures (4.14 and 4.15). These soil moisture contents and water table depth maps were then compared to frost table depths and part of a simplified vegetation classification of the basin to compare these across both space and time for both simulations.

Four dates were selected to compare the variability in soil moisture, water table depth, and active layer thaw over the summer (the 15th of each month). Deep active layer depths that were used overtop of the soil moisture and water table depths were isolated from the active layer maps based on the distribution of depths in the basin. These ranges differed from month to month but were chosen based on the modal distribution of the pixel count graphs for each month. The vegetation overlay was taken from Figure 4.1 and is the tundra classification, where those parts of the basin that were unvegetated and relatively flat was isolated and the birch and alder shrub patches were removed so that potential patterns of thaw based on the locations of these taller shrub patches could be analyzed. These can be seen in Figures 4.12, 4.13, 4.14, and 4.15 below.

In Figure 4.11, a comparison of soil moisture content shows that 2016 overall was much wetter than 2021 for both upper layers of soil over the summer. For both simulations, soil moisture content is high after spring freshet, lowers in July due to infiltration, root uptake and evaporation, and then slowly increases into autumn due to rainfall events. The highest amounts of soil moisture are concentrated in and around the creeks, and variably throughout the rest of the catchment, presumably in either the hummock or inter-hummock zones. The hillslopes in and around the creeks tend to have the lowest amount of soil moisture in both layers of soils and for both simulations. The 2016 simulation shows more variability in moisture contents, especially in the more open, tundra portions of the catchment.

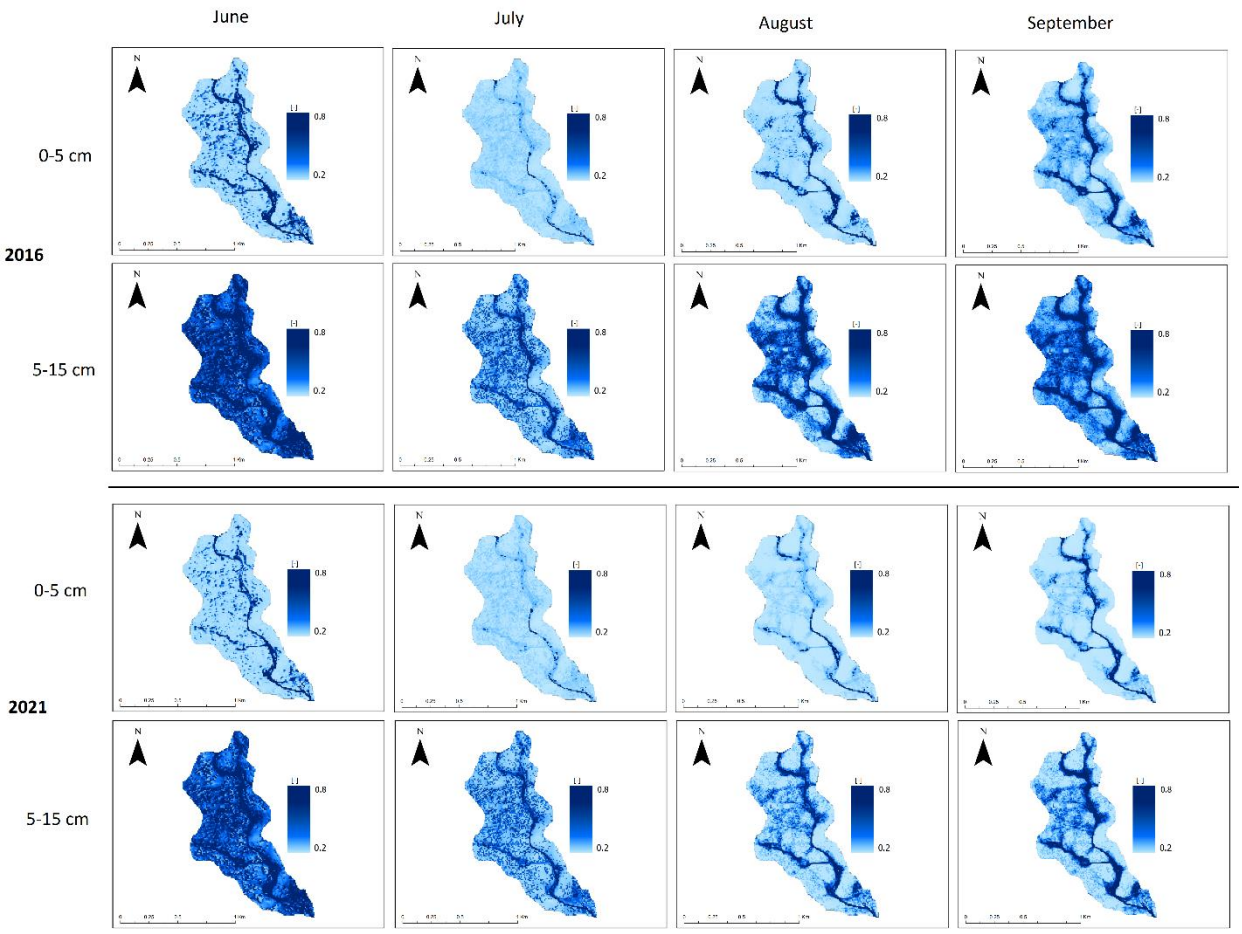

Figure 4.11: Soil moisture content from 0-5 cm and 5-15 cm for the 2016 and 2021 simulations. Darker blues are higher soil moisture content. End of summer soil moisture content is higher for 2016 for both layers of the soil.

As many studies have shown, thaw in northern catchments is highly linked to soil moisture content (Farouki, 1981; Beringer et al., 2001; Mustamo et al., 2019; Zhao et al., 2019). We should expect to see a deeper active layer thaw where soil moisture content is higher, and vice versa. Further, where taller shrubs exist in the catchment because of canopy shading we should see shallower thaw depths, but it is unclear how this might correspond to soil moisture. Figures 4.12 and 4.13 explore these relationships temporally and spatially across Siksik Creek in both simulations.

As shown in Figure 4.12 and Figure 4.13, the active layer progressively deepened over the summer, where depths were deepest in and around the creeks, and at some points in the tundra. Spatial variability in thaw developed further into the summer as the active layer thickened. For both 2016 and 2021, the shallowest thaw tended to be where the tall shrub patches existed, and in the creek (Row B). In Row E the lowest amounts of soil moisture content were

also in these areas. When we overlap the deepest thaw depths for each summer date, the highest amounts of soil moisture content correspond to the deepest active layer thaw depths (Row D). There are also some differences between the two figures as well. For both active layer thaw and soil moisture content, the values and extents are greater for the wet simulation than the dry simulation at almost all points throughout the summer, but especially at the end of the summer.

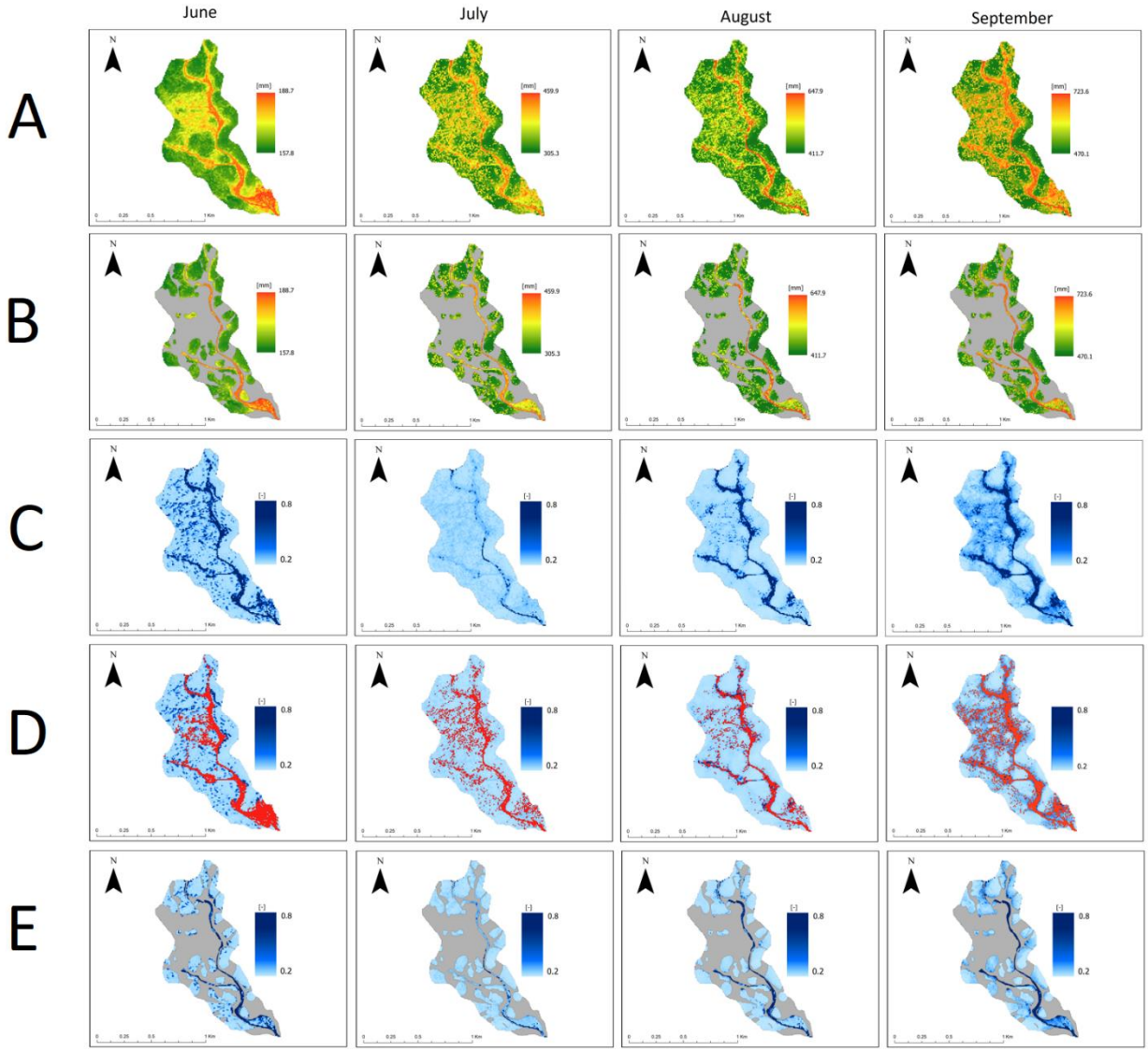

Figure 4.12: A comparison of active layer depths to soil moisture contents and vegetation for 2016. Row A is the unmodified active layer depths from June 15th to September 15th, Row B is the tundra classification over top of the active layer map, Row C is the unmodified soil moisture content maps for the 0-5 cm depths, Row D is the deep active layer depths over top of the soil moisture content map, and Row E is the tundra classification draped over the 0 – 5 cm soil moisture content map.

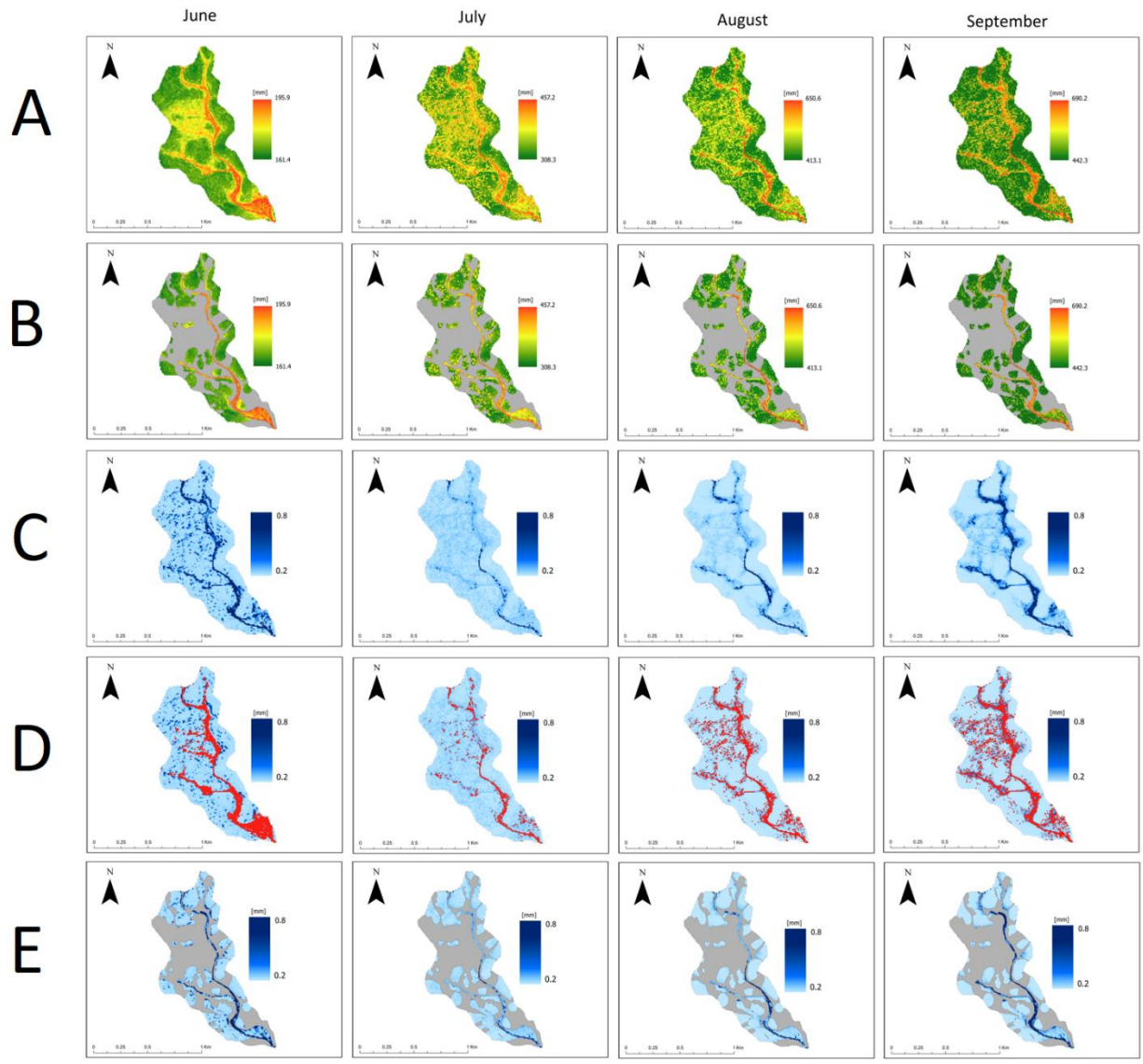

Figure 4.13: A comparison of active layer depths to soil moisture contents and vegetation for 2021. Row A is the unmodified active layer depths from June 15th to September 15th, Row B is the tundra classification over top of the active layer map, Row C is the unmodified soil moisture content maps for the 0-5 cm depths, Row D is the deepest active layer depths over top of the soil moisture content map, and Row E is the tundra classification draped over the soil moisture content map.

When we compare active layer depth to the depths to the water table, seen in Figures 4.14 and 4.15, the 2016 simulation has a more vibrant map in the deeper blues, with the shallowest depths to the water table covering more of the basin. The deepest thaw depths correspond well with the shallowest depths to the water table (Row D). The deepest depths to the water table correspond well with the tall shrub patches (Row E). In June and July, the water table depths correspond with the hummock and inter-hummock zones, but the influence of hummocks seems to disappear as the summer progresses, as noted in Chapter 3. Similar to the soil moisture content

figures above, again in Rows D and E, 2016 had much more of the water table depths show around the overlays than 2021 did. There was deeper thaw, and thus more overlay, and still it showed through this. The same holds true for the tundra overlay, although this overlay did not differ. Where these patterns differed was in the creeks, and near the mouth of the catchment which is flatter than most of the basin.

One of the largest differences between Figures 4.14 and 4.15 however is the seasonal pattern of depths to the water table. For both the 2016 and 2021 simulations, the catchment starts with deeper depths across the catchment except around hummocks and the creek. Into July the water table becomes shallower across the basin, and from here the two years differ. The 2016 simulation continues this pattern into July, whereas the 2021 simulation has much of the basin begin to have deeper depths to the water table. These deeper depths to the water table correspond well with the tall shrub patches. This continues into September, whereas for the 2016 simulation it is only in September where this pattern becomes apparent. There is a lag between the two simulations before plant uptake can affect water table depths.

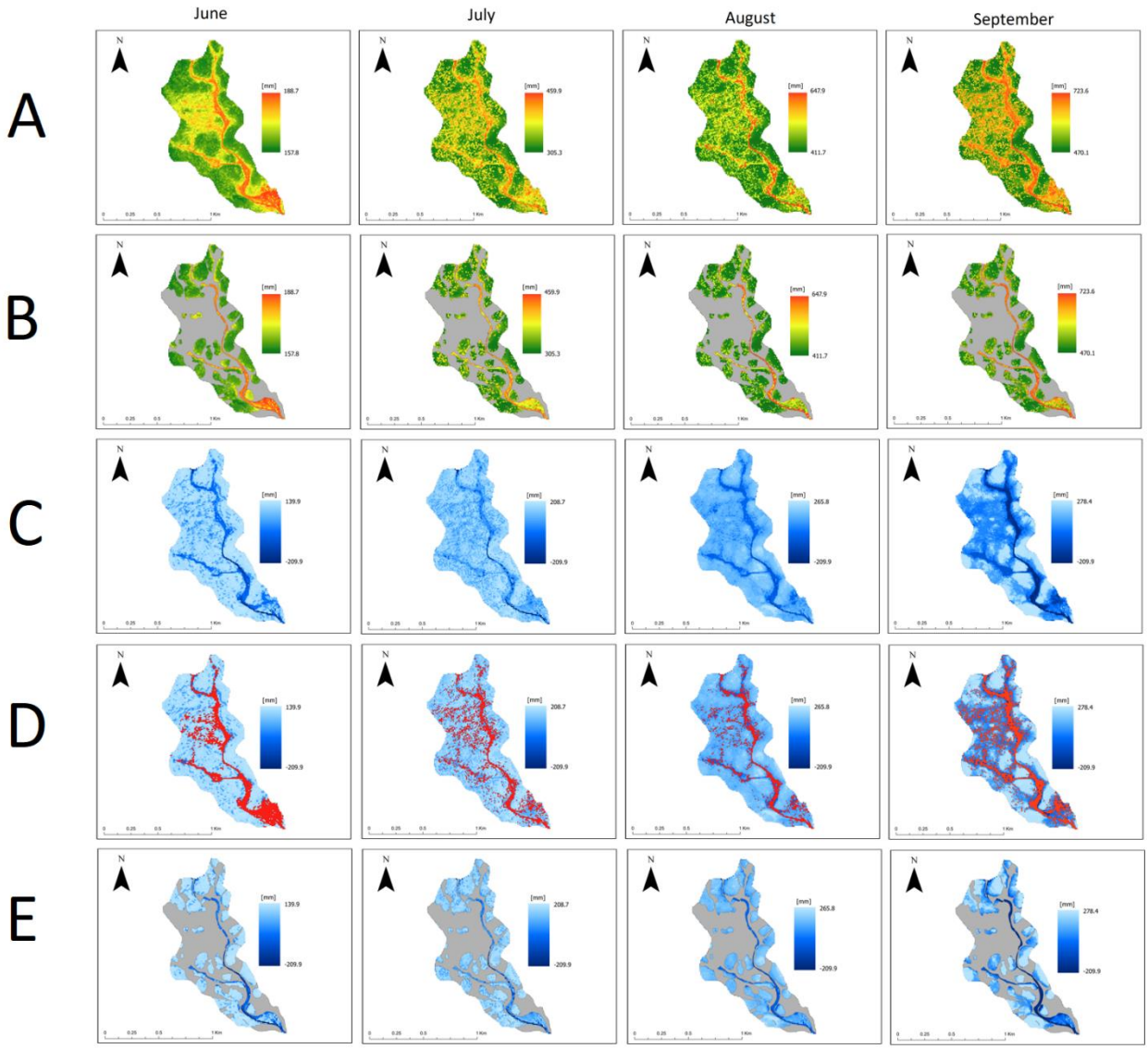

Figure 4.14: A comparison of active layer depths to water table depths and vegetation for 2016. Row A is the unmodified active layer depths from June 15th to September 15th, Row B is the tundra classification over top of the active layer map, Row C is the unmodified Water table depth maps, Row D is the deepest active layer depths over top of the Water table depth map, and Row E is the tundra classification over the Water table depth map.

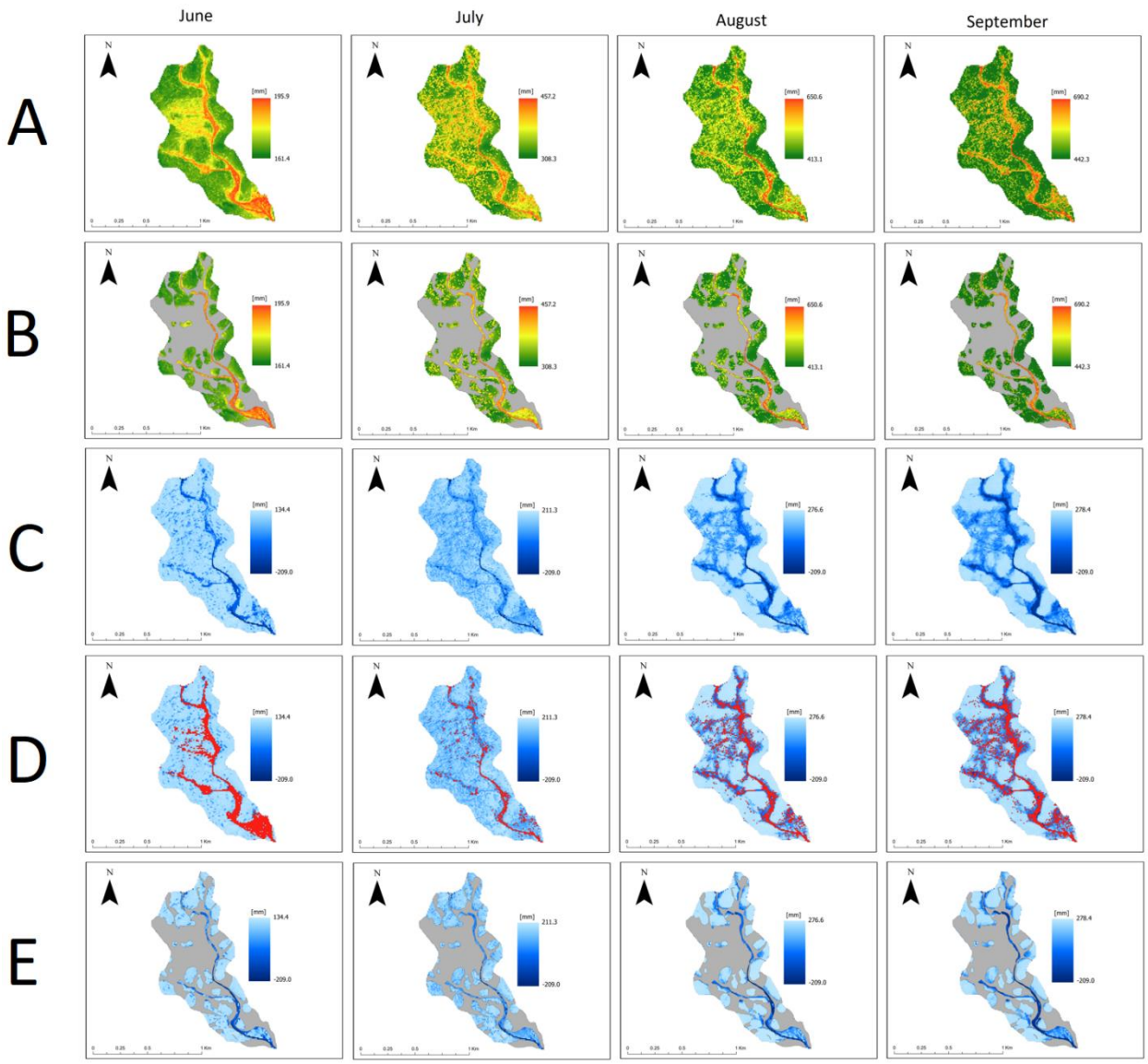

Figure 4.15: A comparison of active layer depths to water table depths and vegetation for 2021. Row A is the unmodified active layer depths from June 15th to September 15th, Row B is the tundra classification over top of the active layer map, Row C is the unmodified Water table depth maps, Row D has the deepest active layer depths over top of the Water table depth map, and Row E has the tundra classification over the Water table depth map.

4.5 Discussion

As seen in Chapter 3, end of summer thaw and water table depths between the various simulations had very little variation and difference in depths. It was speculated that this was likely due to the dry summer and the lack of moisture being held in the soil. The presence of microtopography, such as hummocks, causes spatial variability in soil moisture which will affect active layer thaw (Endrizzi et al., 2011). Results from Chapter 3 had shown shallower thaw depths were simulated likely due to the thermal conductivity of peat being linked to its soil moisture content, where increases in soil moisture increase the thermal conductivity of the soil and vice versa (Oke, 1987; Farouki, 1981). As Farouki (1981) and Mustamo et al. (2019) have noted, thermal conductivities of Arctic soils, and specifically peat, are most strongly controlled by the media occupying its pore space. Whether this is air, water, or ice, these influence the differences in thermal conductivity. In peat soils and organic soils, this increase in thermal conductivity appears to be linear with increasing soil moisture content (Konovalov and Roman, 1973; Kujala et al. 2008). As such, it is expected that a dry year will have less active layer thaw than other years with more water available, at least where peat is found.

The dry summer of 2021 was compared to a normal year (2016) to examine the effects of less available water on active layer thaw, water table depths, and components of the water balance. Thaw throughout the catchment was much greater and more widespread for the normal year than that for the dry year simulation. Mustamo et al. (2019) noted how important soil moisture content is for thaw in these Arctic catchments as the presence or lack of moisture directly corresponds to end of summer thaw depths. The role microtopography plays is to control the spatial variability of soil moisture, which then leads to spatial variability in ground thaw based on the presence or lack of water (Endrizzi et al., 2011).

While we did show this in our results for the 2016 simulation with greater mean and median active layer depths, we did not see much of an increase in the maximum depths of thaw across the catchment. With both the 2021 and 2016 simulations, the end of summer maximum active layer depths were relatively close, being within 2-3 cm of each other, where we expected to see a greater difference in maximum depth between the two simulations. In Figures 4.12 to 4.15, we see that the deepest depths of active layer thaw were in and around the creeks and where hummocks were located; the shallower thaw depths corresponded to the locations of taller

shrub patches in the catchment. In Figure 4.6, the extent of thaw in both the creeks and hummock areas encompassed more of the catchment in 2016 than in 2021. Figure 4.7 confirms this with higher counts of deeper thaw depths. Zipper et al. (2018) noted in their study that heat transport in the subsurface by advection is a function of two sources: the magnitude of groundwater flow, and the energy content of the groundwater. For the 2016 simulations we can assume that the magnitude of groundwater flow is higher, but given the relatively same temperatures, that the energy content is the same per unit area. Based on this, maximum thaw depth in the hummock zones should be consistent for both simulations and deeper in the creeks.

As hummocks typically have a thinner layer of peat (Quinton and Marsh, 2000; Endrizzi et al., 2011), it should take less time for the active layer to thaw through this layer of peat and into the mineral earth soil of the hummocks. These mineral earth soils have higher thermal conductivities than organic soils by several magnitudes (O'Connor et al., 2020). Based on this, hummocks should have deeper active layer thaw. However, hummocks are composed of finer textured soils. Here, the pore space retention of water is significantly higher, even though its hydraulic conductivity is much less than in peat and the inter-hummock zones (O'Connor et al., 2020). Wilcox et al. (2019) did note that the timing of snowmelt, and thus exposure of the ground surface to incoming insolation, does also play a role in determining the maximum extent of active layer thaw. Therefore, the faster thaw rate through the peat layer over top of the hummocks can be explained by the slight difference in depth in hummock zones between the 2016 and 2021 simulations.

Overall, Figures 4.12 to 4.15 imply a relationship between active layer thaw depths and soil moisture. This largely has to do with the Richard's equation in GEOtop and the transfer of heat from the atmosphere into the soil (Rigon et al., 2006; Endrizzi et al., 2011). Volumetric water content is a key component of the transfer of heat into the subsurface in these equations. In Figures 4.12 to 4.15 the reverse is also true, where the soil moisture content is lowest there is also the shallowest active layer thaw depths. These areas match well with the location of taller shrub patches. We can assume that this is a mix of canopy interception of precipitation as well as shading, and even uptake of groundwater by the plants in these areas, thus limiting moisture as well as limiting thaw, similar to what was observed by Wilcox et al. (2019).

The depths to the water table became shallower for the normal year simulation. With active layer depths that typically only reach 50-70 cm (Endrizzi et al., 2011; Wilcox et al., 2019), there is finite space for the water table to exist where the bottom of the active layer is presumed to be impermeable. A shallower depth to the water table means that there is much more water in the sub-surface than deeper depths, and this also means that there is more heat in the system stored in the sub-surface if we consider it a basin of heat instead of per area. For the dry year simulation, water table depths were close to uniform across the basin and deeper. Compared to the normal year however, it appears that many of the deeper values are located in and around alder and birch shrub patches. This is not shown for the dry year simulation as there was little variation in water table depths.

Discharge between the two simulations were different due to differences in summer precipitation and SWE stored on the ground before snowmelt. The summer of 2016 was classified as a normal year with total summer precipitation and summer average temperature similar to the long-term average. As mentioned, the summer of 2021 was a dry summer, as seen in Figure 4.9. The discharge for 2021 was a third of the total compared to 2016, and the 2016 peak discharge was doubled that of 2021 during freshet. Neither year showed much response to precipitation events later into the summer. This likely correlates to the topmost layer of soil moisture in the model simulations being significantly drier than other layers, and thus what little precipitation in either summer that occurred was retained in the vadose zone rather than being allowed to flow. Overall, we found that higher discharge in 2016 did not coincide with a higher maximum water table depth. If we examine Figure 4.9 the total summer volume is different between the two years, however the majority of streamflow for both years occurs after freshet, and in both summers there is almost no discharge after this. Both cumulative lines in this figure flatten out at the same time. If we recall Zipper et al. (2018), the energy content of the water if we consider the air temperatures as identical per unit area, are also identical – and thus there should only be a slightly deeper maximum between the two simulations for the creek areas.

Evapotranspiration showed little change between the two years (Figure 4.10). Both the daily and cumulative graphs were similar, where the daily ET had slightly higher values, and the end of summer cumulative values differed by only 4 mm. This is likely a result of how the simulation for the wet year was set up, as the only difference between the two was precipitation

and SWE. The rest of the meteorological forcing values were the same, such as air temperature, windspeed, and relative humidity, and where the model uses its own internal method to calculate ET.

Summers similar to 2021 are a complete change for both the hydrology of the catchment, as well as for active layer thaw. Wetter summers can lead to deeper thaw depths while a drier summer could produce shallower active layer thaw depths. Soil moisture was determined to be influential, and it can be inferred from this study that wetter summers pose more of a concern to permafrost degradation than drier summers.

4.6 Conclusion

The summer of 2021 when compared to a normal year had overall much shallower thaw, and discharge for the summer was almost 1/3 that of a normal year. While microtopography may influence local variations in thaw variability, it does this by influencing soil moisture spatial variability, and soil moisture is what determines the extent of seasonal thaw for the whole of the catchment. The water table depths for 2016 simulation were shallower than the dry simulation. However, shrubs may act as an influence on water table spatial variability, much like hummocks were for active layer thaw. These results show that the more wet and warm years rather than the dry years pose a threat for thaw reaching into and degrading permafrost.

Chapter 5
Conclusions and Recommendations for Future Research

The drying of the Arctic is a phenomenon that many regions of the Arctic have begun to experience as global warming progresses (Olthof et al., 2015; Webb et al., 2022). This is amplified in Arctic climates by many feedback systems, which make this region more susceptible to change than other parts of the globe (AMAP,2021). This drying has direct repercussions on active layer thaw and permafrost degradation, as well as influencing local hydrological systems. These systems are being altered in ways that have not been fully understood and collecting data in these regions requires lots of resources. Research conducted within this thesis improves the ability to understand how dry summers affect these Arctic catchments affected by global warming by (1) further understanding how dry summers may affect thaw underneath hummocks and inter-hummocks, (2) modelling many of the topographical features that commonly exist in these catchments to see how these affect thaw and various hydrological components, and (3) comparing this dry year to a baseline normal to more-wet year to truly understand how significant dry years can be to the hydrology as well as thaw regimes for these regions. This was done by using a variety of both direct measurements during the summer of 2021 to measure thaw and other watershed characteristics, using the model GEOtop to understand topographical influences on this, as well as to model wetter conditions in the basin. The main goal of this research is to better understand how climate change is affecting the hydrology and thaw in these continuous permafrost regions. This chapter shows how Chapters 2, 3, and 4 contribute to a better understanding of thaw during these phenomena years and outlines future research to address many of the knowledge gaps that exist within this thesis.

5.1 Synthesis of contributions

5.1.1 The Relation of Hummocks and Inter-Hummocks to Peat Thicknesses, And the Role This Has During a Dry Summer on Ground Thaw Variability.

We know from previous research in Siksik Creek that hummocks and inter-hummocks influence ground thaw variability (Quinton and Marsh, 1999; Endrizzi et al., 2011; Wilcox et al., 2019). In this case, this thesis sought to do this within the context of a dry summer. Chapter 2 explores how thaw over the course of such a summer develops, how this varies across the catchment, and explores how peat thicknesses are associated with these features. Results from Chapter 2 show that lichens and mosses seem to be linked to hummocks and inter-hummocks, and suggests that mapping hummocks and inter-hummocks as a proxy by mapping lichens and mosses might be possible; further, that thaw within the basin was shallower than what was expected over the summer, and that these conditions may not actually pose a risk to permafrost degradation because of how peat specifically is affected by soil moisture content. Chapter 3 attempts to map hummocks and inter-hummocks and incorporates them into the model. The simulations in this chapter compare a 1-soil domain, which averaged hummock and inter-hummock properties into one, versus a 2-soil domain that discretized a soil type for each of these. Results showed how these features responded during freshet with the 2-soil domain reaching a peak discharge two days earlier and that thaw in the basin was controlled by microtopography rather than larger topographical features. More work needs to be done to understand thaw directly underneath hummocks in the catchment and how this might affect permafrost.

5.1.2 Modelled Thaw Variability and Hydrological Assessment of a Dry Year

One of the key goals of this thesis was to improve and build upon the work of Endrizzi et al. (2011), where the goal was to add modules available in newer versions of the model GEOtop, such as snow and shrubs, as well as incorporating microtopography to assess ground thaw variability and how these might change some of the hydrological components of the catchment. Specifically, Chapter 3 included both hummocks and inter-hummocks, shrubs, and snow that was present at the beginning of the simulations. Several simulations were explored to

individually test the influences that these have on thaw, water tables, discharge, and evapotranspiration.

It was found that GEOtop can incorporate these features into the model, especially micro-topographical features such as hummocks and inter-hummocks which typically get upscaled or ignored because of their size. While these simulations still upscaled the discretization of the nodes to 10 m, these nodes were all specifically hummock and or inter-hummock. The model was able to properly simulate thaw rates over the course of the summer, as well as simulating peak discharge and cumulative discharge volumes for the summer, and evapotranspiration peaks and cumulative volumes. These all closely matched observations, although later summer precipitation events were not modelled and slightly overestimated ET at the beginning and end of the summer.

The presence of snow and shrubs influenced the timing of peak ET and discharge more than the actual volumes. The simulations with shrubs had freshet begin a day earlier than the snow-only model and had smaller values for ET for most of the summer. Further, the shrub-only simulation generally had shallower thaw. This is limited because of how dry the catchment was for the summer and how thermal conductivities of peat decrease with decreasing soil moisture. Because snow was only on the ground when the active layer was very shallow, very little of this water infiltrated into the ground.

5.1.3 Comparing Thaw Variability and Hydrological Assessments Between a Wet and Dry Summer.

Chapter 4 is the culmination of the previous two chapters and attempts to show how a dry year will affect both the hydrology as well as thaw in Siksik Creek. Further, it helps to give insight into what we might expect to see in both a drying and wetting scenario. General assumptions for what the future will hold include warmer air temperatures, which will lead to longer snow free periods, and thus higher evaporation rates (Black et al., 2021). This will also impact the amount of snow stored over the winter, as well as increasing precipitation over the summer months; earlier snowmelt timings will lead to deeper active layer thaw, and thus permafrost degradation (Wilcox et al., 2019).

Future changes in active layer thaw, discharge and evapotranspiration will be affected by the highly inter-connected, and complex systems that exist in Arctic catchments. Chapter 4 found that soil moisture has a control on the extent of seasonal thaw as wetter summers will have deeper thaw depths. While microtopography influences local variability in thaw, the soil moisture content in the soil will determine the maximum, minimum, and mean thaw depths. Additionally, shallower water table depths mean more water is stored in the subsurface and generates greater values of discharge over the summer. Between the 2016 and 2021 simulations, the normal year had 3x the volume of discharge than the dry summer had, where the peak volume of discharge was doubled. While many studies suggest that evapotranspiration will increase, the wet simulation did not show this, likely because of how the simulation was discretized, and how the model calculates ET. This chapter implies that the wet and warm years, rather than the warm and dry years, will create more permafrost degradation.

5.2 Knowledge Gaps and Future Research

With past studies examining hummocks and inter-hummocks within Siksik Creek (Quinton et al., 1999; Endrizzi et al., 2011; Wilcox et al., 2019), there is still more research needed on the potential drying or wetting of Arctic catchments. As wetting and drying phenomena are going to become more common, and understanding what this might mean both for thaw and hydrologically is crucial for continuing research.

Future changes to precipitation, evaporation, as well as shrub expansion, will have impacts on thaw and the hydrology of these catchments. This thesis sought to improve our understanding of microtopographical and local features, and how these affect thaw and various water balance components on a watershed level. More research needs to be done to understand thaw rates underneath hummocks in relation to permafrost depth underneath these features. One of the findings of this thesis was that it was unlikely for thaw underneath of inter-hummocks during a dry summer to reach the permafrost layer. This was because of how thick the layer of peat was in these areas, and how the thermal conductivity of peat decreased with decreasing soil moisture. Hummocks have a thin to no peat layer on top and due to the thermal conductivity of these mineral soils, which are clay dominated and thus not as affected by soil moisture as peat, this could increase permafrost degradation.

As for the modelling component of this thesis, future research should look at more than just one generic shrub type for the catchment. There are a variety of alder, birch, and willow shrubs that exist either on the hillslopes or in the creeks of these Arctic catchments, and as shrub expansion becomes more ubiquitous in the north, will begin to play a larger role in influencing thaw and the hydrology of these catchments. Wilcox et al., (2019) looked at many of these shrubs and their influence on thaw timing and extent. It is possible that various types of shrubs will amplify or null many of the effects of climate change.

Further, GEOtop is capable of modelling at hyper-scale resolutions. While this thesis only stuck to 10 m resolutions, the issue of scale and truly incorporating hummocks and inter-hummocks is something that needs to be addressed as these features are typically very small (0.5 – 1 m). It would be interesting to see how thaw and many of the water balance components change as the resolution becomes finer. It is possible that many of the over or under-estimation of some of the water-balance components could be solved with this, it is also possible that routing of water in the sub-surface becomes infinitely complex at this scale, especially within a hummock / inter-hummock domain.

Lastly, while this thesis looked at a wet vs dry summer, there is still much to be done to show how different these summers are and how greatly they both impact thaw and the hydrology of Arctic catchments respectively. Specifically, as Chapter 4 showed, the methodology used to model both summers leaves much to be desired. Most predictions for climate change in these Arctic regions suggest changes to evapotranspiration (Lamontagne et al., 2018; Wilcox et al., 2019; Olthof & Rainville, 2021), and this chapter found little change despite the large difference in water available to the system. This likely is due to how GEOtop calculates ET, and because the same air temperature and relative humidity values were used for both simulations. Further simulations should use a variety of years, that have physical measurements available to validate them, that are a mix of warm, cold, dry, and wet, to show how each of these affects both thaw and the hydrology of the catchment, and where each simulation uses its own distinct meteorological variables rather than just changing precipitation and SWE. Further, legacy conditions in the basin, such as soil moisture, can impact the amount of water available in the subsurface for the coming year (Hinkel et al., 2001). This was not explored in this study, but given the discussion around dry and wet conditions, this seems like something pertinent for

future studies determining the true extent of conditions in the catchment. A better understanding of these processes in the ground is still needed for numerical modelling, and while techniques and methodologies are being developed, there is still much room for improvement.

6.0 References

AMAP. (2021). Arctic Climate Change Update 2021: Key Trends and Impacts. Summary for Policy-makers (Arctic Monitoring and Assessment Programme,Ed.). https://www.amap.no/documents/download/6759/inline

Ahmad, J., Coon, E., Painter, S. (2020). Evaluating integrated surface/subsurface permafrost thermal hydrology models in ATF (v0.88) against observations from a polygonal tundra site. *Geoscientific model development* (13). 2259-2276. DOI: 10.5194/gmd-13-2259-2020bonan

Ahmed, R., Prowse, T., Dibike, Y., Bonsal, B. (2021). Effects of climatic drivers and teleconnections on late 20th century trends in spring freshet of four major arctic-draining rivers. *Water (Basel)*, (13). DOI: 10.3390/w13020179

Ajami, H., McCabe, M.F., Evans, J.P. (2015). Impacts of model initializations on an integrated surface water-groundwater model. *Hydrological Processes (29).* 3790-3801.

American Meteorological Society (2021). Glossary of meteorology. Frost table - Glossary of Meteorology (ametsoc.org) Last edited April 25, 2012.

Atchley, A., Coon, E., Painter, S., Harp, D., Wilson, C. (2016). Influence and interactions of inundation, peat, and snow on active layer thickness. *Geophysical Research Letter* (43) 5116-5123.

Batchelor, C.L., Dowdeswell, J.A., Pietras, J.T. (2013) Seismic stratigraphy, sedimentary architecture, and palaeo-galciology of the Mackenzie Trough: evidence for two Quaternary ice advances and limited fan development on the eastern Canadian Beaufort Sea margin. *Quaternary Science Reviews* (65). 73-87.

Bixio, A., Orlandini, s., Paniconi, C., Putti, M. (2000). Physically-based distributed model for coupled surface runoff and subsurface flow formulation at the catchment scale. *Computational Methods in Water Resources* (12). 115-122.

Black, K., Wallace, C., Baltzer, J. (2021). Seasonal thaw and landscape position determine foliar functional traits and whole-plant water use in tall shrubs on the low Arctic tundra. *New Phytologist* (231). 94-107.

Bolduc, C. (2015). Thermal evidence for surface and subsurface water contributions to baseflow in a high arctic river. Queen's University, Masters of science thesis.

Bonan, G. (1996). Sensitivity of a GCM simulation to subgrid infiltration and surface runoff. *Climate Dynamics* (12). 279-285. DOI: 10.1007/BF00219501

Bui, M., Lu, J., Nie, L. (2020). A review of hydrological models applied in the permafrost-dominated arctic region. *Geosciences* (10). DOI: 10.3390/geosciences10100401

Burn, C. R. & Kokelj, S. V. (2009). The Environment and Permafrost of the Mackenzie Delta Area. *Permafrost and Periglacial processes*, 20: 83-105. Doi:10.1002/ppp.655

Carey, S., Woo, M.K. (2007). Field and laboratory estimates of pore size properties and hydraulic characteristics for subarctic organic soils. *Hydrological Processes* (21). 2560-2571. 2007

Choudhury, BJ., Monteith, JL (1988). A four layer model for the heat budget of homogeneous land surfaces. *Meteorological Society* (114). 373-398.

D'Odorico, P., Rigon, R. (2003). Hillslope and channel contributions to the hydrologic response. *Water resources research* (39). DOI: 10.1029/2002WR001708

Endrizzi, S., Marsh, P. (2010) Observations and modeling of turbulent fluxes during melt at the shrub-tundra transition zone 1: point scale variations. *Hydrology Research* (41.6) 471-491.

Endrizzi, S., Quinton, W.L., Marsh, P. (2011). Modelling the Spatial Pattern of Ground Thaw in a Small Basin in the Arctic Tundra. *The Cryosphere Discussions* (5). 367 – 400.

Farouki, O. (1981). The thermal properties of soils in cold regions. *Cold regions science and technology* (5). 67-75. DOI: 10.1016/0165-232X(81)90041-0

Frauenfeld, O., Zhang, T., Barry, RG, Gilichinsky, D. (2004). Interdecadal changes in seasonal freeze and thaw depths in Russia. *Journal of geophysical research* (109).

GEOtop Users Manual (Version 1.0). Edition by Endrizzi, S., Dall'Amico, M., Gruber, S., Rigon, R. www.geotop.org

Glossary of Permafrost and Related Ground-ice Terms (1988). Permafrost subcommittee associate committee on geotechnical research. Nation research council of Canada. Prepared by: S.A. Harris, H.M. French, J.A. Heginbottom, G.H. Johnston, B. Ladanyi, D.C. Sego, R.O. van Everdingen. Technical memorandum No. 142.

Gray, D.M., Granger, R.J., Landine, P.G. (1986). Modelling snowmelt infiltration and runoff in a prairie environment. *American Water Resources Association*, 427-438.

Grunberg, I., Wilcox, E.J., Zwieback, S., Marsh, P., Boike, J. (2020). Linking tundra vegetation, snow, soil temperature, and permafrost. *Biogeosciences* (17). 4261-4279.

Gubler, S., Endrizzi, S., Gruber, S., Purves, R. (2013)/ Sensitivities and uncertainties of modeled ground temperatures in mountain environments. *Geoscientific model development* (6). 1319-1336. DOI: 10.5194/gmd-6-1319-2013

Hansson, K., Simunek, J., Mizoguchi, M., Lundin, van Genuchten, L. M. (2004). Water flow and heat transport in frozen soil numerical solution and freeze-thaw applications. *Vadose Zone Journal* (3). 694-704.

Higgens, F., Chipman, J., Lut, D., Culler, L., Virginia, R., Ogden, L. (2019). Changing Lake Dynamics indicate a drier arctic in western Greenland. Journal of geophysical research. *Biogeosciences* (124). 870-883.

Hinkel, K., Paetzold, F., Nelson, F., Bockheim, J. (2001). Patterns of soil temperature and moisture in the active layer and upper permafrost at Barrow, Alaska: 1993-1990. *Global and Planetary Change* (29). 293-309.

Holden, J., Burt, T. (2003)/ Hydrological studies on blanket peat: the significance of the acrotelm-catotelm model. *The journal of ecology* (91). 86-102. DOI: 10.1046/j.1365-2745.2003.00748.x

Hopkinson, C., Fox, A., Monette, S., Churchill, J., Crasto, N., Chasmer, L. (2011). Investigating the spatial distribution of water levels in the Mackenzie Delta using airborne LiDAR. *Hydrological Process* (25). 2995-3011. https://doi.org/10.1002/hyp.8167

IPCC, 2014: Climate Change 2014: Synthesis Report. Contribution of Working Groups I, II and III to the Fifth Assessment Report of the Intergovernmental panel on Climate Change [Core Writing Team, R.K. Pachauri and L.A. Meyer (eds.)]. IPCC, Geneca, Switzerland, 151 pp.

IPCC, 2019: Climate Change and Land. An IPCC special report on climate change, desertification, land degradation, sustainable land management, food security, and greenhouse gas fluzes in terrestrial ecosystems. [P.R. Shukla, J. Skea, E. Calvo Buendia, V. Masson-Delmotte, H.-O. Pörtner, D. C. Roberts, P. Zhai, R. Slade, S. Connors, R. van Diemen, M. Ferrat, E. Haughey, S. Luz, S. Neogi, M. Pathak, J. Petzold, J. Portugal Pereira, P. Vyas, E. Huntley, K. Kissick, M. Belkacemi, J. Malley, (eds.)]. In press.

James, R., Hinkel, K., Hinkel, N. (1996) Concurrent permafrost aggradation and degradation induced by forest clearing, central Alaska, U.S.A. *Arctic and Alpine Research* (28) No.3, 293-299.

Jiang, Y., Zhuang, Q., O'Donnell, J. (2012). Modeling thermal dynamics of active layer soils and near-surface permafrost using a fully coupled water and heat transport model. *Journal of Geophysical Research: Atmospheres* (117).

Johansen, O. (1975). Thermal conductivity of soils. Ph.D. Thesis. University of Trondheim

Jonckherre, I., Fleck, S., Nackaerts, K., Muys, B., Coppin, P., Weiss, M., Baret, F. (2003) Review of methods for in situ leaf area index determination Part I. Theories, sensors and hemispherical photography. *Agricultural and Forest Meteorology* (121). 19-35

Jorgenson, J., Jorgenson, M., Boldenow, M., Orndahl, K. (2018). Landscape change detected over a half century in the Arctic National Wildlife Refuge using high-resolution aerial imagery. *Remote Sensing* (10).

Juszak, I., Eugster, W., Heijmans, M., Monique, M.P.D., Schaepman-Strub, G. (2016). Contrasting radiation and soil heat fluxes in Arctic shrub and wet sedge tundra. *Biogeosciences* (13). 4049-4064. DOI: 10.5194/bg-13-4049-2016

Kokelj, S. V., Burn, C.R. (2005). Near-surface ground ice in sediments of the Mackenzie Delta, Northwest Territories, Canada. *Permafrost and Periglacial Processes* (16). 291-303.

Konovalov, A., Roman, L. (1973) The thermophysical properties of peat soils. *Soil Mechanics and Foundation Engineering* (10). 179-181.

Kujala, K., Seppala, M., Holappa, T (2008). Physical properties of peat and palsa formation. *Cold Regions Science and Technology* (52). 48-414.

Lafaysse, M., Cluzet, B., Dumont, M., Lejeune, Y., Vionnet, V., Morin, S. (2017) A multiphysical ensemble of numerical snow modelling. *The Cryosphere* (11) 1173-1198.

Lamontagne-Halle, P., McKenzie, J.M., Kurylyk, B.L., Zipper, S.C. (2018). Changing Groundwater Discharge Dynamics in Permafrost Regions. *Environmental Research Letters* (13).

Lamontagne-Halle, P., McKenzie, J.M., Kurylyk, B., Molson, J., Lyon, L. (2020). Guidelines for cold-regions groundwater numerical modeling. *WIREs Water* (7). https://doi.org/10.1002/wat2.1467

Lants, T.C., Marsh, P., Kokelj, S.V. (2013). Recent Shrub proliferation in the Mackenzie Delta Uplands and Microclimatic Implications. *Ecosystems* (16). 47-59.

Lemieux, J., Sudicky, E., Peltier, W., Tarasov, L. (2008). Simulating the impact of glaciations on continental groundwater flow systems: 1. Relevant processes and model formulation. *Journal of Geophysical research* (113). DOI: 10.1029/2007JF000928

Ling, F., Zhang, T. (2003). Numerical simulation of permafrost thermal regime and talik development under shallow thaw lakes on the Alaskan Arctic Coastal Plain. *Journal of Geophysical Research* (108). DOI: 10.1029/2002JD003014

Mackay, J. (1980). The origin of hummocks, western Arctic coast, Canada. *Canadian journal of earth sciences* (17). 996-1006.

Marsh, P., Woo, Ming-Ko. (1981). Snowmelt, glacier melt, and high arctic streamflow regimes. *Canadian Journal of Earth Science* Vol. 18 (8). 1380-1384.

Marsh, P., Pomeroy, J., Pohl, S., Quinton, W., Onclin, C., Russell, M., Neumann, N., Pietroniro, Davidson, A., McCartney, S. (2008). Snowmelt processes and runoff at the arctic treeline: ten years of mags research. In M.-K. Woo (Ed.), *Cold region atmospheric and hydrologic studies*. The Mackenzie gewex experience: hydrologic processes (2). 97-123.

Marsh, P., Bartlett, P., Mackay, M., Pohl, S., Lantz, T. (2010). Snowmelt energetics at a shrub tundra site in the Western Canadian Arctic. *Hydrological Processes* (24). 3603-3620. DOI: 10.1002/hyp.7786

McKenzie, J.M., Voss, C.I. (2013). Permafrost thaw in a nested groundwater-flow system. *Hydrogeology Journal* (21). 299-316.

Morse, P.D., Burn, C.R., Kokelj, S.V. (2012). Influence of snow on near-surface ground temperatures in upland and alluvial environments of the outer Mackenzie Delta, Northwest Territories. *Canadian Journal Earth Science* (49). 895-913.

Mualem, Y. (1976) A new model for predicting the hydraulic conductivity of unsaturated porous media. *Water Resources* (12). 513-522.

Mustamo, P., Ronkanen, A., Berglund, O., Berglund, K., Klove, B. (2019) Thermal conductivity of unfrozen and partially frozen managed peat soils. *Soil & Tillage research* (191). 245-255.

Muster, S., Langer, M., Abnizova, A., Young, K., Boike, J. (2015). Spatio-temporal sensitivity of MODIS land surface temperature anomalies indicates high potential for large-scale land cover change detection in Arctic permafrost landscapes. *Remote Sensing of environment* (168). 1-12.

National Resources Canada. (1995). Canada Permafrost. *National atlas of Canada* (5)

Ng, G., Wickert, A., Somers, L. et al. (2018) GSFLOW-GRASS v1.0.0: GIS-enabled hydrologic modeling of coupled groundwater-surface-water systems (11).

Obu, J., Westermann, S., Bartsch, A. et al., (2019) Northern Hemisphere Permafrost Map Based on TTOP modelling for 2000-2016 at 1km2 Scale. *Earth-Science Reviews* (193). 299-316.

O'Connor, M., Cardenas, M., Ferencz, S., Wu, Y., Neilson, B.T., Chen, J., Kling, G.W. (2020). Empirical Models for Predicting Water and Heat Flow Properties of Permafrost Soils. *Geophysical Research Letters* (47).

Oke, T.R. (1987). Boundary Layer Climates. Routledge, Taylor & Francis Group.

Olthof, I., Fraser, R., Schmitt, C. (2015). Landsat-based mapping of thermokarst lake dynamics on the Tuktoyaktuk Coastal Plain, Northwest Territories, Canada since 1985. *Remote sensing of the Environment*. 194-204. DOI: 10.1016/j.rse.2015.07.001

Olthof, I., Rainville, T. (2022). Dynamic surface water maps of Canada from 1984 to 2019 Landsat satellite imagery. *Remote Sensing of the Environment* (279).

Palmer, M.J., Burn, C.R., Kokelj, S.V. (2012). Factors Influencing Permafrost temperatures across tree line in the uplands east of the Mackenzie Delta, 2004-2010. *Canadian Journal of Earth Science* (49). 877-894.

Paniconi, C., Putti, M. (1994). A comparison of Picard and Newton iteration in the numerical solution of multidimensional variably saturated flow problems. *Water resources research* (30). 3357-3374. DOI: 10.1029/94WR02046

Pomeroy, J.W., Lesack, L., Marsh, P. (1993) Relocation of Major Ions in Snow along the Tundra – taiga ecoton. *Nordic Hydrology* (24). 151-168.

Pomeroy, J., Dion, K. (1996)/ Winter radiation extinction and reflection in a boreal pine canopy: measurements and modelling. *Hydrological Processes* (10). 1591-1608. DOI: 10.1002/(SICI)1099-1085(199612)10:12<1591::AID-HYP503>3.0.CO;2-8

Quinton, W.L., Marsh, P. (1999). A Conceptual Framework for Runoff Generation in a Permafrost Environment. *Hydrological Processes* (13). 2563-2581.

Quinton, W.L., Gray, D.M., Marsh, P. (2000). Subsurface drainage from hummock-covered hillslopes in the Arctic tundra. *Journal of Hydrology* (237. 112-125.

Quinton, W.L., Gray, D. (2003). Subsurface drainage from organic soils in permafrost terrain: the major factors to be represented in a runoff mode, refereed proceedings of the 8th international conference on permafrost, Davos, Switzerland.

Quinton, W.L., Shirazi, T., Carey, S., Pomeroy, J. (2005). Soil Water Storage and Active-layer Development in a Sub-alpine Tundra Hillslope, Southern Yukon Territory, Canada. *Permafrost & Periglacial Processes* (16). 369-382.

Quinton, W., Carey, S. (2008). Towards an energy-based runoff generation theory for tundra landscapes. *Hydrological Processes* (22). 4649-4653.

Rinaldo, A., Marani, A., Rigon, R. (1991). Geomorphological dispersion. *Water Resources* (27). 513-525.

Rantanen, M., Karpechko, A., Lipponen, Y., Nordling, K. Hyvarinen, O., Ruosteenoja, K., Vihma, T., Laaksonen, A. (2022). The Arctic has warmed nearly four times faster than the globe since 1979. *Communications, Earth & environment* (3).

Rigon, R., Bertoldi, G., Over, T. (2006). GEOtop: a distributed hydrological model with coupled water and energy budgets. *Journal of hydrometeorology* (7). 371-388.

Rinke, A., Segger, B., Crewell, S., Maturilli, M., Naakka, T., Nygard, T., Vihma, T., Alshawaf, F., Dick, G., Wickert, J., Keller, J. (2019). Trends of vertically integrated water vapor over the Arctic during 1979-2016: Consistent moistening all over? *Journal of Climate* (32). 6097-6116.

Russel, M. (2002). Water balances across the Arctic tree line and comparisons to a numerical weather prediction model. Master's thesis manuscript, University of Saskatchewan.

Seto, J. (2022). Undergraduate Thesis, Wilfrid Laurier University.

Schoolmeester, T., Gjerdi, H.L., Crump,J., Alfthan, B. Fabres,J., Johnsen, K., Puikkonen, L., Kurvits, T. and Baker, E., 2019. Global Linkages – A Graphic look at the changing Arctic. UN Environment and GRID-Arendal, Nairobi and Arendal. www.grida.no

Sonnentag, O., Hould-Gosselin, G. (2021). Post-processed evapotranspiration data for Siksik Creek at TMM.

Tetzlaff, D., Carey, S., McNamara, J., Laudon, H., Soulsby, C. (2017). The essential value of long-term experimental data for hydrology and water management: long-term data in hydrology. *Water resources research* (53). 2598-2604.

Tetzlaff, D., Piovano, T., Ala-Aho, P., Smith, A., Carey, S. K., Marsh, P., … Soulsby, C. (2018). Using stable isotopes to estimate travel times in a data-sparse Arctic catchment: Challenges and possible solutions. *Hydrological Processes*, *32*(12), 1936–1952. https://doi.org/10.1002/hyp.13146

Van Genuchten, M.T. (1980). A closed-form equation for predicting the hydraulic conductivity of unsaturated soils. *Soil Science* (44). 892-898.

Vavrus, S., Wang, F., Martin, J., Francis, J., Peings, Y., Cattiaux, J. (2017). Changes in north American atmospheric circulation and extreme weather: influence of Arctic amplification and northern hemisphere snow cover. *Journal of Climate* (30). 4317-4333.

Verseghy, D. (1991). Class- a canadian land surface scheme for GCMS. I. soil model. *International journal of climatology* (11). 111-133. DOI: 10.1002/joc.3370110202

Walker, B., Wilcox, E., Marsh, P. (2020). Accuracy assessment of late winter snow depth mapping for tundra environments using structure-from-motion photogrammetry. *Arctic Science* (7) 588-604.

Walker, D., Jia, G., Epstein, H., Raynolds, M., Chapin III, F., Copass, C., Hinzman, L., Knudson, J., Maier, H., Michaelson, G., Nelson, F., Ping, C., Romanovsky, V., Shiklomanov, N. (2003) Vegetation-soil-thaw-depth relationships along a low-arctic bioclimate gradient, Alaska: synthesis

of information from the ATLAS studies. *Permafrost and Periglacial Processes* (14) 103-123. DOI: 10.1002/ppp.452

Way, R.G., Lewkowicz, A.G. (2017). Environmental Controls on Ground Temperature and Permafrost in Labrador, Northeast Canada. *Permafrost and Periglacial Processes* (29). 73-85.

Webb, E., Liljedhal, A., Corddeiro, J., Loranty, M., Witharana, C., Lichstein, J. (2022). Permafrost thaw drives surface water decline across lake-rich regions of the Arctic. *Nature Climate Change* (12). 841-846.

Wilcox, E.J., Keim, D., Jong, T.D., Walker, B., Sonnentag, O., Sniderhan, A.E., Mann, P., Marsh, P. (2019) Tundra shrub expansion may amplify permafrost thaw by advancing snowmelt timing. *Arctic Science* (5). 202-217.

Wojciech, D. (2020). Permafrost active layer. *Earth-science reviews* (208). DOI: 10.1016/j.earscirev.2020.103301

Woo, M-K., Marsh, P. (2005). Snow, frozen soils and permafrost hydrology in Canada, 1999-2002. *Hydrological processes* (19). 215-229. DOI: 10.1002/hyp.5772

Yanhui, Y., Guo, L., Yu, Q., Wang, X., Pan, X., Wu, Q., Wang, D., Wang, G. (2022). Spatial variability and influential factors of active layer thickness and permafrost temperature change on the Qinghai-Tibet plateau from 2012 to 2018. *Agricultural and forest meteorology* (318). DOI: 10.1016/j.agrformet.2022.108913

Ye, Z., Pielke, R. (1993). Atmospheric parameterization of evaporation from non-plant-covered surfaces. *Journal of applied meteorology* (32). 1248-1258.

Yongjiu, D., Zeng, X., Dickinson, R., Baker, I., Bonan, G., Bosilovich, M., Denning, A., Dirmeyer, P., Paul, A., Houser, P., Nui, Guoyue, Oleson, K., Schlosser, C., Yang, Z-L. (2003). The common land model. *Bulletin of the American meteorological society* (84). 1013-1023. DOI: 10.1175/BAMS-84-8-1013

Young, K., Bolton, W.R., Killingtveit, A., Yang, D. (2006) Assessment of Precipitation and Snowcover in Northern Research Basins. *Nordic Hydrology, 37*(4)

Zanotti, F., Endrizzi, S., Bertoldi, G., Rigon, R. (2004). The GEOTOP snow module. *Hydrological processes* (18). 3667-3679.

Zhang, Y., Wang, X., Fraser, R., Olthof, I., Chen, W., Mclennan, D., Ponomarenko, S., Wu, W. (2012) Modelling and mapping climate change impacts on permafrost at high spatial resolution for an Arctic region with complex terrain. *The Cryosphere* (7) 1121-1137.

Zhao, Y., Bingcheng, S., Zhenhua, Z., Min, L., Hailong, H., Hill, R. (2019). A new thermal conductivity model for sandy and peat soils. *Agricultural and forest meteorology* (274). 95-105.

Zipper, S., Lamontagne-Halle, P., McKenzie, J., Rocha, A. (2018). Groundwater controls on postfire permafrost thaw: water and energy balance effects. Journal of Geophysical Research: *Earth Science* (123). 2677-2694.

Appendix

Table 7.1: Piezometric Data collected over the summer of 2021.

Piezometer	Latitude	Longitude	June_1	June_2	July_1	July_2	July_3	July_4	July_5	July_6	July_7	July_8	July_9	Aug_1	Aug_2	Aug_3	Aug_4
SSL-1	68.739554	-133.491											52.7		46.8		66.7
SSL-2	68.740104	-133.49															
SSL-3	68.740305	-133.489	35.1	45.5					63.2		57.6		59.9		58.7		62.5
SSL-4	68.740178	-133.49	6.1														
SSL-5	68.739766	-133.489		15.1					25.5		26.5						28.7
SSL-6	68.740772	-133.488							43.9		43.3		70.8		70.9		63.3
SSL-7	68.739476	-133.492															
SSL-8	68.74037	-133.491															
TMM-1	68.746048	-133.503															
TMM-2	68.746571	-133.503										57.7		57.9	69.4		
CC-1	68.743462	-133.496			28.6			30.9		30.2		31.9			32.9		33.4
SS-1	68.746006	-133.493	4.3		8.2			14.9		9.7		13.1			14.4		20
SM-1	68.745965	-133.495												44.3			
SM-2	68.746571	-133.497								8.1		12.8			11.8	15.3	42.2

SHR-1	68.747 93	-133.50 2								16.9		28.8		19.8	18.9	23.6	29.8
SHR-2	68.748 36	-133.49 9	20.4				29.2			23.9		25.9		27	25.5	29.2	34.8
SHR-3	68.748 045	-133.49 9															
SHR-4	68.747 785	-133.5	7.2							15.2		17.3		18.7			20.5